Calorons, symmetry, and the soliton trinity

Joshua Stephen Cork

Submitted in accordance with the requirements for the degree of Doctor of Philosophy

The University of Leeds

School of Mathematics

Department of Pure Mathematics

August 2018

Abstract

This thesis is concerned with calorons – finite-action, anti-self-dual connections over $S^1 \times \mathbb{R}^3$. We study three major topics: a review of the geometry of calorons, and their different construction techniques; the topic of symmetric calorons, that is, calorons invariant under various isometries; and their role in understanding the links between the Yang-Mills solitons, monopoles and instantons, and the solitons of the Skyrme model, also known as skyrmions.

We emphasise the role of the rotation map – a large gauge transformation which acts on calorons isometrically – in studying symmetric calorons, and provide a classification of cyclically symmetric calorons where the cyclic groups considered involve the rotation map. Our approach utilises a generalisation of the monad matrix data, first understood in the context of calorons by Charbonneau and Hurtubise, and we additionally construct explicit symmetric solutions to Nahm's equations up to the case of charge 2.

Calorons are seen to interpolate between monopoles on $\mathbb{R}^3$ and instantons on $\mathbb{R}^4$, and likewise, these have concrete, and convincing relationships to skyrmions. We refer to this relationship between monopoles, instantons, and skyrmions, as the 'soliton trinity'. In a construction inspired by the Atiyah-Manton-Sutcliffe construction of Skyrme fields from instantons, we show how caloron holonomies may be used to approximate gauged skyrmions on $\mathbb{R}^3$. We observe that this interpolation between monopoles and instantons is similarly exhibited by the gauged Skyrme models that we construct, by exploring monopole-like and instanton-like boundary conditions for spherically symmetric Skyrme fields. Due to the kinship of monopoles and calorons, this relationship between calorons and skyrmions may prove to be a way to explain the apparent links between monopoles and skyrmions.

To my wife.

"Exactly!" said Deep Thought. "So once you do know what the question actually is, you'll know what the answer means."

Douglas Adams,

The hitchhiker's guide to the galaxy.

Acknowledgements

I would not be where I am today without the incredible support of my supervisor, Derek Harland. He is the model example of a PhD supervisor; his patience, insight, gift of encouragement, and ability to get the best out of you, are everything you might want, and more. I'm indebted to his dedication to me as a student, and for the countless helpful discussions we have had.

My time in Leeds has been greatly enhanced by the excellence of the School of Mathematics. My funding was through a Graduate Teaching Assistantship, providing me not only with financial support, but also with the incredible experience of teaching in all settings from small workshops to large lectures. I'm incredibly grateful for this opportunity, and for all of the students who have been an inspiration to teach along the way! In particular I would like to thank Margit Messmer for all of her help with the GTA position. I have also been lucky enough to be a part of a thriving *geometry group* at Leeds, and it has been a great source of community, which I have treasured deeply. Many thanks to all of you for the lunches, coffees, seminars, and pub trips, which have all been intellectually stimulating, and a great joy. Also, thanks particularly go to all those who came to the *differential geometry study group* meetings, for the many hours we spent studying tough topics. A lot of my core understanding developed from these meetings.

Many thanks should go to my office mates, for regularly discussing my thought processes with me at the whiteboard, and in particular Jakob Vidmar for his help with Mathematica. Countless others, inside and outside of the school of maths, have been a help throughout my PhD in various ways both mathematically and socially. It is not possible for me to list every other friend and colleague who has been a support to me over the last four years, but some who come to mind are: Samuel Aylmer, Joe Cook, Alice and Ben Creasey, Ben Daniel-Thorpe, Adam Dent, Steven Dixon, Joe Driscoll, Gabriel Fidler, James Hossein, Maxime Fairon, Stephen Flood, Cesare Gallozzi, Christina Grant, Chris Halcrow, Beth Lingard, Sarah Liddell, James Meredith, Joe Oliver, Liz Rhodes, Nic

Peters, the Swales family, Rachel Swann, Leah Thompson, Christian Watkins, Adam Wells, Richard Whyman, Ken Williams, Tom Winyard, Daniel Wolf, and Tim Woodson. I would also like to thank all of my teachers from school and university who encouraged me to achieve well, and to think for myself.

The love and support of my family over the years has been very important, and their interest in all of my pursuits has never ceased to be an encouragement. My achievements owe no small part to the hard work of my Mum and Dad in my upbringing, and I believe much of my character, ambition, and philosophies, are reflections of their good example of parenting. In fact, I probably would have never studied mathematics at all if it had not been for my Dad's enthusiasm for the subject.

Last, but by no means least, I must thank my wife, Millie. This thesis is a testament of her patience, immeasurable kindness, and love, and I would have struggled to complete it without her. Thank you for normalising my life, and for the many fun adventures we have.

Contents

Notational conventions

The following notational conventions shall be used throughout this thesis, unless otherwise specified, or clear from the context.

$\vec{x}$	A coordinate vector $(x^1, x^2, x^3) \in \mathbb{R}^3$.
$(t, \vec{x})$	Coordinates on $S^1 \times \mathbb{R}^3$.
μ_0	The reciprocal of the radius of the circle S^1.
$(x^0, \vec{x})$	Coordinates on $\mathbb{R}^4$.
r	The radial coordinate $r = \lvert\vec{x}\rvert = \sqrt{(x^1)^2 + (x^2)^2 + (x^3)^2}$.
s	The coordinate on $\mathbb{R} \big/ \mu_0\mathbb{Z}$.
S^2_∞	The 2-sphere at $r = \infty$ of $\mathbb{R}^3$, also the boundary ∂B^3 of the 3-ball.
N	The rank of the vector bundle $V \longrightarrow S^1 \times \mathbb{R}^3$.
Latin indices i through n	Summation or referencing of indexed objects over indices $1, 2, 3$.
Greek indices	Summation or referencing of indexed objects over indices $0, 1, 2, 3$.
Latin indices p, q, r	Referencing of indexed objects over indices $1, \ldots, N$, sometimes $N \sim 0$.
∂_μ	The partial derivative $\frac{\partial}{\partial x^\mu}$.
D^A	A connection with connection 1-form A.
F^A	The curvature 2-form of a connection D^A.
Ω	The parallel transport operator for a connection.
$\Lambda^p(M)$	The space of p-forms on a manifold M.
$\Lambda^p(M, \mathfrak{g})$	p-forms on M whose components are $\mathfrak{g}$-valued.
S_{YM}	The Yang-Mills action.
Q	The Yang-Mills topological charge.
k_p	The magnetic charges of a caloron.

k_0 or k	The instanton number of a caloron.
μ_p	The eigenvalues of the asymptotic Higgs field $-\imath\Phi_\infty$.
$(\vec{m},\vec{\nu})$ or (m_p,ν_p)	The monopole charges and masses of a caloron.
$\mathcal{C}^N(\vec{m},\vec{\nu})$	The moduli space of framed $SU(N)$ calorons.
$\mathcal{C}_u^N(\vec{m},\vec{\nu})$	The moduli space of unframed $SU(N)$ calorons.
$\star$	The Hodge-star operator on a riemannian manifold.
$\star_3$, $\star_4$	The Hodge-star operators on $\mathbb{R}^3$ and $\mathbb{R}^4$ respectively.
ϵ_{ijk}, $\epsilon_{\mu\nu\rho\sigma}$	The totally anti-symmetric Levi-Civita symbols of degree 3 and 4 respectively, with the convention that $\epsilon_{123}=\epsilon_{0123}=1$.
$\langle\cdot,\cdot\rangle$	The inner product on $\mathfrak{su}(N)$-valued forms defined by $\langle\xi,\eta\rangle\mathrm{Vol}_\gamma=-\mathrm{tr}\,(\xi\wedge\star\eta)$, where (M,γ) is a riemmannian manifold with volume form Vol_γ.
$\lvert\cdot\rvert^2$	The norm squared of $\langle\cdot,\cdot\rangle$, defined by $\lvert\xi\rvert^2=\langle\xi,\xi\rangle$.
$\langle\langle\cdot,\cdot\rangle\rangle$	The integral over M of $\langle\cdot,\cdot\rangle$.
$\lvert\lvert\cdot\rvert\rvert^2$	The norm squared of $\langle\langle\cdot,\cdot\rangle\rangle$.
σ^1, σ^2, σ^3	The Pauli matrices $\sigma^1=\begin{pmatrix}0&1\\1&0\end{pmatrix}$, $\sigma^2=\begin{pmatrix}0&-\imath\\\imath&0\end{pmatrix}$, $\sigma^3=\begin{pmatrix}1&0\\0&-1\end{pmatrix}$
$\vec{\sigma}$	The 'vector' of Pauli matrices $(\sigma^1,\sigma^2,\sigma^3)$.
I_p	A subdivision of $[\mu_N,\mu_0+\mu_N]$ defined by $I_p=[\mu_{p+1},\mu_p]$, for $p=1,\ldots,N-1$, and $I_0=[\mu_1,\mu_0+\mu_N]$.
$(T_p^\lambda,(u_p,w_p))$	Caloron Nahm data.
(α,β,u,w)	A Nahm complex on $\mathbb{R}\big/\mu_0\mathbb{Z}$.
(A,B,C,D)	Monad matrices.
C_p, D_p	The p-th column/row of monad matrices C/D, $p=0,\ldots,N-1$.
$\mathcal{M}_k^N$	The moduli space of non-singular monad matrices.
$\mathcal{I}$	The set of all words $\Pi(x_1,x_2)$ in two variables.

ρ	The rotation map.
$\mathfrak{R}(\vec{n},\phi)$	A rotation matrix in $SO(3)$ by angle ϕ about an axis $\vec{n}\in\mathbb{R}^3$.
$\mathfrak{S}_\theta$	An element of $SO(2)$ representing a translation $t\mapsto t+\theta/\mu_0$.
$P_{\vec{\varphi}}$	An element of the maximal torus T^{N-1} in $SU(N)$, with phase vector $\vec{\varphi}=(\varphi_1,\ldots,\varphi_N)$ satisfying $\varphi_1+\cdots+\varphi_N=0$.
S_θ	The circle translation – composition of parallel transport along S^1 with $\mathfrak{S}_\theta$.
S_m or S	The shift matrix $S_m=\left(\begin{array}{ccc\|c} 0 & \cdots & 0 & 1 \\ \hline & & & 0 \\ & \mathbb{1}_{m-1} & & \vdots \\ & & & 0 \end{array}\right)$, or simply S when $m=k$, the instanton number.
$\mathrm{diag}\{x_p\}_{p=1}^m$	The $m\times m$ diagonal matrix $\begin{pmatrix} x_1 & & \\ & \ddots & \\ & & x_m \end{pmatrix}$.
$\mathrm{diag}\{x_p\}_{p=0}^{m-1}$	The $m\times m$ diagonal matrix $\begin{pmatrix} x_0 & & \\ & \ddots & \\ & & x_{m-1} \end{pmatrix}$.
$\mathcal{C}_k^N$	The moduli space of calorons with equal monopole charges and masses, with instanton number k.
$\mathcal{C}_k^N(H)$ or $\mathcal{M}_k^N(H)$	The fixed point set in the moduli space of calorons/monad matrices of a group of isometries H.
$\rho(C_{Nn}^{j,\vec{\varphi}})$	The rotation cyclic groups of order Nn, with $j\in\mathbb{Z}_n$.
$\aleph$	$\gcd(n,Nj)$.
Γ	$\gcd(n,j)$.
β	The period $2\pi/\mu_0$ of a caloron.
U	A Skyrme field $U:\mathbb{R}^3\longrightarrow SU(2)$.

L	The left-invariant current of a gauged Skyrme field: $L = U^{-1}D^B U$.
ψ_n, ψ_+	The Hermite functions and additional Hermite function.
$\phi_n^{(\alpha,\beta)}$, $\phi_+^{(\alpha,\beta)}$	The ultra-spherical functions and additional ultra-spherical function.
E_α	The gauged Skyrme energy derived from periodic Yang-Mills theory.
$f(r)$	The profile function for a spherically symmetric Skyrme field.
$g(r)$	The profile function for a spherically symmetric gauge field.

List of figures

List of tables

Chapter 1

Introduction

Various physically relevant field theories admit topological soliton solutions; particle-like configurations which are stable under continuous deformations. A more precise mathematical definition of what 'topological solitons' are is not to be found in the literature, but usually the 'topological' refers to a classification by homotopy (for instance, the degree of a map), or an integral *charge* (for instance, a Chern number), and the 'soliton' refers to a localization of the density of some *energy functional*, in analogue to the classical wave solitons described by the KdV equations. An excellent review and standard reference for these objects in general is the book by Manton and Sutcliffe [82].

Two prevalent examples of topological solitons, which have attracted the interest of both physicists and mathematicians, are *instantons* and *monopoles*, whose field theories are the 4-dimensional *Yang-Mills*, and 3-dimensional *Yang-Mills-Higgs* respectively. Mathematically, these manifest themselves as finite-action (or energy) solutions to the anti-self-dual equations (or a dimensional reduction of them known as the Bogomolny equations). Instantons and monopoles both possess a very rich geometry, for example, they have moduli spaces, which in particular provide examples of complete hyperkähler manifolds [7, 34, 54]. In fact there is a veritable smörgåsbord of relationships to the wider pure mathematical world. For example, explicit constructions make use of twistor theory

[6, 124], with links to the realms of algebraic geometry [9, 88], and instanton moduli spaces were fundamental in the work of Donaldson regarding topological invariants for four-manifolds [32, 34].

Many of the pure mathematical advances in the study of solitons such as monopoles and instantons have been as a result of physical motivations. Instantons and monopoles are considered to be hypothetical elementary particles within the standard model of particle physics, often given the name of 'pseudoparticles', and they both have important roles to play in various areas of modern theoretical physics. Another example of topological solitons with a key relevance in physics are *skyrmions*. These are critical points of a 3-dimensional field theory called the *Skyrme model*, and are intended as a model of nuclear physics. Skyrmions are in some ways rather different to instantons and monopoles. For instance, the existence of the particles that they are supposed to model is not doubted, but on the other hand, their geometry is less rich, with no moduli spaces or nice twistor constructions. In addition, the topological charges of monopoles and instantons are defined in contrasting ways to that of skyrmions. That said, the study of skyrmions mathematically is still an interesting problem in its own right [78].

There are multiple concrete mathematical and physical relationships between instantons and monopoles [45, 82], and in particular, monopoles can be thought of as *translation-invariant instantons*. Having highlighted their differences, it may come as a surprise to hear that skyrmions are also remarkably similar to instantons and monopoles. One of the most striking resemblances between these objects is observed in the *symmetric* examples, where through various sophisticated means, many examples of symmetric instantons and monopoles correlate well with the existence of corresponding symmetric skyrmions [8, 59, 111, 117]. The mathematical relationship between instantons and skyrmions was first proposed by Atiyah and Manton [8], by approximating skyrmions with instanton holonomies. This technique, and its remarkable accuracy, was later explained and fully understood by Sutcliffe [113]. Regarding monopoles and skyrmions,

one intriguing link between them is their shared relationship to rational maps [59], and there are also important physical reasons to relate skyrmions and monopoles, for example, skyrmions' role in quantum chromodynamics (QCD) may be interpreted in a similar way to monopoles' role in the standard model [127]. Nevertheless, unlike the case of instantons, so far there is no formal understanding of why monopoles and skyrmions appear to be so similar.

Calorons, also known as *periodic instantons*, are topological solitons, which have in recent years seen much interest for a variety of reasons [22, 44, 53, 71, 72, 73, 94]. One of their attributes is that they are seen to interpolate between instantons and monopoles [49, 69, 75, 107], and in particular, their understanding in terms of *constituent monopoles* [44, 72] provides a further link between monopoles and instantons. In addition, like instantons, their holonomies may be used to approximate skyrmions [36, 51, 96]. In the final chapter of this thesis, we propose and explore the possibility that the relationship between monopoles, instantons, and skyrmions – '*the soliton trinity*' – may be best understood by considering all three of their relationships with calorons. In particular, we shall reassess the relationship between calorons and skyrmions in light of the work of Sutcliffe in [113]. Importantly, far less is known in general about calorons compared to instantons and monopoles, especially regarding their symmetric examples, and so this will also be a major topic of this thesis.

The mathematical framework which describes the objects of interest, and that we shall be working in, is that of differential geometry and topology, in particular, the gauge theory of vector bundles, homotopy theory, and Chern-Weil theory. We shall assume the reader is reasonably well-versed in these subjects from the outset, nevertheless, some good references are [47, 119]. For the sake of completeness, in the next few sections we shall formalise the main underlying concepts for this thesis, and expand on what we have just discussed, and the problems to be considered, in greater detail.

1.1 Anti-self-dual connections and the Yang-Mills action

For an oriented, m-dimensional riemannian manifold (M, γ), the *Hodge-star operator* is the map

$$\star : \Lambda^p(M) \longrightarrow \Lambda^{m-p}(M), \tag{1.1}$$

defined by

$$u \wedge \star v = \langle u, v \rangle \mathrm{Vol}_\gamma, \tag{1.2}$$

where $\langle \cdot, \cdot \rangle$ is the inner-product on p-forms induced by the metric γ, and Vol_γ is the volume form on (M, γ). Consider a connection $D^A = d + A$ on a vector bundle $V \longrightarrow M$, with structure group G, so that $A \in \Lambda^1(M, \mathfrak{g})$ with $\mathfrak{g} = \mathrm{Lie}(G)$. Its curvature, defined by $F^A = dA + A \wedge A$, is a $\mathfrak{g}$-valued 2-form, and in particular, $\star F^A$ is an $(m-2)$-form. In the case that $m = 4$, it is therefore possible to ask whether F^A is self- or anti-self-dual with respect to the Hodge-star, that is

$$\star F^A = \pm F^A. \tag{1.3}$$

As a matter of convention, we shall only be interested in the equation $\star F^A = -F^A$, and such connections will be known as **anti-self-dual connections** (ASD). The *self-dual* connections can easily be obtained by reversing the orientation on M. From the outset, we shall also restrict our attention to complex vector bundles with structure group $U(N)$, that is, rank-N hermitian bundles.

ASD connections are interesting for a variety of reasons. Firstly, they naturally minimise the Yang-Mills-action

$$S_{YM} := ||F^A||^2 = -\int_M \mathrm{tr}\,(F^A \wedge \star F^A). \tag{1.4}$$

Indeed, the equations of motion are the *Yang-Mills equations* $D^A \star F^A = 0$, which are trivially satisfied by ASD connections due to the Bianchi identity $D^A F^A = 0$. This is

not only an example of how to solve a second-order PDE by using a first-order PDE, but in this particular case, the most successful attempt at minimising the Yang-Mills action has been through studying ASD connections. Another way to see why this works more directly is the following Bogomolny'i style argument: consider the identity

$$||F^A||^2 = \frac{1}{2}||F^A + \star F^A||^2 + \int_M \mathrm{tr}\,(F^A \wedge F^A). \tag{1.5}$$

Since $||\cdot||^2 \geq 0$, what (1.5) tells us is that the Yang-Mills action satisfies the inequality

$$S_{YM} \geq 8\pi^2 Q, \tag{1.6}$$

where Q is the quantity

$$Q = \frac{1}{8\pi^2}\int_M \mathrm{tr}\,(F^A \wedge F^A). \tag{1.7}$$

The real number (1.7) is known as the **topological charge** of the Yang-Mills connection. The topological significance is, admittedly, dependent on the structure of M and V, but the key importance comes from the (local) formula

$$\mathrm{tr}\,(F^A \wedge F^A) = d\mathrm{tr}\,(A \wedge dA + \frac{2}{3}A \wedge A \wedge A),$$

and so for anti-self-dual connections, the value of the action is essentially only dependent on the behaviour at the boundaries of each trivialisation of V. The bound (1.6) is saturated precisely by the ASD connections. Critical points of functionals which possess topological bounds are often given the title of *topological soliton* [82], and those configurations which attain the bound are often known as *BPS topological solitons*.

A second point of interest is found in the study of *integrable systems*. There are several examples of integrable systems which may be obtained as a dimensional reduction, or symmetry reduction, of the ASD equations. Examples include the Bogomolny equations, Nahm's equations, and the KdV equation. A relatively bold statement, known as 'Ward's conjecture', proposes that all systems of equations which may be considered in some way to be 'integrable', are obtainable as a reduction of the ASD equations (see [84] for more

details of this). Other relationships with integrable systems are observed as a result of the twistor geometric descriptions that many ASD connections possess, and is an idea that shall be remarked upon as we delve deeper into the topics of this thesis.

The final motivation that we shall discuss is the physical significance. To quantize gauge theories, one usually tries to calculate Feynman 'path integrals' where the space of 'paths' is $\mathcal{D}(M')$, the space of all connections over M', where M' is a lorentzian 4-manifold. In general, these integrals do not have a clear definition, and so a standard technique is to 'Wick rotate' M' to the riemannian M, and consider the functional integral

$$K[S] = \int_{A \in \mathcal{D}(M)} p(A) \exp\left(-S_{YM}(A)\right) d[A],$$

where $d[\cdot]$ is a suitable measure on $\mathcal{D}(M)$, and p is a polynomial. Physically K is the 'propagation function' which represents the quantum probability amplitude of the physics described by S_{YM}. A good approximation to K is the semi-classical approximation, which involves expanding the exponential around the 'classical' configurations, that is, the critical points of S_{YM} for which S_{YM} is *finite*. In particular, since ASD connections are critical points, this gives a motivation for the following definition.

Definition 1.1.1 *A (Yang-Mills)* ***instanton*** *is an ASD connection with finite Yang-Mills action.*

Remark 1.1.2 *The word 'instanton' was first coined by 't Hooft in reference to a* 1*-dimensional classical solution in the physics of the double-well potential, which appears to be localised as an instantaneous trajectory between two classically forbidden vacuum states [23, 110]. The instantons of Yang-Mills theory are intended to be* 4*-dimensional analogues of these.*

The initial breakthroughs in finding explicit examples of ASD connections were first made by Belavin, Polyakov, Schwarz, and Tyupkin [11], then later Witten [126], and Corrigan,

Fairlie, and 't Hooft [31, 57] provided some more general examples. These were also the first examples of Yang-Mills instantons, in the most simple case where the base manifold is euclidean $\mathbb{R}^4$. Instantons on $\mathbb{R}^4$ are usually what are being referred to when the word 'instanton' is used. These instantons are in fact geometrically equivalent to instantons on S^4: since the ASD equations (1.3) are conformally invariant, and $\mathbb{R}^4$ is conformally equivalent to $S^4 \setminus \{\infty\}$, every instanton on S^4 gives rise to an instanton on $\mathbb{R}^4$, and a theorem of Uhlenbeck [120] shows that the converse is also true, so that we have that every instanton on $\mathbb{R}^4$ is determined uniquely, via stereographic projection, by an instanton on S^4. By compactness of S^4, the action (1.4) is always finite, so that every anti-self-dual connection on S^4 is an instanton. Vector bundles over S^4 are topologically classified by their second Chern number $c_2(V, S^4)$, an integer which can be computed from the integral

$$c_2(V, S^4) = \frac{1}{8\pi^2} \int_{S^4} \operatorname{tr} (F^A \wedge F^A) \in \mathbb{Z}. \tag{1.8}$$

This is exactly the topological charge (1.7), which in this context is often called the **instanton charge**.

The instantons on $\mathbb{R}^4$ manifest themselves physically as the configurations which describe tunneling between quantum vacuum states. More specifically, the vacuum states of (pure) quantum chromodynamics (QCD) are characterised by an integer $n \in \mathbb{Z}$ [23], and an instanton of charge Q corresponds to a trajectory between vacuum states $|n\rangle$ and $|n+Q\rangle$. Furthermore, restricting the propagator K to K_Q, which integrates only over the spaces of instantons of charge Q, shows how instantons resolve the $U(1)$ problem in QCD [58], that is, they are an explanation of the apparent $U(1)$ symmetry in QCD that is not observed in the real world.

It is worth noting that the notion of an instanton may be generalised to higher dimension than 4, and this is particularly important in the study of M-theories. However this, along with other physical consequences, goes far beyond the scope of this thesis.

1.1.1 Gauge transformations

In general, the space $\mathcal{A}$ of all ASD connections on $V \longrightarrow M$ is quite large, but we can exploit the structure of the bundle V to our advantage. Every bundle map $\gamma : V \longrightarrow V$ induces local **gauge transformations** $g : \mathcal{U} \longrightarrow U(N)$ for $\mathcal{U} \subset M$ open, defined by the restriction to each trivialisation:

$$\begin{array}{rccc} \gamma_{\mathcal{U}} : & \mathcal{U} \times \mathbb{C}^N & \longrightarrow & \mathcal{U} \times \mathbb{C}^N \\ & (x, v) & \mapsto & (x, g(x)v), \end{array}$$

for $x \in \mathcal{U}$, $v \in \mathbb{C}^N$. These form a group $\mathcal{G}$ called the **gauge group**, which acts on connections via

$$A \mapsto gAg^{-1} - dgg^{-1}. \tag{1.9}$$

Under this action, the curvature transforms as $F^A \mapsto gF^Ag^{-1}$, and so it is straightforward to see that the Yang-Mills action (1.4), and charge (1.7) are invariant under these automorphisms of the bundle V. This *gauge invariance* motivates the consideration of the orbit space $\mathcal{M} = \mathcal{A}/\mathcal{G}$ as the true physical space which these objects occupy. $\mathcal{M}$ is called the **moduli space of ASD connections**

1.2 The soliton trinity

Instantons are seen to be topological solitons in four dimensions, and are arguably the only special types of field configurations within this many dimensions. Moving down to three dimensions, there are two major players in the topological soliton scene: monopoles and skyrmions [82]. Both of these solitons have well-established relationships with instantons.

First, monopoles. Let (X, η) be an orientable riemannian 3-manifold, and $W \longrightarrow X$ be a vector bundle over X, which we shall for simplicity take to be trivial, rank N, and hermitian. Let $D^{\widetilde{A}}$ be a connection on W, with curvature $F^{\widetilde{A}}$ and consider also a section

$\Phi \in \Gamma(\mathrm{End}(W))$. With respect to a global trivialisation of W, Φ is simply given by a map $\Phi : X \longrightarrow \mathfrak{u}(N)$. Define a 4-manifold (M, γ) from (X, η) by setting $M = \mathbb{R} \times X$, and $\gamma = dt^2 + \eta$, where t is a coordinate on $\mathbb{R}$. Additionally, we may define a vector bundle $V \longrightarrow M$ as the pull-back $V = p^*W$, where $p : M \longrightarrow X$ is the obvious projection, and a connection D^A on V via $A = \widetilde{A} + \Phi dt$.

It is straightforward to see that the connection D^A is anti-self-dual ($\star_\gamma F^A = -F^A$) if and only if $(\widetilde{A}, \Phi)$ satisfies the **Bogomolny equation**[1]

$$\star_\eta D^{\widetilde{A}} \Phi = -F^{\widetilde{A}}, \tag{1.10}$$

furthermore, its Yang-Mills action is given by

$$S_{YM} = \int_{\mathbb{R}} E_{YMH} dt, \tag{1.11}$$

where E_{YMH} is the Yang-Mills-Higgs energy

$$E_{YMH} := ||F^{\widetilde{A}}||^2 + ||D^{\widetilde{A}}\Phi||^2 = -\int_X \mathrm{tr}\left(F^{\widetilde{A}} \wedge \star F^{\widetilde{A}} + D^{\widetilde{A}}\Phi \wedge \star D^{\widetilde{A}}\Phi\right). \tag{1.12}$$

In short, a **monopole** on X is such a pair $(\widetilde{A}, \Phi)$ satisfying the Bogomolny equation (1.10) for which the Yang-Mills-Higgs energy (1.12) is finite. According to the description above, monopoles may be thought of as *translation-invariant instantons*, where the condition of finite action is replaced by the condition of finite energy. The most common monopoles studied are those where $X = \mathbb{R}^3$, and in general are subject to rather strict boundary conditions, which we shall describe later on in chapter 2.

Similarly to the identity (1.5), the Yang-Mills-Higgs energy (1.12) satisfies

$$||F^{\widetilde{A}}||^2 + ||D^{\widetilde{A}}\Phi||^2 = ||F^{\widetilde{A}} + \star_\eta D^{\widetilde{A}}\Phi||^2 + 2\int_X \mathrm{tr}\,(F^{\widetilde{A}} \wedge D^{\widetilde{A}}\Phi), \tag{1.13}$$

so that we have the energy bound

$$E_{YMH} \geq 2\int_X \mathrm{tr}\,(F^{\widetilde{A}} \wedge D^{\widetilde{A}}\Phi), \tag{1.14}$$

[1] Strictly speaking, this depends on a choice of orientation, and so (1.10) is equivalent to (1.3) within this formalism up to a change of sign.

with equality when $(\widetilde{A}, \Phi)$ satisfy the Bogomolny equation (1.10). This integral in (1.14) is also topological, and in the case of $X = \mathbb{R}^3$, and $N = 2$, is precisely $4m\pi$, where $m \in \mathbb{Z}$ is the *monopole charge* revealed by the boundary data for such a monopole. For this reason, monopoles, like instantons, are known as BPS solitons.

Second, skyrmions. Consider an instanton D^A on $V \longrightarrow M = \mathbb{R}^4$. With respect to a global trivialisation of V, D^A is determined by the connection 1-form $A = \sum_{\mu=0}^{3} A_\mu dx^\mu$, where $A_\mu : \mathbb{R}^4 \longrightarrow \mathfrak{u}(N)$ are the components of A, and x^μ are the standard coordinates on $\mathbb{R}^4$, for $\mu = 0, \ldots, 3$. Let $\Omega : \mathbb{R}^4 \longrightarrow U(N)$ be the solution to the equation

$$\partial_0 \Omega + A_0 \Omega = 0 \tag{1.15}$$

with the boundary condition $\lim_{x^0 \longrightarrow -\infty} \Omega = \mathbb{1}$. The function Ω is well-known to differential geometers as the *parallel transport operator* of D^A along all lines in the x^0-direction. This gives rise to a function $U : \mathbb{R}^3 \longrightarrow U(N)$ defined by $U = \lim_{x^0 \longrightarrow \infty} \Omega$, called the *holonomy*. The instanton is classified by an integer k, namely the second Chern number of the associated bundle over S^4. The constructed function $U : \mathbb{R}^3 \longrightarrow U(N)$ satisfies the boundary condition $U \longrightarrow \mathbb{1}$ as $|\vec{x}| \longrightarrow \infty$, so it descends to a map $U' : S^3 \longrightarrow U(N)$. Such maps are classified too by an integer, given by $\pi_3(U(N)) \cong \mathbb{Z}$, and moreover, from this construction, this integer is precisely the instanton charge k.

The most applicable case of these holonomies is when $N = 2$, and V has structure $SU(2)$. In 1989, Atiyah and Manton [8] proposed interpreting these functions $U : \mathbb{R}^3 \longrightarrow SU(2)$ as candidates for **Skyrme fields**. An $SU(2)$ **skyrmion** is a map $U : \mathbb{R}^3 \longrightarrow SU(2)$ satisfying $U \longrightarrow \mathbb{1}$ as $|\vec{x}| \longrightarrow \infty$, which is a global minimum of the *Skyrme energy functional*:

$$E_S := ||U^{-1}dU||^2 + ||U^{-1}dU \wedge U^{-1}dU||^2. \tag{1.16}$$

The extrema of (1.16) are the solutions to the *Skyrme field equation*

$$\sum_{i,j} \partial_i \left(U^{-1}\partial_i U + \left[U^{-1}\partial_j U, [U^{-1}\partial_i U, U^{-1}\partial_j U] \right] \right) = 0. \tag{1.17}$$

Unlike the exact relationship that we see between monopoles and instantons, this construction sadly does not produce exact solutions to (1.17), but is merely an approximation. Nevertheless, this approximation has proven to be remarkably good in comparison to known results for skyrmions. A formal understanding of this relationship was later provided by Sutcliffe [113] by employing a 'mode expansion' of the gauge field, and we shall expand more on this relationship in chapter 4.

The topological degree of the map $U : \mathbb{R}^3 \longrightarrow SU(2)$ is often denoted by $\mathcal{B}$, and is physically interpreted as the *baryon number*. This has the standard integral formula

$$\mathcal{B} = \frac{1}{24\pi^2} \int_{\mathbb{R}^3} \text{tr} \left(U^{-1}dU \wedge U^{-1}dU \wedge U^{-1}dU \right). \tag{1.18}$$

There is also a topological energy bound for (1.16), originally due to Faddeev [39], which we shall demonstrate in a different manner here. Using the identity

$$E_S = ||dU \wedge dU^{-1} \mp \star dUU^{-1}||^2 \pm 2 \int_{\mathbb{R}^3} \text{tr} \left(U^{-1}dU \wedge U^{-1}dU \wedge U^{-1}dU \right), \tag{1.19}$$

we straightforwardly see that the Skyrme energy satisfies the bound

$$E_S \geq 48\pi^2 |\mathcal{B}|. \tag{1.20}$$

The bound (1.20) is only attained when

$$dU \wedge dU^{-1} = \pm \star dUU^{-1}. \tag{1.21}$$

Equation (1.21) is equivalent to saying that the right-invariant Maurer-Cartan current corresponding to U, defined by $R = dUU^{-1}$ satisfies the equation

$$\star R = \mp dR. \tag{1.22}$$

To understand this equation, consider the Skyrme-field $U : \mathbb{R}^3 \longrightarrow SU(2)$ in components, that is

$$U(\vec{x}) = \phi^0(\vec{x})\mathbb{1} + \imath\vec{\phi}(\vec{x}) \cdot \vec{\sigma},$$

where $\sigma^1, \sigma^2, \sigma^3$ are the Pauli matrices, and $\phi = (\phi^0, \phi^1, \phi^2, \phi^3) : \mathbb{R}^3 \longrightarrow S^3$. Now let η_{S^3} denote the metric on S^3. Then equation (1.22) is equivalent to saying that the *strain tensor* $\phi^* \eta_{S^3}$ has all eigenvalues equal to 1.[2] In other words $\phi : \mathbb{R}^3 \longrightarrow S^3$ is an isometry. But this is impossible since $\mathbb{R}^3$ is not isometric to S^3. Therefore, unlike the case of monopoles and instantons, the Skyrme model is not BPS.

Despite not being a BPS theory, studying the Skyrme model is still an interesting physical and mathematical problem. Physically, skyrmions are supposed to model atomic nuclei, and there are many interesting variational questions regarding the functional (1.16), which is a simple generalisation of the Dirichlet energy whose critical points are the famous harmonic maps. For instance: is there a smooth map $U : \mathbb{R}^3 \longrightarrow SU(2)$ within each homotopy class which minimises E_S? Can E_S be thought of as some sort of Morse function?

As we have discussed, there is a precise understanding of the links between instantons and monopoles, and instantons and skyrmions. For quite some time, there have also been striking observations of links between monopoles and skyrmions, besides the indirect link via instantons on $\mathbb{R}^4$. One example is the rational map ansatz [59]. This is another way of approximating Skyrme fields by considering rational maps $P : S^2 \longrightarrow S^2$, under the novel consideration of identifying the domain of the rational map as concentric spheres in $\mathbb{R}^3$, and the target as spheres of constant latitude in S^3, i.e. a map $\mathbb{R}^3 \longrightarrow S^3$, which is a candidate for a Skyrme field. Besides the many attractive qualities for analysis of the Skyrme energy functional (1.16) within this formalism, the main motivation for this consideration belongs to trying to view monopoles and skyrmions in the same light. Indeed, the moduli space of $SU(2)$ monopoles has important relationships to rational maps $R : S^2 \longrightarrow S^2$, which we shall not delve into here (but for further details see [33, 67, 68]). The point is, every rational map gives rise to a monopole, and it would seem that they also give rise to (approximate) skyrmions, with many valuable applications

[2] See [78].

[79]. There are several other striking resemblances between monopoles and skyrmions, which all fall under the category of 'symmetric solitons', and we shall discuss this in the following section. These similarities between monopoles and skyrmions have not so far been understood in any precise way, but we suspect a more concrete relationship exists.

1.2.1 The role of symmetry

A very common technique in studying variational problems is to hunt for 'symmetric solutions', that is, critical points which are invariant under the action of some group of diffeomorphisms. This is useful for several reasons. Firstly, imposing a symmetric form invariably reduces the difficultly of solving the underlying equations, for example, in a 3-dimensional problem, asking for spherical-symmetry, that is, the fields only depend on their radial component, reduces what was a PDE, into an ODE. This simplification of the defining equations makes explicit construction more realistic. Secondly, there are geometric reasons for studying symmetric solutions. In the cases where the space of solutions is a riemannian manifold, and the group acts by isometries, then it is well-known that the fixed-point sets are totally geodesic riemannian submanifolds, and so information about the geodesic flow in the space of all solutions can be obtained from studying symmetric examples. This may be exploited for the purposes of understanding dynamics – Manton argues in [77], specifically in the context of monopoles, that the geodesic flow on the moduli space is the low-energy approximation to the true dynamics of the solitons. This idea has been rigorously formulated, and validated under certain restrictions, by Stuart in [112]. A third advantage is somewhat philosophical, but has its basis in physical reasoning, namely, that the important solutions to a variational problem are those which possess some degree of symmetry. Indeed, many natural phenomena exhibit high levels of symmetry, for example the spherical formation of soap bubbles, and many simple variational problems are solved by highly symmetric configurations, for example, the closed planar curve of some given length with maximal enclosed area is the

circle. Moreover, the existence of certain symmetries is somewhat axiomatic in theoretical physics [28]. Additionally, the observed symmetric 'shape' of nuclei is one of the many reasons for studying symmetric skyrmions, which are supposed to model nuclear physics, and is an important consideration for quantization.

Remark 1.2.1 *The construction of symmetric solutions is dependent on the applicability of the principle of symmetric criticality [99], which states that the symmetric critical points are precisely the critical symmetric points, that is, the critical points of the symmetrically reduced field theory. This principle does not hold in full generality, however it is true for all of the relevant examples that we have discussed.*

The existence of symmetric instantons, monopoles, and skyrmions, has been fundamental in advancing the field, with a plethora of examples available to study [3, 10, 13, 14, 43, 55, 60, 61, 62, 83, 95, 104, 111, 116, 117, 123]. In fact, the first example of a monopole on $\mathbb{R}^3$ was the Prasad-Sommerfield solution [105] to (1.10), which takes the $O(3)$-symmetric form

$$\begin{aligned}\Phi &= -f(r)\frac{\vec{x}\cdot\vec{\sigma}}{r},\\ A &= \frac{\imath}{2}\left(g(r)-1\right)\frac{\vec{x}\times\vec{\sigma}}{r^2}\cdot d\vec{x},\end{aligned}$$

where $r = |\vec{x}|$, $\vec{\sigma}$ is the vector of Pauli matrices, and $f, g : (0,\infty) \longrightarrow \mathbb{R}$ are given by[3]

$$\begin{aligned}f(r) &= \coth 2r - \frac{1}{2r},\\ g(r) &= \frac{2r}{\sinh 2r}.\end{aligned}$$

Sadly, most of the symmetric examples do not provide us with analytic formulae like this monopole solution, and in the case of skyrmions, only numerical methods have been successful. However, the trade-off is that almost all of the cases (at least for instantons and monopoles) make use of the various 'twistor' construction techniques, highlighting not

[3] Up to some choice of length scale, which we have here set equal to 1.

only their importance in understanding the objects' geometric structure, but also in finding 'explicit' examples, which can then be constructed numerically from the associated data. In figures 1.1-1.2, we show plots of the charge densities of symmetric monopoles and skyrmions respectively, which are all constructed from numerical solutions.[4]

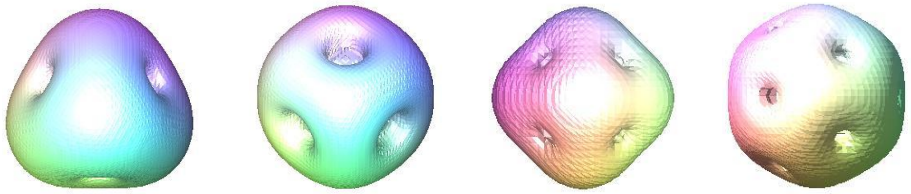

Figure 1.1: The abelian charge density isosurfaces of monopoles with platonic symmetries. These monopoles have charges $3, 4, 5$, and 7 respectively. Images courtesy of Derek Harland.

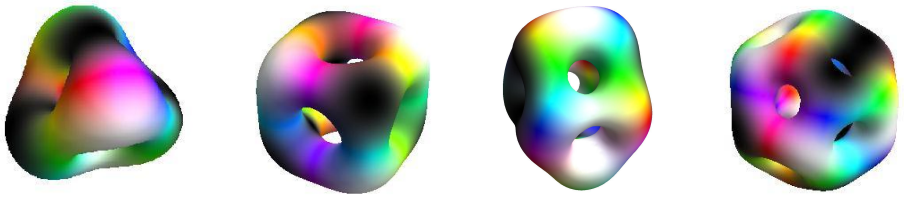

Figure 1.2: The charge density isosurfaces of low charge skyrmions, taking the form of polyhedral 'shell-like' structures. These skyrmions have baryon numbers $3, 4, 5$, and 7 respectively. Images courtesy of Chris Halcrow, and colouring scheme coded by Dankrad Feist, explained in [40].

It doesn't take much imagination to notice that there are some striking resemblances between some of these monopoles and skyrmions. Indeed, in the cases $\mathcal{B} = 3, 4$, and 7, the symmetric skyrmions have precisely the same symmetries as the $m = 3, 4$, and 7 monopoles respectively! Similarly, although not shown in pictures, the charge 1 and 2 monopoles and skyrmions also share the same symmetries, namely spherical, and

[4]Many thanks go to Derek Harland and Chris Halcrow for providing me with these images.

toroidal. It seems unlikely that such similarities would be only coincidental. These relationships with the symmetries are somewhat explained by the rational map ansatz [59]. More precisely, there is a unique (up to a choice of orientation) degree 3 rational map $P : S^2 \longrightarrow S^2$ with tetrahedral symmetry,[5] namely

$$P(z) = \frac{\sqrt{3}\imath z^2 - 1}{z^3 - \sqrt{3}\imath z}, \tag{1.23}$$

also a degree 4 rational map with cubic symmetry:

$$P(z) = \frac{z^4 + 2\sqrt{3}\imath z^2 + 1}{z^4 - 2\sqrt{3}\imath z^2 + 1}, \tag{1.24}$$

and a degree 7 rational map with dodecahedral symmetry:

$$P(z) = \frac{z^5 - 3}{3z^7 + z^2}. \tag{1.25}$$

By a theorem of Jarvis [67, 68], these define the tetrahedral, cubic, and dodecahedral monopoles of charges $3, 4$, and 7 respectively, and via the rational map ansatz, go some way towards explaining why the $\mathcal{B} = 3$, $\mathcal{B} = 4$, and $\mathcal{B} = 7$ skyrmions have those symmetries also. However, there are counter-examples to this apparent sequence of symmetric solitons. For example, the $\mathcal{B} = 5$ skyrmion does not seem to exhibit much symmetry at all other than an order 2 dihedral symmetry [82]. On the contrary, there is, as seen in figure 1.1, and in [60], a charge 5 monopole with octahedral symmetry. Thus, the verdict over whether there is a direct link between skyrmions and monopoles is still undecided.

These links that we have discussed between instantons, monopoles, and skyrmions, are summarised in figure 1.3. The dashed line between monopoles and skyrmions highlights the gaps in understanding, but with a respect for the fact that there are many convincing reasons to expect a concrete link to exist.

[5] The group $SO(3)$ acts on the space of rational maps by pull-back of an $SU(2)$ Möbius transformation.

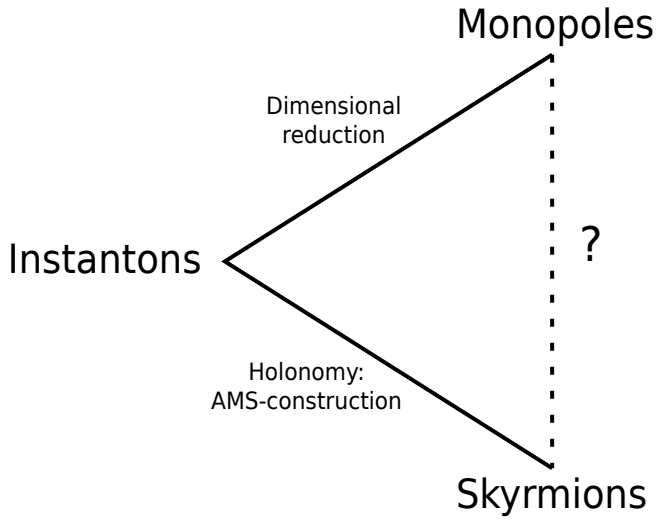

Figure 1.3: The triangle of ideas relating the 'soliton trinity'.

1.2.2 The role of calorons

Very loosely, calorons are instantons on $S^1 \times \mathbb{R}^3$, and we study them at great depth in chapter 2. An important feature of calorons is how they relate to instantons on $\mathbb{R}^4$ and monopoles on $\mathbb{R}^3$. Specifically, calorons can be viewed as 'loops of monopoles' [44], calorons are embedded in the space of instantons [22, 32], and in particular, they are seen to interpolate between these two solitons in certain limiting cases [49, 75, 107, 122]. Due to the kinship between monopoles and calorons, any link between calorons and skyrmions may be able to provide an understanding for the apparent links between monopoles and skyrmions. Our idea is to consider the Atiyah-Manton-Sutcliffe construction of Skyrme fields from instantons in the context of calorons, and to study the Skyrme fields generated within the knowledge of this interpolation between instantons and monopoles. In summary, the proposition is that the diagram of the soliton trinity in figure 1.3 may be better understood by introducing calorons, and considering instead the diagram in figure

1.4. All of these ideas are to be explored in more detail in chapter 4.

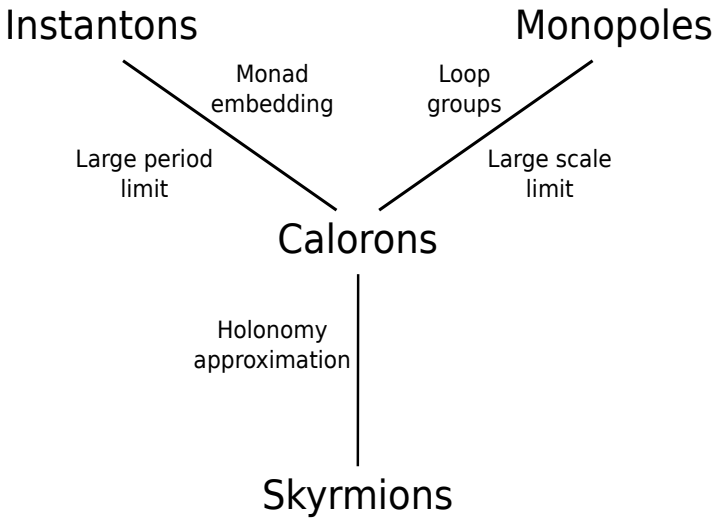

Figure 1.4: The soliton trinity from the perspective of calorons.

Remark 1.2.2 *It is worth mentioning that some work, beyond the study of the rational map ansatz, to compare monopoles and skyrmions was done in [48, 101] by adding a 'Skyrme term' to the usual Yang-Mills-Higgs energy. In contrast, our approach in chapter 4 does not make any modifications to the underlying theories.*

1.3 Overview of thesis

Besides this introductory chapter, this thesis is separated into three main chapters which cover the topics of 'calorons, symmetry, and the soliton trinity'.

In chapter 2, we formalise the notion of what a caloron is, with a precise overview of their definitions and boundary conditions. We then cover some brief examples, and discuss some important properties of the geometry of their moduli spaces, including a correspondence called *the rotation map*, which we will use later on when discussing

symmetries. We also review their relationships to instantons on $\mathbb{R}^4$, and monopoles on $\mathbb{R}^3$. We conclude this chapter with a review of the various related data to calorons. Specifically, we describe the famous *Nahm transform* in the context of calorons, and also a set of matrix data called *monad matrices*. This matrix data and its relationship to calorons was first understood by Charbonneau and Hurtubise [22] in the case of $SU(2)$ calorons, and we generalise it to a special case of $SU(N)$ calorons (those with all magnetic charges equal to zero).

Chapter 3 is devoted to *symmetric calorons*. Firstly, we introduce the isometries on the moduli space of calorons, and how they act on the associated Nahm and monad matrix data. We follow this by proving some necessary conditions for the existence of invariant solutions. The main results of this chapter are within the discussion of *cyclic calorons*, that is, calorons invariant under the action of various cyclic groups. Here we show the existence of charge k, $SU(N)$ calorons, which are invariant under the action of cyclic groups of order Nk, by utilising both the monad matrix data, and a special isometry of the moduli space, which is the rotation map. We conclude the chapter with a discussion of, and an explicit construction of, the corresponding cyclic Nahm data for some low charge cases.

In the final chapter, chapter 4, we study the relationship between calorons and skyrmions alluded to in figure 1.4, by reassessing the holonomy approximation in light of Sutcliffe's work in [113]. As we shall see, calorons provide a natural way to incorporate a gauge field into the Skyrme model, and hence may be considered as good approximations to *gauged skyrmions*. In particular, by expanding the caloron in terms of the *ultra-spherical functions*, we may derive a one-parameter family of gauged Skyrme models, which we show to reduce to the ordinary Skyrme model in a particular limit. The bulk of this chapter is then concentrated on numerically studying the most simple examples – those with spherical symmetry, and how they relate to calorons and monopoles. The main conclusion is that the gauged skyrmions appear to exhibit the same interpolation

between ‘instanton-like’ solutions, and ‘monopole-like’ solutions, which is a property of calorons. We conclude this chapter by relating these gauged skyrmions, and their caloron approximations, to skyrmions in the ordinary Skyrme model.

Chapter 2

Calorons

The main objects of study in this thesis are calorons. Loosely speaking, calorons are periodic instantons, that is finite-action, anti-self-dual connections on $S^1 \times \mathbb{R}^3$. Their name is due to their physical interpretation, which is instantons at 'finite temperature'[1], where, according to the Matsubara formalism, the euclidean time is seen to be periodic. Calorons are arguably more relevant physically than both instantons[2] and monopoles [2, 46, 65, 72, 121].

Unlike in the case of S^4, in general, an ASD connection on $S^1 \times \mathbb{R}^3$ will not have finite action, and so boundary conditions need to be carefully defined to allow for this. To simplify things, we shall restrict our attention to the case of $SU(N)$ calorons, for $N \geq 2$, which means that the vector bundle V is a trivial, rank N hermitian bundle, equipped with a parallel volume form. The boundary conditions we shall describe for these calorons were first formulated by Nye [97], and recent work by Cherkis and colleagues on Taub-NUT instantons [27] suggests that they are in fact equivalent to the condition of finite action.

[1] That is, non-zero.

[2] That is, instantons on $\mathbb{R}^4$.

2.1 Boundary conditions

For the purpose of having well-defined boundary conditions, we shall compactify $\mathbb{R}^3$ by thinking of it as the interior of the closed ball B^3, then calorons will be defined on all of $S^1 \times B^3$, with conditions on $S^1 \times \partial B^3$. We will always denote the boundary as the 2-*sphere at infinity*, that is $\partial B^3 \cong S^2_\infty$. In order to understand the boundary conditions, we first need to develop a conceptual framework.

Definition 2.1.1 *Let M be a manifold, and $M' \subset M$ be a submanifold. Let $V \longrightarrow M$ be a vector bundle of rank r and let V' denote its restriction to M'. A **framing** for V over M' is a bundle isomorphism*

$$f : V' \longrightarrow W',$$

*where W' is a trivial, rank r bundle over M'. A **framed vector bundle** is a pair (V, f). (V, f) is said to be **framed by** W'.*

Consider the circle S^1 of radius $1/\mu_0$, for some $\mu_0 > 0$, as the quotient $S^1 \cong \mathbb{R} \Big/ \frac{2\pi}{\mu_0}\mathbb{Z}$. We denote coordinates on $S^1 \times \mathbb{R}^3$ by (t, x^1, x^2, x^3), and equip it with the euclidean metric induced from $\mathbb{R}^4$. Let V and W be trivial, rank N hermitian vector bundles over $S^1 \times B^3$, and B^3 respectively, each equipped with a parallel volume form. We denote by V_∞ and W_∞ their restrictions to $S^1 \times S^2_\infty$ and S^2_∞ respectively in each case. We introduce the framing for V over $S^1 \times S^2_\infty$

$$\begin{array}{rccc} f: & V_\infty & \longrightarrow & p_\infty^* W_\infty, \\ & (t,x,v) & \mapsto & (t,x,\varphi(t,x)v) \end{array}, \tag{2.1}$$

where $p_\infty : S^1 \times S^2_\infty \longrightarrow S^2_\infty$ is the projection, and $\varphi : \mathbb{R} \times S^2_\infty \longrightarrow SU(N)$ satisfies

$$\varphi(t,x) = \varphi(t + 2\pi/\mu_0, x), \quad \forall\, t \in \mathbb{R},\ x \in S^2_\infty.$$

We are interested in the behaviour of the caloron connection 1-form A on the restriction to $S^1 \times S^2_\infty$, and so via the framing (2.1), this depends on the properties of the bundle W_∞, which we shall now prescribe.

Let W_∞ decompose into line bundles[3]

$$W_\infty = \mathcal{O}(k_1) \oplus \cdots \oplus \mathcal{O}(k_N), \tag{2.2}$$

where k_p are integers which sum to 0. We also equip W_∞ with a connection 1-form a_∞, which we impose to be diagonal with respect to the splitting (2.2). Specifically,

$$a_\infty = \sum_{p=1}^{N} a_p,$$

where a_p is the unique connection 1-form on $\mathcal{O}(k_p)$ with curvature $da_p = \frac{k_p}{2}\imath\Omega$, where here Ω denotes the volume form on S^2_∞ with the round metric. In addition to the connection a_∞, we consider a section $\Phi_\infty \in \Gamma(\mathrm{End}(W_\infty))$ whose eigenbundles are $\mathcal{O}(k_p)$, that is, there exist $\mu_p \in \mathbb{R}$ satisfying

$$\Phi_\infty s_p = \imath\mu_p s_p, \quad \forall\, s_p \in \Gamma\left(\mathcal{O}(k_p)\right).$$

Note that we have $d\Phi_\infty + [a_\infty, \Phi_\infty] = 0$. We will order the splitting (2.2) so that the eigenvalues satisfy $\mu_N \leq \cdots \leq \mu_1$. Since the structure group is $SU(N)$, we also have $\sum_{p=1}^{N} \mu_p = 0$. In general, we shall consider the eigenvalues to be distinct for the purposes of construction. This choice is known as the condition of *maximal symmetry breaking*. Finally, for further purposes of construction, and later interest, we shall restrict ourselves to the situation where these numbers satisfy

$$\mu_0 - (\mu_1 - \mu_N) \geq 0. \tag{2.3}$$

These definitions are consistent with that of Nye [97], and we are now in a position to define what a caloron is.

Definition 2.1.2 *Let (V, f) be a trivial, rank N, framed, hermitian bundle over $S^1 \times B^3$, framed by $p^*_\infty W_\infty$ on $S^1 \times S^2_\infty$. A connection D^A on V is said to be an $SU(N)$-**caloron***

[3] We remark that such a decomposition is a general feature of holomorphic vector bundles over $S^2_\infty \cong \mathbb{C}P^1$ by the Birkhoff-Grothendieck theorem [56].

configuration *if it is anti-self-dual, and*

$$(f^{-1})^* \, A|_{S^1 \times S^2_\infty} = (\Phi_\infty \circ p_\infty) dt + p_\infty^* a_\infty. \tag{2.4}$$

Here $p_\infty : S^1 \times S^2_\infty \longrightarrow S^2_\infty$ is the projection, and W_∞, a_∞, and Φ_∞ are defined as above.

2.1.1 Topological charges and constituent monopoles

Associated to a caloron are a set of numbers which are determined by the boundary conditions we have just described, and are the main classifying data for calorons. These are a tuple

$$(\vec{m}, \vec{\nu}) \equiv (m_1, \ldots, m_N, \nu_1, \ldots, \nu_N), \tag{2.5}$$

where $m_p \in \mathbb{N}$ and $\nu_p \in [0, \mu_0]$ such that $\sum_p \nu_p = \mu_0$. The numbers ν_p are called the **monopole masses** of the caloron, and are formed from the eigenvalues $\imath\mu_p$ of Φ_∞ via

$$\begin{aligned} \nu_p = \mu_p - \mu_{p+1}, \quad p = 1, \ldots, N-1, \\ \nu_N = \mu_0 + \mu_N - \mu_1. \end{aligned} \tag{2.6}$$

Note that the condition of *maximal symmetry breaking* is equivalent to saying that $\nu_p \neq 0$ for all $p = 1, \ldots, N$. The integers m_p are topological quantities known as the **monopole charges**, and are defined in terms of $N+1$ related integers called the **magnetic charges** and **instanton number** of the caloron. The **magnetic charges** $k_1, \ldots, k_N$ are the first Chern numbers of the line bundles in the splitting (2.2). The **instanton number**, which we denote by k_0, may be interpreted as a 'relative second Chern number' of the bundle (V, f). More explicitly, recall that the framing for V (2.1) is determined by a function

$$\varphi : \mathbb{R} \Big/ \tfrac{2\pi}{\mu_0}\mathbb{Z} \times S^2_\infty \longrightarrow SU(N).$$

For fixed $t \in \mathbb{R}$, this determines a function $\varphi_t : S^2_\infty \longrightarrow SU(N)$, which represents an element of $\pi_2(SU(N))$. This is a trivial group, so the homotopy extension theorem says

we may extend the framing via homotopy to a function defined on the interior of B^3:

$$\begin{array}{rccc} F_t: & V|_{\{t\}\times B^3} & \longrightarrow & p^*W \\ & (t,x,v) & \mapsto & (t,x,\Psi_t(x)v), \end{array} \tag{2.7}$$

where $p : \{t\} \times B^3 \longrightarrow B^3$ is the projection, and $\Psi_t : B^3 \longrightarrow SU(N)$ satisfies the boundary condition

$$\Psi_t(z) = \varphi(t,z), \quad \forall\, z \in S^2_\infty,$$

but is not necessarily periodic on the interior of $S^1 \times B^3$. Let $\epsilon > 0$. The maps F_t, for all $t \in (-\epsilon, \epsilon + 2\pi/\mu_0)$, define a continuous one-parameter family, and we interpolate between them via the *clutching functions*

$$\kappa_t(x) := \Psi_{t+2\pi/\mu_0}(x)\Psi_t(x)^{-1}. \tag{2.8}$$

For each t, $\kappa_t : B^3 \longrightarrow SU(N)$ gives an automorphism of W, and one can easily check that $\kappa_t|_{S^2_\infty}$ is the identity, so κ_t descends to a map $\kappa_t : S^3 \longrightarrow SU(N)$ by one-point compactification of $\mathbb{R}^3$. The clutching functions are clearly homotopic for each t, and represent an element of $\pi_3(SU(N)) \cong \mathbb{Z}$. The integer representative of these maps is precisely the instanton number k_0.

Finally, in order to define the monopole charges m_p, we must impose that

$$\sum_{q=0}^{p} k_q \geq 0, \quad \forall\, p = 1, \ldots, N. \tag{2.9}$$

Then, the monopole charges are determined as

$$m_p = \sum_{q=0}^{p} k_q. \tag{2.10}$$

Remark 2.1.3 *The choice to describe calorons in terms of the monopole charges and masses $(\vec{m}, \vec{\nu})$ is quite clearly equivalent to describing them in terms of the data $(k_0, k_1, \ldots, k_N, \mu_0, \mu_1, \ldots, \mu_N)$, but is the convention which makes a lot of later discussion neater and more transparent.*

An $SU(N)$-caloron is thought of as having N constituent monopoles, each with charges and masses (m_p, ν_p). This notion is formalised in terms of *the loop group* point of view, discussed in section 2.3.2. In general, a caloron with boundary data $(\vec{m}, \vec{\nu})$ will be known as a $\vec{m}$**-caloron**, with monopole masses $\vec{\nu}$. From the boundary data, we may extract another important topological quantity – the caloron charge. This is given by the Yang-Mills charge (1.7), which is computed in this context by the integral

$$Q = \frac{1}{8\pi^2} \int_{S^1 \times \mathbb{R}^3} \mathrm{tr}\,(F^A \wedge F^A). \tag{2.11}$$

It is possible to show (for example in [97]) that the charge is expressed neatly in terms of the monopole masses and charges as

$$Q = \frac{1}{\mu_0} \sum_{p=1}^{N} m_p \nu_p. \tag{2.12}$$

Another characteristic quantity for a caloron is the **holonomy** $U : \mathbb{R}^3 \longrightarrow SU(N)$ around the circle, also known as the *Polyakov loop*. This is given in terms of the solution

$$\Omega : [0, 2\pi/\mu_0] \times \mathbb{R}^3 \longrightarrow SU(N)$$

to the parallel transport equation

$$\partial_t \Omega + A_t \Omega = 0,$$

formally written as the path-ordered exponential

$$U(\vec{x}) := \Omega\left(\frac{2\pi}{\mu_0}, \vec{x}\right) = \mathcal{P} \exp\left(-\int_{S^1} A_t(s, \vec{x}) dt\right). \tag{2.13}$$

Here $\mathcal{P}$ in (2.13) denotes the 'path-ordering' [47] of the factors of A_t with respect to the loop

$$\begin{array}{rccc} \gamma_{\vec{x}} : & [0, 2\pi/\mu_0] & \longrightarrow & S^1 \times \mathbb{R}^3 \\ & t & \mapsto & (t, \vec{x}). \end{array}$$

Information regarding the boundary data may be extracted from the holonomy. For example, when the magnetic charges satisfy $k_p = 0$ for all $p = 1, \ldots, N$, $U(\vec{x})$ is globally

constant on S^2_∞, so it descends to a map $U' : S^3 \longrightarrow SU(N)$, representing an element of $\pi_3(SU(N)) \cong \mathbb{Z}$. This is homotopic to the clutching maps defined in (2.8), and hence its 'degree' is the instanton number k_0. Another important idea is that of *trivial holonomy*.

Definition 2.1.4 *An $SU(N)$-caloron caloron is said to have **trivial holonomy** if $U(\infty) := \lim_{r\longrightarrow\infty} U(\vec{x})$ belongs to the centre of $SU(N)$.*

The situation of trivial holonomy is a condition on the eigenvalues μ_p, and is simple to characterise in the case of $N = 2$. In this case the eigenvalues satisfy $\mu_1 = -\mu_2 \equiv \mu$, and trivial holonomy is equivalent to $\mu = 0$ or $\mu = \mu_0/2$.

2.2 Examples

In this section, we shall present and discuss some simple examples of $SU(N)$-calorons which appear in the literature.

2.2.1 Harrington-Shepard calorons

The first examples of calorons were $SU(2)$-calorons, written down explicitly by Harrington and Shepard [52], utilising the Corrigan-Fairlie-'t Hooft ansatz for instantons:

$$A_\mu = \frac{\imath}{2}\eta_{\mu\nu}\partial_\nu \log\phi, \tag{2.14}$$

where $\phi : S^1 \times \mathbb{R}^3 \longrightarrow \mathbb{R}$, and $\eta_{\mu\nu}$ is the self-dual 't Hooft tensor, defined by

$$\eta_{\mu\nu} = \begin{cases} \sigma^j, & \mu = j,\ \nu = 0,\ j = 1,2,3, \\ -\sigma^j, & \mu = 0,\ \nu = j,\ j = 1,2,3, \\ \epsilon_{jkl}\sigma^l, & \mu = j,\ \nu = k,\ j,k = 1,2,3. \end{cases} \tag{2.15}$$

It is straightforward to show that the ASD equations for (2.14) are equivalent to the Laplace equation $\partial_\mu \partial^\mu \phi = 0$. The Harrington-Shepard solution for calorons is given by the general harmonic function on $S^1 \times \mathbb{R}^3$:

$$\phi = 1 + \sum_{j=1}^{k} \frac{\lambda_j^2}{2r_j} \frac{\sinh(\mu_0 r_j)}{\cosh(\mu_0 r_j) - \cos(\mu_0(t - \theta_j))}, \tag{2.16}$$

where $\lambda_j > 0$, and $r_j = |\vec{x} - \vec{a}_j|$, for some different points $\vec{a}_j \in \mathbb{R}^3$, and $\theta_j \in S^1$. It is possible to show that this gauge field defines a (k, k)-caloron with monopole masses $(0, \mu_0)$, that is, one with trivial holonomy. These are often interpreted as k $(1, 1)$-calorons, with centres $(\theta_j, a_j) \in S^1 \times \mathbb{R}^3$, and 'scales' $\lambda_j > 0$.

2.2.2 Monopoles

Recall that monopoles on $\mathbb{R}^3$ are a pair $(\widetilde{A}, \Phi)$ consisting of a connection 1-form $\widetilde{A}$ on a rank N vector bundle $W \longrightarrow \mathbb{R}^3$, and a section $\Phi \in \Gamma(\mathrm{End}(W))$ called the **Higgs field**, which are solutions to the Bogomolny equation (1.10) with finite Yang-Mills-Higgs energy (1.12). Like calorons, monopoles may be thought of as being defined on B^3, with $\mathbb{R}^3$ identified as the interior, and an additional structure given on the boundary $\partial B^3 \cong S^2_\infty$. The bundle W_∞, that is, the restriction of W to S^2_∞, is equipped with a connection 1-form $\widetilde{a}_\infty$ and endomorphism section Φ_∞ which are defined in the same way as with calorons to be simultaneously diagonalisable with respect to the splitting (2.2). The pair $(\widetilde{A}, \Phi)$ are then subject to the conditions that they both admit extensions to all of B^3, and that $A|_{S^2_\infty} = \widetilde{a}_\infty$ and $\Phi|_{S^2_\infty} = \Phi_\infty$. An $SU(N)$-monopole has $N - 1$ constituent charges and masses defined analogously to a caloron. The Higgs field at infinity Φ_∞ has eigenvalues $\imath\mu_p$ and corresponding eigenspaces $\mathcal{O}(k_p)$, where $\mu_N \leq \cdots \leq \mu_1$, $\sum_{q=1}^{p} k_q \geq 0$ for all p, and $\mu_1 + \cdots + \mu_N = k_1 + \cdots + k_N = 0$. The constituent charges are $\widetilde{m}_p = \sum_{q=1}^{p} k_q$, which are imposed to be non-negative, and constituent masses are $\widetilde{\nu}_p = \mu_{p+1} - \mu_p$. As with calorons, monopoles possess maximal symmetry breaking if $\widetilde{\nu}_p \neq 0$ for all $p = 1, \ldots, N - 1$.

A caloron can be obtained from an $SU(N)$-monopole by setting the caloron connection 1-form as

$$A = \widetilde{A} + \Phi dt. \tag{2.17}$$

Since via this construction, the anti-self-dual equation is equivalent to the Bogomolny equation, we see that this represents a $\vec{m}$-caloron with instanton charge $k_0 = 0$, i.e. a $(\vec{\widetilde{m}}, 0)$-caloron. Its monopole masses $\vec{\nu}$ are determined as usual by the eigenvalues of Φ_∞ and the reciprocal radius μ_0. In fact, every such caloron arises in this way, but to be precise, the condition (2.3) must be satisfied in order for a caloron to be generated. This is okay though, since we are free to choose μ_0 so that this holds as it is not part of the monopole data.

2.2.3 Calorons with non-trivial holonomy

Besides monopoles, there are more generic examples of calorons with non-trivial holonomy which have been written down explicitly. In 1998, both Lee and Lu [75], and Kraan and van Baal [73], independently studied the first examples of $SU(2)$ calorons with non-trivial holonomy. They considered $(1, 1)$-calorons, and in particular the moduli space and metric was explicitly constructed, and found to given by the product of $S^1 \times \mathbb{R}^3$ with the Taub-NUT space modulo an action of $\mathbb{Z}_2$ [71, 73]. These results have been generalised to the case of $(1, \ldots, 1)$-calorons [70]. All of these calorons have magnetic charges $k_p = 0$ for all $p = 1, \ldots, N$. Calorons with a mixture of magnetic and instanton charge are significantly less understood, however some interesting explicit examples may be found in [20, 49, 69].

By far the most successful method of constructing calorons has been the *Nahm transform*, which we shall describe for calorons with all magnetic charges zero in section 2.4. This construction was explicitly utilised for the construction of the $k_0 = 1$ calorons in [70, 73, 75]. A few other examples of calorons have been implicitly described via the $SU(2)$

Nahm transform. Some charge (k, k) cases were considered in [19], and many examples of $(2, 2)$-calorons have been written down implicitly [18, 89, 93]. Examples which exploit symmetry are given by Harland [49], Nakamula and Sawado [90], and Ward [122], but only considering low charge (k, k), and $(k+1, k)$ cases, and the latter two only with trivial holonomy. Some of the implicit calorons of [49] were recently constructed explicitly in [69], again via the Nahm transform.

2.2.4 Limits of calorons

In the limit $\mu_0 \longrightarrow 0$ (that is, the *large period limit*), the function (2.16) reduces to

$$\phi = 1 + \sum_{j=1}^{k} \frac{\lambda_j^2}{r_j^2 + (t - \theta_j)^2}, \tag{2.18}$$

which within the ansatz (2.14) generates a charge k instanton on $\mathbb{R}^4$. Another interesting limit to consider is the *large scale limit*, where the scales λ_j are significantly large compared to the period. In this limit, (2.16) is dominated by the non-constant terms, and takes the form

$$\phi = \sum_{j=1}^{k} \frac{\lambda_j^2}{2r_j} \frac{\sinh(\mu_0 r_j)}{\cosh(\mu_0 r_j) - \cos(\mu_0(t - \theta_j))}. \tag{2.19}$$

One can show [49] that this generates a $(k-1, k)$-caloron of constituent masses $(0, \mu_0)$. The $k = 1$ case has only one non-trivial constituent monopole (that is, with non-zero mass and charge), and can be shown [107] to be related via the action of a *large gauge transformation* $g : \mathbb{R} \times \mathbb{R}^3 \longrightarrow SU(2)$ to a $(1, 0)$-caloron with masses $(\mu_0, 0)$, i.e. an $SU(2)$ monopole. In fact, this monopole is the Prasad-Sommerfield monopole [105]. This gauge transformation was the first example of an explicit *rotation map*, the idea of which we shall discuss further in section 2.3.3.

Various other examples of limits of calorons have been studied [49, 75, 122], and in each case, the resulting limiting object is observed to be either an instanton, or a caloron of

lower charge (by which we mean, at least one of the constituents' charges is reduced). The upshot is that calorons are seen to interpolate between monopole-like solitons at large scales (in the limit $\mu_0 \longrightarrow \infty$) and instanton-like solitons at large periods (in the limit $\mu_0 \longrightarrow 0$). This understanding is something that we shall return to again in chapter 4 when we discuss the relationship between calorons and skyrmions, in an attempt to complete the links between the soliton trinity.

2.3 Moduli spaces

The group of gauge transformations acts on calorons via (1.9), and can be used to form moduli spaces of $SU(N)$-caloron configurations with boundary data $(\vec{m}, \vec{\nu})$. In order to do this properly, we require that our gauge transformations preserve all the boundary conditions of the framed bundle (V, f).

A *framed bundle map* $\gamma : V \longrightarrow V$ is one such that its restriction $\gamma_\infty : V_\infty \longrightarrow V_\infty$ satisfies $f \circ \gamma_\infty = f$, where f is the framing (2.1). This is equivalent to saying that the gauge transformation is identity as $|\vec{x}| \longrightarrow \infty$. Such maps preserve the framed bundle (V, f), and together they form the *framed gauge group*, isomorphic to the group of **framed gauge transformations**[4]

$$\mathcal{G} = \{g : S^1 \times \mathbb{R}^3 \longrightarrow SU(N) \ : \ g \longrightarrow \mathbb{1} \text{ as } |\vec{x}| \longrightarrow \infty\}.$$

It is usual to consider calorons which differ by framed gauge transformations to be equivalent, hence we form the moduli spaces $\mathcal{C}^N(\vec{m}, \vec{\nu})$ of **framed $\vec{m}$- calorons** as the $\mathcal{G}$-orbits of $SU(N)$ caloron configurations with boundary data $(\vec{m}, \vec{\nu})$.

[4]In this context, all other gauge transformations will be known as **unframed**.

2.3.1 The moduli space geometry

Constructing the moduli spaces $\mathcal{C}^N(\vec{m},\vec{\nu})$ requires knowledge of the solutions to the ASD equations (1.3) with the correct boundary conditions. Since $S^1 \times \mathbb{R}^3$ is unbounded, it is not immediate[5] that the moduli space is a finite-dimensional manifold. The most direct way to gain any knowledge is to construct the calorons explicitly, but as we have seen, explicit examples of calorons are few and far between. The most promising method for understanding the moduli space involves the use of a non-linear transform known as the *Nahm transform*, which we shall describe in section 2.4, along with an explicit parameterisation in terms of some matrix data, which we describe in section 2.5. These descriptions allow us to predict that the moduli space $\mathcal{C}^N(\vec{m},\vec{\nu})$ is a complex manifold of dimension $2\sum_{p=1}^{N} m_p$, and this is confirmed in the case $N = 2$ [21]. Furthermore, it is equipped with a natural metric, which we describe briefly in section 3.1, and this metric is conjectured to be hyperkähler.

Unframing

By definition, along each 'time slice' of S^1, every caloron is asymptotically isomorphic to a connection a_∞ and asymptotic Higgs field Φ_∞ on W_∞, which decomposes into the line bundles $\mathcal{O}(k_p)$ via the splitting (2.2), and this isomorphism is given by the framing (2.1). The group of automorphisms of W_∞ is given by the maximal torus T^{N-1} in $SU(N)$. We define the **unframed moduli space** $\mathcal{C}_u^N(\vec{m},\vec{\nu})$ as the quotient of $\mathcal{C}^N(\vec{m},\vec{\nu})$ by this T^{N-1} action.

[5] For example, by analysing the ASD equations and using an index theorem.

2.3.2 The loop group point of view

We have already observed in section 2.2.2 that monopoles give rise to calorons. In fact, this relationship between calorons and monopoles goes deeper than this relatively trivial example. Something that we have not been very transparent about so far is the reasoning behind the terminology 'constituent monopoles' when describing the boundary data for calorons. For $SU(N)$ monopoles, the case where $\widetilde{m}_q = \widetilde{\nu}_q = 0$ for all $q \neq p$, for some $p \in \{1, \ldots, N-1\}$, is known as the p-th *fundamental monopole*. A general $SU(N)$ monopole, with maximal symmetry breaking, is therefore in some way made up of $N-1$ fundamental monopoles, hence the term 'constituents'. More precisely, these constituents are embeddings of $SU(2)$ monopoles into the space of $SU(N)$ monopoles by associating each to one of the $N-1$ simple roots of the Lie group $SU(N)$. In a similar fashion, we claim that we may interpret $SU(N)$ calorons, with maximal symmetry breaking, as a superposition of N constituent $SU(2)$ monopoles [72]. This interpretation is formalised in the work of Garland and Murray [44] in the context of *loop groups* [106].

The **loop group** LG of a Lie group G is the group of smooth gauge transformations of the trivial G-bundle over S^1, that is

$$LG := \{g : S^1 \longrightarrow G \ : \ g \text{ smooth}\}, \tag{2.20}$$

with point-wise composition. There is a natural action of $U(1)$ on LG via the pull-back of the corresponding isometry $S^1 \longrightarrow S^1$. This action defines the **intertwined loop group** $\widehat{L}G := LG \rtimes U(1)$. The main result regarding loop groups and calorons is the following:

Theorem 2.3.1 (Garland and Murray (1988) [44]) *There is a 1-1 correspondence between $SU(N)$ calorons and monopoles on $\mathbb{R}^3$ whose gauge group is the intertwined loop group $\widehat{L}SU(N) = LSU(N) \rtimes U(1)$.*

The N monopole constituents of the caloron are identified as the N simple roots of the group $\widehat{L}SU(N)$, and some examples of their Dynkin diagrams are given in figure 2.1.

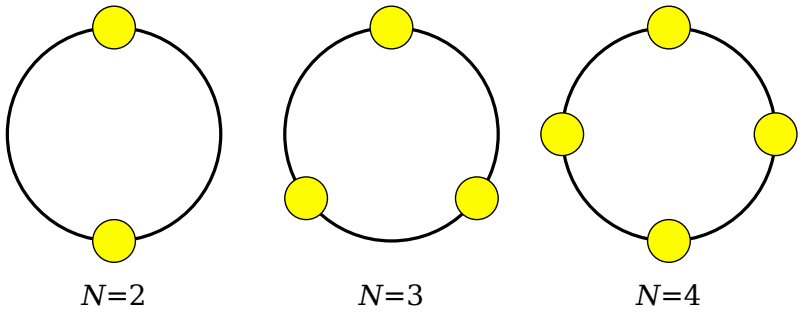

Figure 2.1: The Dynkin diagrams for the loop groups $\widehat{L}SU(N)$ in the cases $N = 2, 3,$ and 4.

Remark 2.3.2 *This relationship between solitons via loop groups is not unique to calorons. For example, in [50], Harland relates chains in $\mathbb{C}P^n$ sigma models to loops of multi-kinks. Further generalisations of this sort of observation have also been made, usually under the name the caloron correspondence [53], and there are also various other applications of loop groups within the wider study of solitons and integrable systems [56].*

2.3.3 The rotation map

In accordance with the loop group point of view, an $SU(N)$-caloron may be thought of as N constituent $SU(2)$ monopoles with charges and masses m_p and ν_p respectively, represented by the simple roots of the loop group $\widehat{L}SU(N)$. There is an obvious symmetry here. Note that the ordering of these roots is somewhat arbitrary; a caloron with boundary data $(\vec{m}, \vec{\nu})$ is essentially the same as one with boundary data $(\vec{m}', \vec{\nu}')$, when $(\vec{m}, \vec{\nu})$ and $(\vec{m}', \vec{\nu}')$ are related by a cyclic permutation of the masses and charges. To put this another way, rotating the Dynkin diagram of $\widehat{L}SU(N)$ by a multiple of the angle $2\pi/N$, that is, cyclically permuting the constituent monopoles, does not affect the structure of the moduli space. Therefore, one expects such calorons to be related by a well-defined map $h_{\mathcal{C}} : \mathcal{C}^N(\vec{m}, \vec{\nu}) \longrightarrow \mathcal{C}^N(\vec{m}', \vec{\nu}')$.

It turns out that such a map may be described by a *large gauge transformation* – a gauge transformation at infinity which is not itself periodic, but still preserves the periodicity of the caloron, that is $h : \mathbb{R} \times S^2_\infty \longrightarrow SU(N)$ such that

$$h(t + 2\pi/\mu_0, z) = \lambda h(t, z), \quad \forall t \in \mathbb{R}, z \in S^2_\infty,$$

for some $\lambda \in U(1)$. The quintessential example of such a large gauge transformation is *the rotation map*. This corresponds directly to the outer automorphism of $\widehat{L}SU(N)$ which rotates the Dynkin diagram by one constituent, that is

$$\rho_{\mathcal{C}} : \mathcal{C}^N(m_1, \ldots, m_N, \nu_1, \ldots, \nu_N) \longrightarrow \mathcal{C}^N(m_2, \ldots, m_N, m_1, \nu_2, \ldots, \nu_N, \nu_1). \tag{2.21}$$

Given the existence of such a map (which we shall describe explicitly very shortly), one is able to gain a full understanding of various moduli spaces by only considering a small subset of possible boundary data.

Definition 2.3.3 *A set of caloron boundary data is called* ***principal*** *if the monopole charges m_p satisfy*

$$m_p \geq k_0 \quad \forall\, p = 1, \ldots, N,$$

with k_0 the instanton number.

Due to the way the rotation map is defined, every caloron moduli space is related to one with principal boundary data by $\rho^r_{\mathcal{C}}$ for some $r = 1, \ldots, N$. This observation is exploited by Nye with regards to defining the Nahm transform for calorons [97].

The rotation map is defined[6] by first considering the bundle map $\varrho : p^*W_\infty \longrightarrow p^*W_\infty$ given by its action on sections with respect to the splitting (2.2), namely

$$\varrho s_p = \begin{cases} \exp\left(-\imath t \mu_0\right) s_p, & p = 1, \\ s_p, & 2 \leq p \leq N, \end{cases} \qquad s_p \in \Gamma(\mathcal{O}(k_p)). \tag{2.22}$$

[6]It is important to note that our definition is different to that of Nye's [97], but its properties are the same.

From this we define the object

$$\widetilde{\rho} = \exp\left(\imath \frac{t\mu_0}{N}\right) \varrho. \tag{2.23}$$

which defines a large gauge transformation $\rho : \mathbb{R} \times S^2_\infty \longrightarrow SU(N)$ satisfying

$$\rho(t + 2\pi/\mu_0, z) = \exp\left(\frac{2\pi\imath}{N}\right) \rho(t, z). \tag{2.24}$$

This large gauge transformation is what we refer to as **the rotation map**. Since (2.23) is not an automorphism of p^*W_∞, it is not at all obvious how this acts on calorons. To understand this, note that (2.23) defines a bundle map $\widetilde{\rho} : p^*W_\infty \otimes L_\infty \longrightarrow p^*W_\infty$, where $L \longrightarrow S^1 \times \mathbb{R}^3$ the trivial line bundle defined by

$$L = \mathbb{R} \times \mathbb{R}^3 \times \mathbb{C}\,/_\sim, \quad (t, \vec{x}, w) \sim \left(t + \frac{2\pi}{\mu_0}, \vec{x}, e^{-\imath\frac{2\pi}{N}} w\right), \tag{2.25}$$

and L_∞ is its restriction to $S^1 \times S^2_\infty$. Also note that the framing (2.1) naturally induces a map $\widetilde{f} : V_\infty \otimes L_\infty \longrightarrow p^*W_\infty \otimes L_\infty$, defined by $\widetilde{f} = f \otimes \mathbb{1}_L$, where $\mathbb{1}_L$ is the identity on L_∞. The action on calorons (bundle, framing, and connection (V, f, A)) is then given by

$$\rho \cdot (V, f, A) = \left(V \otimes L, \widetilde{\rho} \circ \widetilde{f}, A \otimes 0\right). \tag{2.26}$$

This rotation map can be thought of as an overall $\mathbb{Z}_N$ action on the space of all $SU(N)$ caloron configurations, namely the correspondence (2.21), which is the context we shall discuss further in chapter 3. To see that (2.26) corresponds precisely to the map (2.21) on the moduli spaces, we shall summarise the argument of Nye [97]. Note that by (2.4), ρ acts on the boundary field Φ_∞ via

$$\Phi_\infty \mapsto \rho^{-1}\Phi_\infty\rho + \rho^{-1}d\rho.$$

Hence, for $s_p \in \Gamma(\mathcal{O}(k_p))$, we have

$$\Phi_\infty s_p \mapsto \begin{cases} \imath\left(\mu_1 + \dfrac{\mu_0}{N} - \mu_0\right) s_1, & p = 1, \\ \imath\left(\mu_p + \dfrac{\mu_0}{N}\right) s_p, & 2 \leq p \leq N. \end{cases} \tag{2.27}$$

This shows that the eigenvalues have transformed non-trivially. To see how to make sense of it, the transformed eigenvalues $\widetilde{\mu}_p$ must preserve the conditions $\mu_N < \cdots < \mu_1$, and (2.3). This makes sense in terms of (2.27) if they transform such that

$$\begin{aligned} \mu_p \mapsto \mu_{p+1} + \frac{\mu_0}{N} \equiv \widetilde{\mu}_p, \quad p = 1, \ldots, N-1, \\ \mu_N \mapsto \mu_1 + \frac{\mu_0}{N} - \mu_0 \equiv \widetilde{\mu}_N. \end{aligned} \tag{2.28}$$

Clearly μ_0 is unchanged, so this transformation of the eigenvalues corresponds to the masses transforming via $\nu_p \mapsto \nu_{p+1}$, and $\nu_N \mapsto \nu_1$. The eigenbundles of Φ_∞ are preserved by ρ, and since the connection 1-form a_∞ splits up accordingly with respect to the eigenbundle decomposition, the rotation map has no effect on it. Furthermore, the eigenbundle with eigenvalue $\widetilde{\mu}_p$ has Chern number $\widetilde{k}_p$, where

$$\begin{aligned} \widetilde{k}_p = k_{p+1}, \quad p = 1, \ldots, N-1, \\ \widetilde{k}_N = k_1. \end{aligned} \tag{2.29}$$

Finally, to see how the instanton number transforms, we appeal to the fact that the total caloron charge (2.11) will remain unchanged by the rotation map, so that if $k_0 \mapsto \widetilde{k}_0$, then using the formula (2.12) and the transformed data above, we have

$$Q \mapsto \widetilde{k}_0 + \frac{1}{\mu_0}\left(k_2\mu_2 + \cdots + k_N\mu_N + k_1(\mu_1 - \mu_0)\right),$$

which equals Q if and only if $\widetilde{k}_0 = k_0 + k_1$. Comparing this with the transformed magnetic charges, we see that $m_p \mapsto m_{p+1}$ and $m_N \mapsto m_1$. Consequently, the rotation map as defined above has exactly the effect described by (2.21).

2.4 The Nahm transform

Besides the examples given in the previous section, finding explicit, generic, solutions to the ASD equations is a difficult problem, which makes getting a handle on the moduli spaces hard as well. In this section and the next we shall describe two sets of objects

– Nahm data, and monad matrices – both which have moduli in correspondence with calorons. These objects do not rely on solving PDEs to write them down, and so studying them provides a more user-friendly approach to understanding the moduli spaces of calorons.

In general, a *Nahm transform* is a correspondence between moduli of anti-self-dual connections on a space $\mathbb{R}^4/\Gamma$, where $\Gamma \subset \mathbb{R}^4$ is a closed group of translations acting freely on $\mathbb{R}^4$, with moduli of anti-self-dual connections defined on a "dual" space $(\mathbb{R}^4)^*/\Gamma^*$, where Γ^* is the "dual" of the group Γ, given by

$$\Gamma^* = \{x \in (\mathbb{R}^4)^* \,:\, x(\Gamma) \subset \kappa\mathbb{Z}\},$$

for some real constant $\kappa > 0$, usually set to 1. The "dual" moduli space is usually known as the moduli space of *Nahm data*. A good review of these general Nahm transforms may be found in [66]. Recently this concept has been generalised further to understand Nahm transforms for higher dimensional analogues of ASD connections [24, 25, 88, 100, 109], but this goes far beyond the scope of this thesis.

The origins of the Nahm transform lie in the $ADHM$ construction of instantons [6], which considers the case of Γ trivial, and hence $\Gamma^* \cong \mathbb{R}^4$. The dual objects (here called *ADHM data*) are solutions to 'anti-self-dual equations' over the single-point space $\mathbb{R}^4/\mathbb{R}^4$, that is, a set of solutions to purely algebraic equations. This construction was adapted and generalised by Nahm (hence the term 'Nahm transform'), with particular emphasis on the construction of monopoles ($\Gamma \cong \mathbb{R}$, $\Gamma^* \cong \mathbb{R}^3$) [86], and there is a full description for monopoles for all[7] classical gauge groups [64]. For general ASD connections, that is for general gauge groups and base manifold, even the *existence* of a Nahm transform is not completely understood, and still an interesting open problem.

[7] Assuming maximal symmetry breaking.

2.4.1 Nahm data for calorons

The Nahm transform that we are interested in is that for $SU(N)$ calorons. This was rigorously defined and analysed by Nye [97], together with Singer [98], but has only been proven to be a bijection in the case $N = 2$ by Charbonneau and Hurtubise [21]. We will focus on the special case where all the magnetic charges are 0, that is, the Nahm transform for $(k, \ldots, k)$-calorons. The other general cases are similar, but with some added complexity which is not necessary for the purposes of this thesis.

Calorons are anti-self-dual connections on $M = \mathbb{R}^4 \Big/ \frac{2\pi}{\mu_0}\mathbb{Z}$, and their Nahm data are "anti-self-dual connections" on the dual space $M^* = \mathbb{R}^4 \big/ \mu_0\mathbb{Z} \times \mathbb{R}^3 \cong S^1$. By this we mean anti-self-dual connections on $(\mathbb{R}^4)^*$, which are $\Gamma^* \cong \mu_0\mathbb{Z} \times \mathbb{R}^3$-invariant. Giving $(\mathbb{R}^4)^*$ coordinates $\{s, q_1, q_2, q_3\}$, we may define a Γ^*-invariant, $U(k)$-connection on $(\mathbb{R}^4)^*$ via the 1-form

$$\mathfrak{A}(s) = T^0(s)ds + \sum_{j=1}^{3} T^j(s)dq_j, \tag{2.30}$$

where $T^\lambda : \mathbb{R} \big/ \mu_0\mathbb{Z} :\longrightarrow \mathfrak{u}(k)$ are smooth functions for $\lambda = 0, 1, 2, 3$. The condition of anti-self-duality of (2.30) is equivalent to the functions T^λ satisfying

$$\frac{dT^j}{ds} + [T^0, T^j] + \frac{1}{2}\sum_{k,l=1}^{3} \epsilon_{jkl}[T^k, T^l] = 0, \tag{2.31}$$

for $j = 1, 2, 3$, where ϵ_{jkl} is the Levi-Civita symbol, and $\epsilon_{123} = 1$. These three equations are known as **Nahm's equations**, and are the underlying equations which govern the space of Nahm data. As should be evident by now, since the dual space we are dealing with is 1-dimensional, determining the Nahm data requires finding the solution to a system of ODEs. This is in many ways the reason why this transform is so useful – it has reduced the problem of solving PDEs into solving ODEs.

In order for this Nahm data to correspond to $SU(N)$ calorons, we need a way to extract all of the boundary data, including the masses $\nu_1, \ldots, \nu_N$. It turns out that the solution to this

amounts to covering the circle M^* by N intervals of lengths ν_p, namely[8] $I_p = [\mu_{p+1}, \mu_p]$, for $p = 1, \ldots, N-1$, and $I_0 = [\mu_1, \mu_0 + \mu_N]$, and defining N pieces of Nahm data, one over each interval, with boundary conditions at the end-points. We formalise this in the following definition.

Definition 2.4.1 *Let $T_p^\lambda(s) : I_p \longrightarrow \mathfrak{u}(k)$ be smooth functions, and $(u_p, w_p) \in (\mathbb{C}^k \times \mathbb{C}^k)\backslash\{(0,0)\}$, for $p \in \{0, \ldots, N-1\}$ and $\lambda \in \{0,1,2,3\}$. Define the matrix-valued functions*

$$A_p(s)(\zeta) = T_p^2(s) + \imath T_p^3(s) + 2\imath T_p^1(s)\zeta + (T_p^2(s) - \imath T_p^3(s))\zeta^2, \quad s \in I_p,\ \zeta \in \mathbb{C},$$

*for $p = 0, \ldots, N-1$. A set of k-**Nahm data** is given by a collection*

$$(T_p^0, T_p^1, T_p^2, T_p^3, (u_p, w_p))_{p=0,\ldots,N-1}$$

with the following conditions:

1. *For each $p = 0, \ldots, N-1$, T_p^λ satisfy Nahm's equations*

$$\frac{d}{ds}T_p^j + [T_p^0, T_p^j] + \frac{1}{2}\sum_{k,l=1}^{3} \epsilon_{jkl}[T_p^k, T_p^l] = 0, \tag{2.32}$$

   for $j \in \{1,2,3\}$.

2. *The matrices $A_p(s)(\zeta)$ have well-defined limits at the endpoints ∂I_p in a local gauge where $T_p^0 = 0$. Then the column vectors (u_p, w_p) and the matrices $A_p(s)(\zeta)$ satisfy the matching conditions*

$$\begin{aligned} A_0(\mu_0 + \mu_N)(\zeta) - A_{N-1}(\mu_N)(\zeta) &= (u_0 - w_0\zeta)(w_0^\dagger + u_0^\dagger\zeta), \\ A_p(\mu_p)(\zeta) - A_{p-1}(\mu_p)(\zeta) &= (u_p - w_p\zeta)(w_p^\dagger + u_p^\dagger\zeta), \end{aligned} \tag{2.33}$$

   for all $p = 1, \ldots, N-1$ and $\zeta \in \mathbb{C}$.

[8] It is worth noting that our convention here is slightly different, but equivalent, to Nye's. Nye's convention is to replace I_0 by $I_N = [\mu_1 - \mu_0, \mu_N]$. This is a simply change of coordinates of the circle $\mathbb{R}/\mu_0\mathbb{Z}$.

Remark 2.4.2 *We may think of the matrices T_p^j, $j = 1, 2, 3$, as endomorphisms of a rank k hermitian vector bundle K_p over I_p with gluing conditions given by the matching equations (2.33) above to make a hermitian bundle K over the circle M^*. The matrices T_p^0 may be thought of as connection one-forms on K_p. This understanding will be useful later.*

Definition 2.4.3 *A collection of k-Nahm data is called **irreducible** if there are no parallel sections of K_p invariant under the matrices T_p^j for each $p = 0, \ldots, N-1$, $j = 1, 2, 3$.*

The notion of irreducibility turns out to be crucial regarding the existence and invertibility of the Nahm transform [21]. We describe the total irreducible k-Nahm-data configuration space $\mathcal{T}(k, \vec{\nu})$ as the set of tuples containing all **Nahm matrices** T_p^λ for all intervals, along with the corresponding **matching vectors** (u_p, w_p). For notational brevity, we will often write the elements of $\mathcal{T}(k, \vec{\nu})$ as $(T_p^\lambda, (u_p, w_p))$, with the understanding that the tuple is ordered with p running over $0, \ldots, N-1$, and λ running over $0, \ldots, 3$. If we wish to talk about the Nahm matrices for $\lambda = 1, 2, 3$, we will usually use the Latin index j.

2.4.2 Constructing calorons from Nahm data

We shall now briefly describe the Nahm transform for calorons, that is, the method of obtaining the corresponding $(k, \ldots, k)$-caloron from a set of k-Nahm data. For further details, see [97]. In practice, performing the Nahm transform requires solving an additional ODE, and one is usually able to, at least implicitly, derive the caloron via the Nahm transform with quite a lot of accuracy. In the case $k = 1$, this has been done explicitly [70, 73, 75]. For higher charge cases, besides one special example [69], the success has so far been only with numerical methods. For calorons, this has been done only for very special cases [85, 91], but many examples have been considered in the case of monopoles [115]. Recent work by Braden and Enolski [15] has shed light on

how to construct monopoles explicitly from their corresponding Nahm data, yet it is still unknown whether these results apply to calorons.

Let

$$\mathcal{V} = C^\infty(S^1, \mathbb{C}^k) \otimes \mathbb{C}^2 \cong C^\infty(S^1, \mathbb{C}^k \otimes \mathbb{C}^2),$$
$$\mathcal{W} = \mathcal{V} \oplus \mathbb{C}^N.$$

Given a set of k-Nahm data $(T_p^\lambda, (u_p, w_p))$, define

$$T^\lambda(s) = T_p^\lambda(s), \quad s \in I_p, \tag{2.34}$$
$$v_p = \frac{1}{\sqrt{2}} \begin{pmatrix} w_p - u_p \\ w_p + u_p \end{pmatrix} \in \mathbb{C}^k \otimes \mathbb{C}^2, \tag{2.35}$$

for $p = 0, \ldots, N-1$. Let $(t, \vec{x}) \in S^1 \times \mathbb{R}^3$, where here $S^1 = \mathbb{R} \Big/ \frac{2\pi}{\mu_0}\mathbb{Z}$, and denote

$$T = T^0 \otimes \mathbb{1}_2 - \imath \sum_{j=1}^{3} T^j \otimes \sigma^j, \quad \text{and} \quad x = -\imath t \mathbb{1}_k \otimes \mathbb{1}_2 - \sum_{j=1}^{3} x^j \mathbb{1}_k \otimes \sigma^j,$$

where σ^j are the Pauli matrices. The **Nahm operator** $\not{D}_{(t,\vec{x})} : \mathcal{W} \longrightarrow \mathcal{V}$ is defined as

$$\not{D}(\psi, \vec{\zeta}) := -\left(\frac{d}{ds} + T + x\right)\psi + \zeta_0 v_0 \delta(s - \mu_0 - \mu_N) + \sum_{p=1}^{N-1} \zeta_p v_p \delta(s - \mu_p), \tag{2.36}$$

where $\vec{\zeta} = (\zeta_0, \ldots, \zeta_{N-1}) \in \mathbb{C}^N$, and $\delta(\cdot)$ is the Dirac-delta. $\mathcal{W}$ has a natural L^2 inner product given by

$$\langle (\psi, \vec{\zeta}), (\psi', \vec{\zeta}') \rangle_{\mathcal{W}} = \sum_{p=0}^{N-1} \overline{\zeta_p} \zeta_p' + \int_{\mu_N}^{\mu_0 + \mu_N} \psi(s)^\dagger \psi'(s)\, ds, \tag{2.37}$$

and one may show that the space $\mathrm{Ker}(\not{D}) \subset \mathcal{W}$ is of (complex) rank N. The vector bundle $V \longrightarrow S^1 \times \mathbb{R}^3$ is formed in such a way that the fibre over $(t, \vec{x})$ is the vector space $\mathrm{Ker}(\not{D}_{(t,\vec{x})})$. One may find an L^2-orthonormal basis $\{(\psi^q, \vec{\zeta}^q)\}_{q=1}^N \subset \mathrm{Ker}(\not{D})$, where the basis elements are functions of both $s \in [\mu_N, \mu_0 + \mu_N]$ and $(t, \vec{x}) \in S^1 \times \mathbb{R}^3$. This set of

solutions are used to construct the caloron as follows: identifying t with x^0, the caloron is given by the matrix of 1-forms

$$A^{ij} = \sum_{\lambda=0}^{3} \left\langle (\psi^i, \vec{\zeta^i}), (\partial_\lambda \psi^j, \partial_\lambda \vec{\zeta^j}) \right\rangle_{\mathcal{W}} dx^\lambda. \tag{2.38}$$

In practice, finding the kernel of the Nahm operator amounts to solving a set of N differential equations, one on each interval I_p, to obtain functions ψ_p, which describe ψ on each I_p. One then finds the vector components ζ_p by solving matching conditions at each point μ_p, namely

$$\begin{aligned} \psi_{p-1}(\mu_p) - \psi_p(\mu_p) &= \zeta_p v_p, \\ \psi_{N-1}(\mu_N) - \psi_0(\mu_0 + \mu_N) &= \zeta_0 v_0. \end{aligned} \tag{2.39}$$

2.4.3 The moduli space of caloron Nahm data

There are gauge transformations which act on Nahm data given by the elements of the gauge group

$$\begin{aligned} \mathcal{G}(k, \vec{\nu}) &= \left\{ g \in \prod_p \mathrm{Maps}\,(I_p, U(k)) \quad : \quad \begin{array}{c} g_p(\mu_p) = g_{p-1}(\mu_p) \\ g_0(\mu_0 + \mu_N) = g_{N-1}(\mu_N) \end{array} \right\} \\ &\cong \mathrm{Maps}\left(S^1, U(k)\right), \end{aligned} \tag{2.40}$$

which, for $g = (g_1, \ldots, g_N) \in \mathcal{G}(k, \vec{\nu})$, acts on $\mathcal{T}(k, \vec{\nu})$ via $g \cdot (T_p^\lambda, (u_p, w_p)) = \left(g \cdot T_p^\lambda, g \cdot (u_p, w_p)\right)$, where

$$\begin{aligned} \left(g \cdot T_p^j\right)(s) &= g_p(s) T_p^j(s) g_p(s)^{-1}, \quad j \in \{1, 2, 3\}, \\ \left(g \cdot T_p^0\right)(s) &= g_p(s) T_p^0(s) g_p(s)^{-1} - \frac{dg_p}{ds}(s) g_p(s)^{-1}, \\ g \cdot (u_p, w_p) &= g_p(\mu_p)(u_p, w_p), \quad p = 0, \ldots, N-1, \\ g \cdot (u_N, w_N) &= g_N(\mu_0 + \mu_N)(u_N, w_N). \end{aligned}$$

The moduli space of k-Nahm data is given by $\mathcal{N}^N(k, \vec{\nu}) = \mathcal{T}(k, \vec{\nu}) \Big/ \mathcal{G}(k, \vec{\nu})$.

In general, one may define Nahm data for $\vec{m}$-calorons, where $\vec{m}$ is principal[9], in an analogous way by forming Nahm matrices of rank m_p on I_p. The key difference is that of the boundary conditions on the boundaries of two intervals with differing rank. For these we refer the reader to Nye's thesis [97]. From this more generic data, one may analogously form gauge groups and hence moduli spaces $\mathcal{N}^N(\vec{m}, \vec{\nu})$, and we have described the spacial case of $\vec{m} = (k, \ldots, k)$. The main result regarding relationships between Nahm data and calorons is the following, due to Nye and Singer (2000) [98], Nye (2001) [97], and Charbonneau and Hurtubise (2007) [21]:

Theorem 2.4.4 *There exist well-defined maps* $\mathcal{N}^N(\vec{m}, \vec{\nu}) \longrightarrow \mathcal{C}^N(\vec{m}, \vec{\nu})$ *and* $\mathcal{C}^N(\vec{m}, \vec{\nu}) \longrightarrow \mathcal{N}^N(\vec{m}, \vec{\nu})$. *Moreover, in the case that* $N = 2$*, these maps are mutually inverse, hence*

$$\mathcal{N}^2(m_1, m_2, \nu_1, \nu_2) \cong \mathcal{C}^2(m_1, m_2, \nu_1, \nu_2).$$

The mappings referred to in Theorem 2.4.4 are the *Nahm transform* and *inverse Nahm transform* respectively. It is still unknown whether the proof in the case $N = 2$ [21] may be extended to the general case. Nevertheless, this theorem tells us that the structure of the caloron moduli spaces may be studied by considering the moduli spaces of Nahm data, and one obtains a complete understanding in the case that $N = 2$.

With this in mind, we shall now prove some useful properties of $\mathcal{N}^N(k, \vec{\nu})$ to be used later on.

Lemma 2.4.5 *Every* $(T_p^\lambda, (u_p, w_p)) \in \mathcal{T}_k$ *is gauge equivalent to one such that* T_p^0 *is some constant* $\Theta \in \mathfrak{u}(k)$ *for all* $p = 0, \ldots, N-1$.

Proof

Define a function $T^0 : \bigcup_p I_p = [\mu_N, \mu_0 + \mu_N] \longrightarrow \mathfrak{u}(k)$ by setting $T^0 = T_p^0$ on I_p. By the

[9] See definition 2.3.3.

standard existence results in ODE theory, for all $s' \in [\mu_N, \mu_0 + \mu_N]$ there exists $\delta_{s'} > 0$, such that there exists $g_{s'} : [\mu_N, \mu_0 + \mu_N] \cap (s' - \delta_{s'}, s' + \delta_{s'}) \longrightarrow U(k)$ solving

$$g_{s'}(s)T^0(s)g_{s'}(s)^{-1} - \frac{dg_{s'}}{ds}(s)g_{s'}(s)^{-1} = 0,$$

with the initial condition $g_{s'}(s') = \mathbb{1}$. Now, the set

$$\{[\mu_N, \mu_0 + \mu_N] \cap (s' - \delta_{s'}, s' + \delta_{s'}) \ : \ s' \in [\mu_N, \mu_0 + \mu_N]\}$$

is an open cover of $[\mu_N, \mu_0 + \mu_N]$, and since $[\mu_N, \mu_0 + \mu_N]$ is compact, there exists a finite subcover, determined by a finite set $\{s_1, \ldots, s_r\} \in [\mu_N, \mu_0 + \mu_N]$. Therefore, we may form a global gauge transformation $g : [\mu_N, \mu_0 + \mu_N] \longrightarrow U(k)$ from the functions $g_{s_1}, \ldots, g_{s_r}$ which solves $g \cdot T^0 = 0$.

Importantly, we cannot guarantee that this g is periodic, so it is not necessarily in $\mathcal{G}(k, \vec{\nu})$. To obtain such a transformation, consider the map $h : \mathbb{R} \longrightarrow U(k)$ defined by

$$h(s) = \exp\left(-\Theta s\right),$$

where $\Theta \in \mathfrak{u}(k)$ is a constant such that $h(\mu_0) = g(\mu_N)g(\mu_0 + \mu_N)^{-1}$. Then $hg \in \mathcal{G}(k, \vec{\nu})$, and satisfies $hg \cdot T^0 = \Theta$. Since T^0 is gauge-equivalent to a constant, it follows that T^0_p is also for all $p = 0, \ldots, N-1$. □

Proposition 2.4.6 *The following equivalence relation holds in $\mathcal{N}^N(k, \vec{\nu})$:*

$$\left(T^0_p, T^j_p, (u_p, w_p)\right) \sim \left(T^0_p + \imath\frac{2n\pi}{\mu_0}\mathbb{1}, T^j_p, e^{\imath\left(\varphi - \widehat{\mu}_p \frac{2n\pi}{\mu_0}\right)}(u_p, w_p)\right), \tag{2.41}$$

for all $n \in \mathbb{Z}$, $\varphi \in \mathbb{R}$, where $\widehat{\mu}_p = \mu_p$ for $p = 1, \ldots, N-1$, and $\widehat{\mu}_p = \mu_N$ for $p = 0$.

Proof

This is evident by performing a $U(1)$ gauge transformation, namely

$$g_p = \exp\left(\imath\varphi - \imath\frac{2n\pi}{\mu_0}s\right)\mathbb{1}.$$

□

The unframed moduli space

Like with calorons, there is a natural action of T^{N-1} on the moduli space $\mathcal{N}^N(k,\vec{\nu})$. This is given by the action of a *phase vector* $\vec{\varphi} = (\varphi_1, \ldots, \varphi_N)$, where $\varphi_1 + \cdots + \varphi_N = 0 \pmod{2\pi}$, via

$$(T^\lambda_p, (u_p, w_p)) \mapsto \begin{cases} \left(T^\lambda_0, e^{\imath\varphi_N}(u_0, w_0)\right), & p = 0, \\ \left(T^\lambda_p, e^{\imath\varphi_p}(u_p, w_p)\right), & p = 1, \ldots, N-1. \end{cases} \tag{2.42}$$

The orbit space in $\mathcal{N}^N(k,\vec{\nu})$ under the action (2.42) is called the moduli space of **unframed Nahm data**, which we denote by $\mathcal{N}^N_u(k,\vec{\nu})$. This is the analogue in the Nahm data universe to the unframed space $\mathcal{C}^N_u(k,\vec{\nu})$.

The rotation map

Like with the action of T^{N-1}, there is similarly an analogue of the rotation map on caloron Nahm data. Recall that the rotation map affects the boundary data via (2.28) and (2.29). This translates to the intervals I_p as

$$\begin{aligned} I_p &\mapsto (\mu_{p+2} + \mu_0/N, \mu_{p+1} + \mu_0/N), \\ I_{N-1} &\mapsto (\mu_1 + (1-N)\mu_0/N, \mu_N + \mu_0/N). \end{aligned} \tag{2.43}$$

This change in the intervals means that there needs to be a corresponding map which affects the data $(T^\lambda_p, (u_p, w_p))$. This map is given by

$$\begin{aligned} T^\lambda_p(s) &\mapsto \begin{cases} T^\lambda_{p+1}(s - \mu_0/N), & p = 0, \ldots, N-2, \\ T^\lambda_0(s + (N-1)\mu_0/N), & p = N-1, \end{cases} \\ (u_p, w_p) &\mapsto (u_{p+1}, w_{p+1}), \\ (u_{N-1}, w_{N-1}) &\mapsto (u_0, w_0). \end{aligned}$$

It is straightforward to check that these transformed data belong to $\mathcal{N}(k,\vec{\nu'})$, where $\vec{\nu'}$ represents the transformed masses $\nu'_p = \nu_{p+1}$, and are compatible with the change of intervals (2.43).

Remark 2.4.7 *Note that for the Nahm data we have described, that is where $k_q = 0$, $q = 1, \ldots, N$, the rank of the data on I_p will not have changed under the rotation map. In the general space $\mathcal{N}^N(\vec{m}, \vec{\nu})$, the rotation map will also have an effect on the rank of the data on I_p, namely changing from m_p to m_{p+1}.*

Phases and the rotation map within the Nahm transform

The existence of the Nahm transform $\mathcal{N}^N(\vec{m}, \vec{\nu}) \longrightarrow \mathcal{C}^N(\vec{m}, \vec{\nu})$, as in Theorem 2.4.4 has only been proven in the case that the boundary data is principal (see definition 2.3.3). As pointed out by Nye [97], the rotation map allows for the construction of calorons via the Nahm transform, even with non-principal boundary data. Indeed, suppose you have a set of Nahm data with boundary data which is not necessarily principal. Then you may apply the rotation map $\rho_{\mathcal{N}}$ as many times as necessary until its boundary data is principal, from which, the Nahm transform may be implemented, and then the caloron rotated back by using $\rho_{\mathcal{C}}$ until the boundary data agrees with that of the original Nahm data. This is of course true if the diagram

$$\begin{array}{ccc} \mathcal{N}^N(\vec{m}, \vec{\nu}) & \xrightarrow{\rho_{\mathcal{N}}} & \mathcal{N}^N\left(\rho(\vec{m}, \vec{\nu})\right) \\ \text{Nahm}\downarrow\text{transform} & & \text{Nahm}\downarrow\text{transform} \\ \mathcal{C}^N(\vec{m}, \vec{\nu}) & \xrightarrow{\rho_{\mathcal{C}}} & \mathcal{C}^N\left(\rho(\vec{m}, \vec{\nu})\right) \end{array}$$

commutes. This follows from the fact that $\mathrm{Ker}(\not{D})$ is unaffected by the action of $\rho_{\mathcal{N}}$,[10] and so the constructed calorons at the bottom of the diagram must be related by a large gauge transformation, which is easily seen to be $\rho_{\mathcal{C}}$.

In a similar fashion, we conjecture that quotienting by the actions of T^{N-1} on Nahm data (2.42), and on calorons, as described in section 2.3.1, also commutes with the Nahm

[10] Strictly speaking we have only described this for the case $k_q = 0$, $q = 1, \ldots, N$, but the general case also holds (see [97]).

transform, i.e. the diagram

$$\begin{array}{ccc} \mathcal{N}^N(k,\vec{\nu}) & \xrightarrow{/T^{N-1}} & \mathcal{N}_u^N(k,\vec{\nu}) \\ \text{Nahm}\downarrow\text{transform} & & \text{Nahm}\downarrow\text{transform} \\ \mathcal{C}^N(k,\vec{\nu}) & \xrightarrow{/T^{N-1}} & \mathcal{C}_u^N(k,\vec{\nu}) \end{array}$$

commutes. The missing ingredient for this lies in how the Nahm transform defines the framing (2.1). This is explained in Nye's thesis [97], but we do not fully understand this part of the construction.

2.4.4 Spectral curves and integrability

Recall the matrix-valued functions $A_p(s)(\zeta)$ which appear in the definition of caloron Nahm data 2.4.1, given by

$$A_p(s)(\zeta) = T_p^2(s) + \imath T_p^3(s) + 2\imath T_p^1(s)\zeta + (T_p^2(s) - \imath T_p^3(s))\zeta^2, \tag{2.44}$$

for $\zeta \in \mathbb{C}$, and $s \in I_p$. Introducing the additional linear combination of Nahm matrices

$$A_p^\star(s)(\zeta) = T_p^0(s) + \imath T_p^1(s) + (T_p^2(s) - \imath T_p^3(s))\,\zeta, \tag{2.45}$$

it is straightforward to show that Nahm's equations (2.32) are equivalent to the equation

$$\frac{dA_p}{ds} = [A_p, A_p^\star] \quad \forall\, \zeta \in \mathbb{C}. \tag{2.46}$$

In other words, the Nahm equations may be written as a **Lax pair**, given by the combinations A and $A^\star$, which qualifies them to the status of an 'integrable system'.

An important consequence of this is that the quantities $k_n = \mathrm{tr}\,((A_p)^n)$ are not only gauge invariant, but are constant for each $n \in \mathbb{N}$. This is since

$$\begin{aligned} \frac{dk_n}{ds} &= n\mathrm{tr}\,\left(A_p^{n-1}\frac{dA_p}{ds}\right) \\ &= n\mathrm{tr}\,\left(A_p^{n-1}[A_p, A_p^\star]\right) \\ &= n\mathrm{tr}\,\left([A_p^n, A_p^\star]\right) = 0 \end{aligned}$$

by the cyclicity of the trace. Since the trace is the sum of the eigenvalues, this implies that any symmetric polynomial in the eigenvalues η of T_p must be gauge invariant and constant as well, which in particular means that the characteristic polynomial for $-A_p(\zeta)$

$$\chi_\zeta(\eta) = \det\left(\eta \mathbb{1}_k + A_p(\zeta)\right)$$

must be gauge invariant and constant for all $\eta, \zeta \in \mathbb{C}$. We can extend this so that (ζ, η) are coordinates on the tangent bundle of the Riemann sphere $T\mathbb{C}P^1$, which is isomorphic to Hitchin's mini twistor space. Then the curves defined by

$$\mathcal{C}_p = \left\{(\zeta, \eta) \in T\mathbb{C}P^1 \mid \det(\eta \mathbb{1}_k + A_p(\zeta)) = 0\right\} \subset T\mathbb{C}P^1 \tag{2.47}$$

are known as the **spectral curves** for the charge $(k, \ldots, k)$ Nahm data, and there is one curve for each interval I_p.

2.4.5 Examples

The first example we shall present is both the simplest, and most famous – the construction of charge $(1, 1)$ $SU(2)$ calorons with non-trivial holonomy. This case was first understood independently by Kraan and Van Baal [73], and Lee and Lu [75], within the $Sp(1)$ formulation, which is equivalent since $Sp(1) \cong SU(2)$. Here we shall present it using the notation that we have developed so far, that is, in the $SU(2)$ formulation.

We require functions $T_1^\alpha : [-\mu, \mu] \longrightarrow \imath\mathbb{R}$, and $T_0^\alpha : [\mu, \mu_0 - \mu] \longrightarrow \imath\mathbb{R}$, satisfying the simple differential equation

$$\frac{dT_p^j}{ds} = 0, \quad j = 1, 2, 3, \ p = 0, 1.$$

Fixing a gauge such that the T_p^0 are constant and equal (by Lemma 2.4.5), this has general solution

$$T_p = \left(\imath\frac{\theta}{\mu_0}, \imath x_p, \imath y_p, \imath z_p\right) \quad \theta, x_p, y_p, z_p \in \mathbb{R}. \tag{2.48}$$

It is worth remarking that (2.48) is the generic form of $k = 1$ Nahm matrices for any rank N caloron. To completely describe the $(1,1)$-Nahm data, we also need to solve the matching conditions (2.33). In this case, we may translate these as follows: we require vectors $(u_p, w_p) = (\lambda_p e^{\imath\alpha_p}, \kappa_p e^{\imath\beta_p})$, $p = 0, 1$, such that

$$\begin{aligned}
x_0 - x_1 &= \frac{1}{2}(\lambda_1^2 - \kappa_1^2) = \frac{1}{2}(\kappa_0^2 - \lambda_0^2),\\
y_0 - y_1 &= \lambda_1\kappa_1 \sin(\beta_1 - \alpha_1) = \lambda_0\kappa_0 \sin(\alpha_0 - \beta_0),\\
z_0 - z_1 &= \lambda_1\kappa_1 \cos(\alpha_1 - \beta_1) = -\lambda_0\kappa_0 \cos(\alpha_0 - \beta_0).
\end{aligned}$$

We may use the remaining gauge freedom from Proposition 2.4.6 in light of these equations to fix $\alpha_0 = -\alpha_1$. Then, a straightforward calculation and relabelling of parameters shows that

$$\begin{aligned}
T_1^0 &= \imath\frac{\theta}{\mu_0}, & T_0^0 &= \imath\frac{\theta}{\mu_0}\\
T_1^1 &= \imath x, & T_0^1 &= \imath\left(x + \frac{1}{2}(\lambda_1^2 - \lambda_0^2)\right),\\
T_1^2 &= \imath y, & T_0^2 &= \imath\left(y + \lambda_1\lambda_0 \sin(\beta)\right),\\
T_1^3 &= \imath z, & T_0^3 &= \imath\left(z + \lambda_1\lambda_0 \cos(\beta)\right),\\
u_1 &= \lambda_1 e^{\imath\alpha}, & w_1 &= \lambda_0 e^{\imath(\beta+\alpha)},\\
u_0 &= \lambda_0 e^{-\imath\alpha}, & w_0 &= -\lambda_1 e^{\imath(\beta-\alpha)},
\end{aligned} \tag{2.49}$$

is a generic representative for all points in the moduli space of $(1,1)$-Nahm data, and hence $\mathcal{C}^2(1,1,\nu_1,\nu_2)$ by Theorem 2.4.4.

In light of Theorem 2.4.4, we may exploit the data (2.49) to analyse the moduli space $\mathcal{C}^2(1,1,\nu_1,\nu_2)$. Firstly, we observe that there are 8 real parameters. The parameters $(x,y,z) \in \mathbb{R}^3$ are interpreted as the location in $\mathbb{R}^3$ of one constituent monopole. The parameters $\beta \in {}^{\mathbb{R}}/_{2\pi\mathbb{Z}}$, and $(\lambda_1, \lambda_2) \in \mathbb{R}^2_+ \setminus \{(0,0)\}$ are *separation* parameters for the constituent monopoles. The parameter $\alpha \in {}^{\mathbb{R}}/_{2\pi\mathbb{Z}}$ contributes an overall phase, and according to Proposition 2.4.6, the parameter θ is only periodic when $\mu \equiv \mu_1$ is a rational multiple of μ_0.

Understanding the Nahm data for charge $k > 1$ is significantly harder than that of $k = 1$, due to the increased complexity of solving the Nahm equations (2.32). For $k = 2$, Bruckmann, Nógrádi, and van Baal [18] showed that the most general set of Nahm matrices may be written in the form[11]

$$T_p^j(s) = \zeta_p(s) h_p \left(\imath \alpha_p^j \mathbb{1}_2 + \imath \sum_{a=1}^{3} \mathfrak{R}_p^{ja} \frac{D_p}{2} f_p^a(D_p(s+s_p)) \sigma^a \right) h_p^\dagger \zeta_p(s)^\dagger, \tag{2.50}$$

where $\alpha_p^j, D_p, s_p \in \mathbb{R}$, $h_p \in U(2)$, $\mathfrak{R}_p \in O(3)$, and

$$\zeta_p(s) = \exp\left(-T_p^0(s+s_p)\right),$$

where we have set T_p^0 constant in accordance with Lemma 2.4.5. The $3N$ functions $f_p^1, f_p^2, f_p^3 : I_p \longrightarrow \mathbb{R}$ are determined by Nahm's equations, which here reduce to the Euler-top equations

$$\frac{df_p^1}{ds} = -f_p^2 f_p^3, \quad \frac{df_p^2}{ds} = -f_p^3 f_p^1, \quad \frac{df_p^3}{ds} = -f_p^1 f_p^2. \tag{2.51}$$

The general solution to these equations is well-known to be given by the Jacobi elliptic functions

$$\Phi_1(s) = -\frac{\kappa'}{\mathrm{cn}_\kappa(s)}, \quad \Phi_2(s) = \frac{\kappa' \mathrm{sn}_\kappa(s)}{\mathrm{cn}_\kappa(s)}, \quad \Phi_3(s) = \frac{\mathrm{dn}_\kappa(s)}{\mathrm{cn}_\kappa(s)}. \tag{2.52}$$

Here the parameter $\kappa \in [0,1]$ is the *elliptic modulus*, and $\kappa' = \sqrt{1-\kappa^2}$. For details see [1]. Our notation is slightly different, but may be translated simply via $\kappa \leftrightarrow \sqrt{m}$. We will also often adopt Glaisher's notation for quotients, for example $\mathrm{sn}\,(s)/\mathrm{cn}\,(s) \equiv \mathrm{sc}\,(s)$, etc.

The final challenge in fully describing the $k = 2$ Nahm data is to solve to matching conditions (2.33) and obtain the matching vectors (u_p, w_p). Many examples have been found in the case $N = 2$, initially in [18], where three families of solutions are described. Two of these are shown to have axial symmetry in [49], and the remaining solutions

[11] In fact, they described the data locally so as to set $T^0 = 0$. Here we have described the global data with T_p^0 constant.

are known as the 'crossed' solutions, possessing an order 4 cyclic symmetry, which we discuss further in section 3.6.3. A particularly detailed analysis of the $N = k = 2$ Nahm data was done by Nakamula and Sakaguchi in [89], in the case where the trace-less part of T_p^0 is 0. Recently, in [30], we found an example which has T_p^0 with explicitly non-zero trace-less part. This was found by exploiting cyclic symmetries and the rotation map, and we describe this solution in detail in section 3.6.3. In general, it is not possible to write all of the solutions to the matching conditions in one closed form, as was the case for $k = 1$, and as far as we can tell, nobody has ever considered matching these data for $N > 2$.

The case $k > 2$ is even less well-understood, with only a few scattered examples of explicit Nahm data known [19, 90, 122]. On top of this, no explicit implementations of the Nahm transform have been applied to Nahm data for $k > 1$.[12] The only case where the Nahm transform has been invoked is an example which uses numerical methods to generate approximate caloron configurations, in the case of cyclically symmetric $k = 3$ data [91].

2.5 Nahm complexes and the monad construction

The Nahm transform associates calorons – solutions to a system of PDEs – with Nahm data – solutions to a system of ODEs, thus making the construction of calorons more accessible. To further classify calorons, it is possible to consider a Kobayashi-Hitchin correspondence, by sacrificing some structure and extracting a holomorphic piece. Charbonneau and Hurtubise [22] have shown that $SU(2)$-calorons may be thought of, under this correspondence, as holomorphic bundles over $\mathbb{C}P^1 \times \mathbb{C}P^1$, via a *monad construction*, defined by a tuple of matrices subject to a set of algebraic equations, and

[12] There is one further example, in addition to that of [73], of an explicit construction using the Nahm transform to be found in [69], but this is in the case of charge $(2, 1)$, so not applicable to what we have described.

some additional constraints. This matrix data may be extracted from solutions to a holomorphic version of the Nahm data known as a *Nahm complex*. The relationship between monads and instantons first appeared in the work of Donaldson [32], has more recently been established for more generalised instantons [26], and there are several other instanton and caloron related algebro-geometric ideas which stem from the same lines of thought [88, 118].

In this section, we shall describe these Nahm complexes, and matrix data, along with some basic properties, generalised to the case of charge $(k, \ldots, k)$ $SU(N)$-calorons.

2.5.1 Nahm data and Nahm complexes

Writing

$$\alpha_p(s) = T_p^0(s) + \imath T_p^1(s), \quad \text{and} \quad \beta_p(s) = T_p^2(s) + \imath T_p^3(s) \tag{2.53}$$

for $p = 0, \ldots, N-1$, Nahm's equations are equivalent to the *complex* and *real* equations

$$\frac{d\beta_p}{ds}(s) + [\alpha_p(s), \beta_p(s)] = 0, \tag{2.54}$$

$$\frac{d}{ds}\left(\alpha_p(s) + \alpha_p(s)^\dagger\right) + [\alpha_p(s), \alpha_p(s)^\dagger] + [\beta_p(s), \beta_p(s)^\dagger] = 0. \tag{2.55}$$

Equation (2.54) is invariant under the action of $g_p : I_p \longrightarrow GL(k, \mathbb{C})$, where

$$\alpha_p(s) \mapsto g_p(s)\alpha_p(s)g_p(s)^{-1} - \frac{dg_p}{ds}g_p(s)^{-1}, \tag{2.56}$$

$$\beta_p(s) \mapsto g_p(s)\beta_p(s)g_p(s)^{-1}, \tag{2.57}$$

however, (2.55) is not so fortunate to possess this symmetry, and is only invariant under unitary transformations, as with Nahm data.

Definition 2.5.1 *Let $\pi_p : K_p \longrightarrow I_p$ be a complex vector bundle of rank k over the interval I_p, equipped with a smooth connection α_p and a parallel section β_p of* $\mathrm{End}(\mathrm{K_p})$*,*

that is

$$\frac{d\beta_p}{ds}(s) + [\alpha_p(s), \beta_p(s)] = 0 \quad \forall\, s \in I_p. \tag{2.58}$$

Let $u_p \in \pi_p^{-1}(\mu_p)$, $w_p^\dagger \in \left(\pi_p^{-1}(\mu_p)\right)^*$, $u_0 \in \pi_0^{-1}(\mu_0 + \mu_N)$, *and* $w_0^\dagger \in \left(\pi_0^{-1}(\mu_0 + \mu_N)\right)^*$. *Then a tuple* $(\alpha_p, \beta_p, (u_p, w_p))_{p=0,\ldots,N-1}$ *is called a* k***-Nahm complex*** *on the circle* $\mathbb{R}\,/\mu_0\mathbb{Z}$ *if there exist isomorphisms*

$$\begin{aligned} &i_0 : \pi_0^{-1}(\mu_0 + \mu_N) \longrightarrow \pi_{N-1}^{-1}(\mu_N), \\ &i_p : \pi_p^{-1}(\mu_p) \longrightarrow \pi_{p-1}^{-1}(\mu_p), \quad p = 1, \ldots, N-1, \end{aligned}$$

such that the maps

$$\begin{aligned} \beta_0(\mu_0 + \mu_N) - i_0^{-1}\beta_{N-1}(\mu_N) i_0, \\ \beta_p(\mu_p) - i_p^{-1}\beta_{p-1}(\mu_p) i_p \end{aligned} \tag{2.59}$$

are rank one, and coincide with the products $u_p w_p^\dagger$. *A Nahm complex is called* ***reducible*** *if there exist parallel subbundles* $V_p \subset K_p$ *with respect to* α_p, *which are invariant under* β_p, *mapping to each other via the isomorphisms* i_p *at the boundaries, and proper on at least one of the intervals* I_p. *Otherwise, the complex is called* ***irreducible***.

The gauge group for a Nahm complex is the set of complex gauge transformations $\mathrm{Maps}(S^1, GL(k, \mathbb{C}))$ in analogy to (2.40). These act on the data $(\alpha, \beta, (u, w))$ in the natural way, and on the isomorphisms as

$$\begin{aligned} &i_0 \mapsto g_{N-1}(\mu_N) i_0 g_0(\mu_0 + \mu_N)^{-1}, \\ &i_p \mapsto g_{p-1}(\mu_p) i_p g_p(\mu_p)^{-1}, \quad p = 1, \ldots, N-1. \end{aligned}$$

Remark 2.5.2 *We note that the points* $(u_p, w_p^\dagger)$ *in* $K_p \times K_p^*$ *are represented by vectors* $(u_p, w_p) \in (\mathbb{C}^k \times \mathbb{C}^k) \setminus \{(0,0)\}$. *There is a* T^{N-1} *action on these vectors* (u_p, w_p) *for a Nahm complex, given analogously by (2.42), and this determines a 'framed' moduli space as a* T^{N-1} *bundle over an 'unframed' moduli space.*

Fixing a gauge such that $i_p = \mathbb{1}$, and using (2.53), shows that every set of k-Nahm data gives rise to a k-Nahm complex. It turns out, as shown by Donaldson [33] in the context of $SU(2)$ monopoles, that the orbits of solutions to (2.54) under the action of $GL(k,\mathbb{C})$ contain a unique solution to both (2.54) and (2.55), and hence one only need consider (2.54) modulo the action of $\mathrm{Maps}(S^1, GL(k,\mathbb{C}))$ to give all solutions to Nahm's equations. The only caveat is that the boundary conditions are different to those considered by Donaldson. Luckily, the boundary conditions that we are interested in, namely (2.33) and (2.59), appear analogously in the boundary conditions for $SU(N)$ monopoles, and this statement regarding the solutions of the real equation (2.55) has been established for $SU(N)$ monopoles [63, 64]. The irreducibility of a Nahm complex is clearly equivalent to the irreducibility of Nahm data. Hence the moduli space of irreducible k-Nahm complexes on the circle is equivalent to the moduli space of irreducible k-Nahm data for calorons.

2.5.2 Monad matrices

Definition 2.5.3 *Let $A, B \in Mat_{k\times k}(\mathbb{C})$, $C \in Mat_{k\times N}(\mathbb{C})$ and $D \in Mat_{N\times k}(\mathbb{C})$. Then the matrices (A, B, C, D) are called **monad matrices** if they satisfy*

1. *The monad equation:*

$$[A, B] + CD = 0. \tag{2.60}$$

2. *The full-rank conditions: the linear maps defined by*

$$\begin{pmatrix} A - y\mathbb{1}_k \\ B - x\mathbb{1}_k \\ D \end{pmatrix}, \quad \textit{and} \quad \begin{pmatrix} x\mathbb{1}_k - B & A - y\mathbb{1}_k & C \end{pmatrix}, \tag{2.61}$$

are injective and surjective respectively for all $x, y \in \mathbb{C}$.

We denote the set of all monad matrices by $\widetilde{\boldsymbol{Md}}_k^N$.

For the purposes of brevity, unless explicitly clear in context, we will always denote by C_p and D_p the p-th column of C and the p-th row of D respectively, for $p = 0, \ldots, N-1$, that is

$$C = \begin{pmatrix} C_0 & C_1 & \cdots & C_{N-1} \end{pmatrix}, \quad D = \begin{pmatrix} D_0 \\ D_1 \\ \vdots \\ D_{N-1} \end{pmatrix}. \tag{2.62}$$

The gauge group $GL(k, \mathbb{C})$ acts on monad matrices via

$$g \cdot (A, B, C, D) = (gAg^{-1}, gBg^{-1}, gC, Dg^{-1}), \tag{2.63}$$

and the moduli space $\widetilde{\mathcal{M}}_k^N := \widetilde{\mathbf{Md}}_k^N \Big/ GL(k, \mathbb{C})$ is known as the **moduli space of monad matrices**.

Remark 2.5.4 *Like the Lax pair decomposition of Nahm's equation (2.46), and hence the interest from the integrable systems perspective, the monad equation (2.60) also appears in the literature of integrable systems in the context of the Calogero Moser systems [125].*

Definition 2.5.5 *A set of monad matrices* (A, B, C, D) *such that* $A \in GL(k, \mathbb{C})$ *is called* ***non-singular****. We denote the set and moduli space of all non-singular monad matrices by* $\boldsymbol{Md}_k^N$ *and* $\mathcal{M}_k^N := \boldsymbol{Md}_k^N \Big/ GL(k, \mathbb{C})$ *respectively.*

The relationship between $(k, \ldots, k)$-calorons and monad matrices is given by the following theorem, a generalisation of a theorem of Charbonneau and Hurtubise [22]:

Theorem 2.5.6 *The following are holomorphically equivalent:*

1. *The moduli space* $\mathcal{N}^N(k, \vec{\nu})$ *of irreducible, caloron Nahm data;*

2. The moduli space $\mathcal{M}_k^N$ of non-singular monad matrices.

Proof

Let $\mathcal{N}_C^N(k,\vec{\nu})$ denote the moduli space of Nahm complexes on the circle. By the discussion in section 2.5.1, we know that $\mathcal{N}_C^N(k,\vec{\nu}) \cong \mathcal{N}^N(k,\vec{\nu})$ holomorphically, so it remains to show that there exists a bijection

$$\xi : \mathcal{N}_C^N(k,\vec{\nu}) \longrightarrow \mathcal{M}_k^N.$$

Given a Nahm complex (α,β,u,w) on the circle, in a gauge where $i_p = \mathbb{1}$ for all p, we may obtain a set of non-singular monad matrices in the following way. Consider any point $\chi \in I_{N-1}$, and the connection on $[\chi, \mu_0+\chi]$ given by

$$\widetilde{\alpha}(s) = \begin{cases} \alpha_{N-1}(s), & s \in [\chi, \mu_{N-1}], \\ \alpha_p(s), & s \in I_p,\ p \neq N-1, \\ \alpha_{N-1}(\mu_0 - s), & s \in [\mu_0+\mu_N, \mu_0+\chi]. \end{cases} \tag{2.64}$$

Extending $\widetilde{\alpha}$ periodically gives a connection on the circle $\mathbb{R}/\mu_0\mathbb{Z}$. Let $\Omega(s,s_0)$ denote the parallel transport from s_0 to s along $\widetilde{\alpha}$. Then we set[13]

$$\begin{aligned} A &= \Omega(\mu_0+\chi,\chi)^{-1}, & B &= \beta_{N-1}(\chi), \\ C_0 &= \Omega(\mu_0+\mu_N,\chi)^{-1}u_0, & C_p &= \Omega(\mu_p,\chi)^{-1}u_p, \\ D_0 &= w_0^\dagger\Omega(\mu_0+\chi,\mu_0+\mu_N)^{-1}, & D_p &= w_p^\dagger\Omega(\mu_0+\chi,\mu_p)^{-1}, \end{aligned} \tag{2.65}$$

for $p = 1,\ldots,N-1$. The gauge transformations acting on these matrices via (2.63) as constructed are given by $g = g_{N-1}(\chi)$, where g_{N-1} is the I_{N-1} component of a gauge transformation $G \in \mathrm{Maps}(S^1, GL(k,\mathbb{C}))$. We need to check two things: that the complex Nahm equation (2.58) and matching conditions (2.59) imply the monad equation (2.60), and that the irreducibility of the Nahm complex implies the full-rank conditions (2.61), and hence (2.65) defines a mapping $\xi : \mathcal{N}_C^N(k,\vec{\nu}) \longrightarrow \mathcal{M}_k^N$.

[13] That is, A is the inverse holonomy from χ to $\mu_0+\chi$, C_p is the parallel transport of u_p to $\mu_0+\chi$ and D_p is the parallel transport of $w_p^\dagger$ from χ. This choice is in order for isomorphism to be equivalent to that described in [22] in the context of $SU(2)$ calorons.

First note that the complex Nahm equations (2.58) tell us

$$\begin{aligned}\beta_p(s) &= \Omega(s,\mu_{p+1})\beta_p(\mu_{p+1})\Omega(s,\mu_{p+1})^{-1}, \quad \forall s \in I_p,\ p = 0,\dots,N-2,\\ \beta_{N-1}(s) &= \Omega(s,\chi)\beta_{N-1}(\chi)\Omega(s,\chi)^{-1}, \qquad\qquad s \in I_{N-1}.\end{aligned}$$

Comparing the two forms of $\beta_0(\mu_0+\mu_N)$, from above, and from the matching conditions, and iterating through the matching points μ_p, we obtain

$$\begin{aligned}\Omega(\mu_0+\mu_N,\chi)\beta_{N-1}(\chi)\Omega(\mu_0+\mu_N,\chi)^{-1} - \Omega(\mu_0+\chi,\mu_0+\mu_N)^{-1}\beta_{N-1}(\chi)\Omega(\mu_0+\chi,\mu_0+\mu_N)\\ - u_0w_0^\dagger - \sum_{p=1}^{N-1}\Omega(\mu_0+\mu_N,\mu_p)u_pw_p^\dagger\Omega(\mu_0+\mu_N,\mu_p)^{-1} = 0.\end{aligned}$$

Using the constructed data (2.65), this becomes

$$\begin{aligned}\Omega(\mu_0+\mu_N,\chi)B\Omega(\mu_0+\mu_N,\chi)^{-1} - \Omega(\mu_0+\chi,\mu_0+\mu_N)^{-1}B\Omega(\mu_0+\chi,\mu_0+\mu_N)\\ - \Omega(\mu_0+\mu_N,\chi)CD\Omega(\mu_0+\chi,\mu_0+\mu_N) = 0.\end{aligned}$$

Unconjugating the CD term, and using $\Omega(\mu_0+\chi,\chi) = A^{-1}$, we obtain

$$[A,B] + CD = 0,$$

which is the monad equation. To check that the irreducibility of the Nahm complex implies the full-rank conditions for the data (2.65), there are two cases to consider:

1. Suppose there exists a 1-dimensional subspace $L \subset \mathbb{C}^k$ such that

$$L \subset \mathrm{Ker}\begin{pmatrix} A - y\mathbb{1}_k \\ B - x\mathbb{1}_k \\ D \end{pmatrix},$$

   for some $x, y \in \mathbb{C}$.

2. Suppose there exists $x, y \in \mathbb{C}$ such that

$$\mathrm{Im}\begin{pmatrix} x\mathbb{1}_k - B & A - y\mathbb{1}_k & C \end{pmatrix} \subset V,$$

   for some proper co-dimension 1 subspace $V \subset \mathbb{C}^k$.

It is relatively straightforward to see that case 1 corresponds to the existence of a sub-line bundle of K_p, for all p, which is both parallel, and invariant under β_p. Similarly, case 2 corresponds to the existence of a co-rank 1 parallel subbundle of K_p for all p, which is invariant under β_p.

Next we construct a mapping $\psi : \mathcal{M}_k^N \longrightarrow \mathcal{N}_C^N(k, \vec{\nu})$. To do this, first note that by using gauge transformations g_p such that

$$\frac{dg_0}{ds} = g_0\alpha_0 + \frac{d\gamma}{ds}\gamma^{-1}g_0, \quad \frac{dg_p}{ds} = g_p\alpha_p,\ p = 1, \ldots, N-1,$$

where $\gamma : I_0 \longrightarrow GL(k, \mathbb{C})$ is a path such that $\gamma(\mu_1) = \mathbb{1}$, and $\gamma(\mu_0 + \mu_N) = A^{-1}$, we may always transform a Nahm complex to a configuration such that $\alpha_p = 0$, $\beta_p = B_p$, for all $p = 1, \ldots, N-1$, $\alpha_0 = -d\gamma/ds\gamma^{-1}$, and $\beta_0 = \gamma B_0 \gamma^{-1}$, where B_p are constant matrices. Then, given a set of monad matrices (A, B, C, D), we may describe $\psi(A, B, C, D)$ by setting α as above,

$$\left(\left(u_0, w_0^\dagger\right), \left(u_p, w_p^\dagger\right)\right) = \left(\left(A^{-1}C_0, D_0\right), \left(C_p, D_pA^{-1}\right)\right), \tag{2.66}$$

for $p = 1, \ldots, N-1$, and

$$B_p = B - \sum_{q=p+1}^{N-1} C_q D_q A^{-1}, \quad p = 0, \ldots, N-1. \tag{2.67}$$

This may be easily shown to be a Nahm complex in the given gauge, furthermore, a gauge transformation (2.63) of the monad matrices corresponds to a constant gauge transformation of the Nahm complex. Finally, is a straightforward exercise to show that $\xi \circ \psi = \mathbb{1}_{\mathcal{M}_k^N}$ and $\psi \circ \xi = \mathbb{1}_{\mathcal{N}_C^N(k,\vec{\nu})}$, hence $\psi = \xi^{-1}$. □

Remark 2.5.7 *The isomorphism demonstrated between Nahm complexes and monad matrices (and hence between Nahm data and monad matrices) is not unique. For example, varying the choice of interval I_p where the base point χ belongs will give different isomorphisms. This variation corresponds to the action of the rotation map on the space of monad matrices.*

Combined with Theorem 2.4.4, Theorem 2.5.6 has some important consequences for calorons. Indeed, in the case $N = 2$, since the Nahm transform is a bijection, it follows that $\mathcal{M}_k^2$ fully parameterises the space $\mathcal{C}^2(k, \vec{\nu})$, so the moduli space of $SU(2)$ calorons may be understood by studying the moduli space of non-singular monad matrices. This is the result of Charbonneau and Hurtubise [22]. Now, whilst we do not necessarily have a bijective Nahm transform for $SU(N)$, Theorem 2.5.6 shows existence of a subspace of $\mathcal{C}^N(k, \vec{\nu})$ which is at most a complex manifold of dimension $2Nk$, but we conjecture that the monad description is a full parameterisation for all N.

Remark 2.5.8 *The full moduli space $\widetilde{\mathcal{M}}_k^N$ of monad matrices is well-known to parameterise the moduli space of charge k instantons on S^4 [32], and hence, Theorems 2.4.4 and 2.5.6 for $N = 2$ provide an embedding of $SU(2)$-caloron moduli into the space of $SU(2)$-instantons. In this way, calorons with all magnetic charges 0 are the most 'instanton-like' calorons.*

2.5.3 Basic properties of monad matrices

We shall conclude this chapter by covering some basic properties of monad matrices which will be utilised later on. Many of these results were first described in [43] with regards to the $N = 2$ monad matrices. We have reformulated them for our own purposes and generalised for all N.[14]

Let $\mathcal{I}$ denote the set of all words $\Pi(x_1, x_2)$ in two variables x_1 and x_2.

Lemma 2.5.9 $(A, B, C, D) \in \widehat{\boldsymbol{Md}}_k$ *if and only if* $[A, B] + CD = 0$ *and the following conditions hold:*

$$\text{For all } v \in \mathbb{C}^k \setminus 0, \text{ there exists } \Pi \in \mathcal{I} \text{ such that } D\Pi(A, B)v \neq 0. \tag{2.68}$$

[14] The notation we use for monad matrices may be translated to that in [43] via $(A, B, C, D) \leftrightarrow (\alpha_1, \alpha_2, b, a)$.

$$\sum_{\Pi\in\mathcal{I}} \Pi(A,B)\mathrm{Im}(C) = \mathbb{C}^k. \tag{2.69}$$

Proof

Let (A,B,C,D) satisfy the monad equations (2.60), and the conditions (2.68) and (2.69) stated in the lemma. Let $x, y \in \mathbb{C}$. For all $u \in \mathrm{Ker}(A - y\mathbb{1}) \cap \mathrm{Ker}(B - x\mathbb{1}) \cap \mathrm{Ker}(D)$, we have $D\Pi(A,B)u = 0$ for all $\Pi \in \mathcal{I}$. Thus, by (2.68), $u = 0$. Furthermore,

$$\mathbb{C}^k = \sum_{\Pi\in\mathcal{I}} \Pi(A,B)\mathrm{Im}(C) \subset \mathrm{Im}(A - y\mathbb{1}) + \mathrm{Im}(B - x\mathbb{1}) + \mathrm{Im}(C).$$

Hence (2.61) holds, so $(A,B,C,D) \in \widehat{\mathbf{Md}}_k$.

Conversely, let $(A,B,C,D) \in \widehat{\mathbf{Md}}_k$. Consider $V = \mathrm{Ker}(D)$, and define the subspace $V_\infty \subset V$ as

$$V_\infty = \{u \in V \,:\, \Pi(A,B)u \in V,\ \forall \Pi \in \mathcal{I}\}.$$

By the monad equations (2.60), $[A,B](V_\infty) = 0$, furthermore, V_∞ is both A and B invariant. So if $V_\infty \neq 0$, there exists a non-zero $u \in V_\infty$ which is a common eigenvector of A and B. But this violates the full-rank conditions (2.61), a contradiction. Thus $V_\infty = 0$. Now, let $v \in \mathbb{C}^k \setminus \{0\}$. If $v \notin V$, then $D\mathbb{1}v = Dv \neq 0$. If $v \in V$, since $V_\infty = 0$, this means there must exist some $\Pi \in \mathcal{I}$ such that $\Pi(A,B)v \notin V$, and hence $D\Pi(A,B)v \neq 0$. So in each case we have shown that (2.68) holds. Let $W = \sum_{\Pi\in\mathcal{I}} \Pi(A,B)\mathrm{Im}(C)$. Then $A(W), B(W), \mathrm{Im}(C) \subset W$, so A and B induce well-defined maps $a, b : \mathbb{C}^k/W \longrightarrow \mathbb{C}^k/W$, and the monad equations imply that

$$[a,b]\left(\mathbb{C}^k/W\right) = 0.$$

If $W \neq \mathbb{C}^k$, this means there is a shared eigenvector of a and b in $\mathbb{C}^k/W$, which since $\mathrm{Im}(C) \subset W$, contradicts the full-rank conditions (2.61). So $W = \mathbb{C}^k$, i.e. (2.69) holds. □

Corollary 2.5.10 *Let* $(A,B,C,D) \in \widehat{\mathcal{M}}_k$. *Then* $C, D \neq 0$.

Proof

If $C = 0$ or $D = 0$, this violates (2.69) or (2.68) respectively. □

Lemma 2.5.11 *The action of gauge transformations (2.63) is free on* $\widehat{\boldsymbol{Md}}_k$.

Proof

Let $(A, B, C, D) \in \widehat{\mathbf{Md}}_k$ and suppose that $g \in GL(k, \mathbb{C})$ is such that

$$(A, B, C, D) = (gAg^{-1}, gBg^{-1}, gC, Dg^{-1}).$$

Then for all $\Pi \in \mathcal{I}$, we have $\Pi(A, B) = g\Pi(A, B)g^{-1}$. Let $U = \mathrm{Im}(\mathbb{1} - g)$, and $u = (\mathbb{1} - g)v \in U$. Then for all $\Pi \in \mathcal{I}$, we have

$$D\Pi(A, B)u = D\left(\Pi(A, B)v - g\Pi(A, B)g^{-1}gv\right) = D\Pi(A, B)v - Dg^{-1}g\Pi(A, B)v = 0.$$

Hence, by Lemma 2.5.9 condition (2.68), we must have $U = 0$, i.e. $g = \mathbb{1}$. □

2.6 Summary and open problems

This chapter has, for the most part, been a review of $SU(N)$-calorons. We have carefully described their classifying data $(\vec{m}, \vec{\nu})$, and have emphasised some important properties of their moduli spaces, including the torus action, the interpretation in terms of constituent monopoles, and the existence of a large gauge transformation which cyclically permutes the constituents, namely the rotation map. We have additionally given a brief overview of the relationships between calorons, instantons, and monopoles. Indeed, calorons interpolate between instantons at the large period limit ($\mu_0 \longrightarrow 0$), and monopoles at the large scale limit ($\mu_0 \longrightarrow \infty$). Calorons are also explicitly related to monopoles on $\mathbb{R}^3$ via the loop group interpretation, and also in how monopoles are a special case of

calorons. We have also seen how $SU(2)$ calorons are naturally embedded into the space of instantons via the monad matrix description.

The key techniques for understanding calorons, which we shall utilise throughout the next chapter, are the Nahm and monad matrix data for calorons. We have only described this data in the case where all of the magnetic charges are 0, as this is the only case for which we will be interested later. In particular, the $(k, \ldots, k)$-caloron Nahm data has been described in terms of a monad construction, determined by a moduli space of complex matrices, and this is our generalisation of a result given for $SU(2)$-calorons by Charbonneau and Hurtubise in [22]. In fact, they go further, by defining monad matrices which parameterise $\mathcal{C}^2(\vec{m}, \vec{\nu})$, for all charges $\vec{m}$, not just $\vec{m} = (k, k)$. We expect that the same can be done analogously for $SU(N)$-calorons, but this remains to be considered.

Probably the most important open problem that remains from what we have discussed so far is the bijectivity of the Nahm transform for all N. If this is true, then a full monad description of $\vec{m}$-calorons could be a way to prove that the moduli space really is a complex manifold of dimension $2\sum_p m_p$. Another important open problem in this area is whether the Nahm transform is a hyperkähler isometry, which has been shown to be true for a variety of cases of instantons and monopoles.

Chapter 3

Symmetric calorons

3.1 The instanton metric

Let D^A be a connection on a vector bundle $V \longrightarrow M$, which we shall assume is hermitian for simplicity. In the moduli space $\mathcal{D}(M)/\mathcal{G}$ of connections, a natural way to find a tangent vector to D^A is by linearisation, that is, identify tangent vectors with a one-form $a \in \Lambda^1(M, \mathfrak{u}(N))$ such that a is orthogonal to the gauge orbits. An infinitesimal gauge transformation $\exp(\epsilon\delta g)$ induces a tangent vector $[\delta g, A] - d\delta g$, which is L^2-orthogonal to a if and only if

$$\begin{aligned} 0 &= \int_M \mathrm{tr}\left([\delta g, A] \wedge \star a - d\delta g \wedge \star a\right) \\ &= \int_M \mathrm{tr}\left(\delta g A \wedge \star a - A\delta g \wedge \star a + \delta g d \star a\right) \\ &= \int_M \mathrm{tr}\ \left(\delta g(A \wedge \star a + \star a \wedge A + d \star a)\right), \end{aligned}$$

where in the last two lines we have used integration by parts, the cyclicity of the trace, and the anti-commutability of the wedge-product on coordinate 1-forms. We thus require that a satisfies the equation

$$d \star a + A \wedge \star a + \star a \wedge A = 0. \tag{3.1}$$

Note that with respect to local coordinates $\{e_0, \ldots, e_3\}$ of M, we have

$$\begin{aligned} D^A \star a &= \frac{1}{6} \left(\partial_\mu (\star a)_{\nu\rho\sigma} + [A_\mu, (\star a)_{\nu\rho\sigma}]\right) de^\mu \wedge de^\nu \wedge de^\rho \wedge de^\sigma \\ &= \frac{1}{6} \left((\partial_\mu (\star a)_{\nu\rho\sigma} + A_\mu (\star a)_{\nu\rho\sigma}) \, de^\mu \wedge de^\nu \wedge de^\rho \wedge de^\sigma \right. \\ &\qquad \left. + (\star a)_{\nu\rho\sigma} A_\mu de^\nu \wedge de^\rho \wedge de^\sigma \wedge de^\mu \right) \\ &= d \star a + A \wedge \star a + \star a \wedge A, \end{aligned}$$

so that, locally, (3.1) is equivalent to $D^A \star a = 0$.

Let T_A denote the space of all such tangent vectors to the connection D^A. A metric g^A for the moduli space of connections is hence given by the L^2 metric on T_A, i.e. for $a_1, a_2 \in T_A$,

$$g^A(a_1, a_2) := -\int_M \mathrm{tr} \, (a_1 \wedge \star a_2) \, . \tag{3.2}$$

If D^A is anti-self-dual, we also require that the linearisation of the curvature

$$da + A \wedge a + a \wedge A, \tag{3.3}$$

is an anti-self-dual element of $\Lambda^2(M, \mathfrak{u}(N))$. Therefore, the tangent space T_A to an instanton D^A is given by all $a \in \Lambda^1(M, \mathfrak{u}(N))$ satisfying (3.1) and (3.3), with metric (3.2).

For various examples of instantons, and monopoles, it is possible to show that the metric (3.2) is hyperkähler [7, 12, 34, 54]. This notion arises by recognising the three components of the ASD equations as moment maps, which can be used to describe a hyperkähler quotient. The moduli space of Nahm data is also equipped with a hyperkähler metric, constructed in an analogous way [25], and the Nahm transform for monopoles has been shown to be an isometry [87]. In the case of $(1, \ldots, 1)$ calorons, the moduli space and metric have been explicitly constructed [70], and the Nahm transform shown to be a hyperkähler isometry. It is still only conjectured that that the same holds for all $(\vec{m}, \vec{\nu})$-calorons, including whether its metric is hyperkähler in general.

3.2 Isometries

In this section, we shall describe various actions on the moduli spaces $\mathcal{C}^N(\vec{m},\vec{\nu})$ which are isometries of the moduli space metric (3.2) for calorons. These can be classified into three types:

- 'Euclidean isometries' induced from isometries of $S^1 \times \mathbb{R}^3$;
- 'Gauge group isometries' given by unframed gauge transformations;
- 'Large gauge transformations', given by strictly un-periodic gauge transformations at infinity, which nevertheless leave the caloron periodic.

We shall describe all of these actions on the space of caloron *configurations*, and they are all unique up to gauge transformations. Therefore, there is a unique induced action on the moduli space.

3.2.1 Euclidean isometries

It is straightforward to show that the anti-self-dual equations (1.3) are invariant under orientation-preserving conformal transformations $\phi : M \longrightarrow M$, where the effect on D^A is the pull-back $A \mapsto \phi^* A$. Since $\phi^* V$ is isomorphic to V, this defines an action on the space of all anti-self-dual connections which is unique up to gauge transformations, and hence induces an action on the moduli space. When ϕ is an isometry of M, this action on the moduli space is clearly an isometry of (3.2).

For calorons, $M = S^1 \times \mathbb{R}^3$, and the set of conformal maps is exactly the set of isometries. The orientation preserving subgroup is given by

$$\mathrm{Isom}(S^1 \times \mathbb{R}^3)_+ \cong (O(2) \times E(3))_+, \tag{3.4}$$

where $O(2)$ denotes the isometries of S^1, $E(3)$ is the euclidean group generated by rotations, translations, and reflections in $\mathbb{R}^3$, and the subscript $+$ denotes orientation preserving. The notion of 'orientation preserving' here is decoded by only including elements $(\mathfrak{S}, \mathfrak{R}) \in O(2) \times O(3)$ satisfying

$$\det \mathfrak{S} \det \mathfrak{R} > 0. \tag{3.5}$$

In order for these transformations to be well-defined on the moduli spaces of calorons, we also need to check that the framing (2.1) is preserved, that is $\phi^*(V, f) \cong (V, f)$ for all $\phi \in \mathrm{Isom}(S^1 \times \mathbb{R}^3)_+$. It is easy to see that for subgroups of $SO(2) \times SO(3)$, and translations of $\mathbb{R}^3$, this holds. However, there is one generator of $\mathrm{Isom}(S^1 \times \mathbb{R}^3)_+$ which affects the boundary data non-trivially, namely the *parity transformation* $\sigma \in (O(2) \times O(3))_+$ defined by $\sigma(t, \vec{x}) = (-t, -\vec{x})$. This transforms the asymptotic connection a_∞ and Higgs field Φ_∞, seen in (2.4), as

$$\Phi_\infty(z) \mapsto -\Phi_\infty(-z), \quad (a_\infty)_i(z) \mapsto -(a_\infty)_i(-z),$$

where $z = (z_1, z_2)$ is a coordinate on S^2_∞, and $i = 1, 2$. As a result, the eigenvalues μ_p, and magnetic charges k_p transform as

$$\begin{aligned} \mu_p &\mapsto -\mu_{N-p+1}, \\ k_p &\mapsto -k_{N-p+1}, \end{aligned} \tag{3.6}$$

for all $p = 1, \ldots, N$, and so as it stands, the parity transformation σ is a map between two not necessarily equal moduli spaces. The condition for which the moduli spaces are the same is when the set of all μ_p and k_p is preserved under (3.6). This may be seen as setting the μ_p (and k_p) for $p = 1, \ldots, \lfloor \frac{N}{2} \rfloor$ to be strictly positive, and for $p = \lceil \frac{N}{2} \rceil + 1, \ldots, N$ to be strictly negative, in direct reflectional symmetry to the positive half. In the case N is odd, this forces $\mu_q = k_q = 0$ for $q = \lceil \frac{N}{2} \rceil$. Only in these cases does σ induce a well-defined isometric action on the corresponding caloron moduli spaces.

The actions of subgroups of the group (3.4) on the appropriate moduli spaces of calorons are known as the **euclidean isometries**.

3.2.2 Unframed gauge transformations

Recall that caloron moduli spaces are defined as the orbits of caloron configurations under *framed gauge transformations*, that is $g : S^1 \times \mathbb{R}^3 \longrightarrow SU(N)$ such that $g = \mathbb{1}$ on S^2_∞. An **unframed gauge transformation** is a gauge transformation such that $g \neq \mathbb{1}$ on S^2_∞. The action of unframed gauge transformations is an isometry of the space of all ASD connections via (1.9), simply because the metric is gauge invariant. However, this action does not necessarily extend to the moduli spaces $\mathcal{C}^N(\vec{m}, \vec{\nu})$. This extension exists only when the gauge transformations at ∞, given by $g|_{S^2_\infty}$, are automorphisms of W_∞, that is, they respect the decomposition (2.2) into line bundles. These correspond to an action of the maximal torus T^{N-1} in $SU(N)$, and may be summarised as the set of bundle automorphisms $P(\vec{\varphi}) : V \longrightarrow V$, such that the restriction $P(\vec{\varphi})_\infty : W_\infty \longrightarrow W_\infty$ is of the form

$$P(\vec{\varphi})_\infty = e^{-\imath\varphi_p}, \quad \text{on } \mathcal{O}(k_p), \quad p = 1, \ldots, N, \tag{3.7}$$

where $\vec{\varphi} = (\varphi_1, \ldots, \varphi_N)$ is a *phase vector* satisfying $\varphi_1 + \cdots + \varphi_N = 0 \pmod{2\pi}$. We will often refer to this action of T^{N-1} as a **phase action**, or **phase vector action**.

3.2.3 The rotation map

Recall from section 2.3.3 that the rotation map is a correspondence

$$\rho_{\mathcal{C}} : \mathcal{C}^N(m_1, \ldots, m_N, \nu_1, \ldots, \nu_N) \longrightarrow \mathcal{C}^N(m_2, \ldots, m_N, m_1, \nu_2, \ldots, \nu_N, \nu_1).$$

This correspondence is given explicitly by a 'large gauge transformation', namely the bundle map (2.23). Whilst the associated gauge transformation is not periodic, it still has a well-defined action on the space of all calorons, given by (2.26). It is straightforward to see that the rotation map is an isometry between the corresponding moduli spaces as the metric is gauge-invariant.

In general, the rotation map corresponds to an overall $\mathbb{Z}_N$ action on the union of all caloron moduli spaces, but is not automorphic, and so not an isometry 'action' on a specific moduli space. As was the case with the parity transformation σ, certain conditions on the boundary data need to be met in order for the rotation map to induce a well-defined action. From (2.21), we see that in the cases such that $m_p = m_q$ and $\nu_p = \nu_q$ for all $p, q \in \{1, \ldots, N\}$, the rotation map is an example of an isometry of a single moduli space. This specific set of boundary data corresponds to the case where the magnetic charges satisfy $k_p = 0$, and the masses ν_p of each monopole constituent is equal to μ_0/N, for all $p = 1, \ldots, N$. These are a subset of the calorons that we have described in detail with regards to their Nahm and monad matrix data at the end of chapter 2, namely the $(k, \ldots, k)$-calorons of equal monopole mass.

Since we will be ultimately interested in fixed points under the action of groups containing the rotation map, we shall mostly concern ourselves with the moduli spaces for which the rotation map acts, namely $\mathcal{C}^N_k := \mathcal{C}^N(k, \ldots, k, \mu_0/N, \ldots, \mu_0/N)$. We shall also denote the corresponding configuration space by $\mathcal{A}^N_k$. We note that in these moduli spaces, the magnetic charges satisfy $k_p = 0$ for all $p = 1, \ldots, N$, and the eigenvalues μ_p take the form

$$\mu_p = \frac{N + 1 - 2p}{2N}\mu_0, \quad p = 1, \ldots, N, \tag{3.8}$$

so that under the rotation map, they are preserved. As a consequence, the intervals I_p are preserved under the rotation map $\rho_{\mathcal{N}}$ on Nahm data. In addition, the action of the parity transformation $\sigma(t, \vec{x}) = (-t, -\vec{x})$ preserves this choice of magnetic charges and eigenvalues, as can easily be checked from (3.6).

3.2.4 Isometry groups and symmetric calorons

The group $\mathcal{F}$, consisting of all euclidean isometries, unframed gauge transformations, and the rotation map, acts on the space $\mathcal{A}^N_k$ in a way that is unique up to gauge transformations.

The total group of isometries of the moduli space $\mathcal{C}_k^N$ (and its metric (3.2)) is therefore given by $\mathcal{S} := \mathcal{F}/\mathcal{G}$, and satisfies the isomorphism

$$\mathcal{S} \cong \left(T^{N-1} \rtimes \mathbb{Z}_N\right) \rtimes \left(O(2) \times E(3)\right)_+ . \tag{3.9}$$

The semi-direct products appear in (3.9) due to the fact that the rotation map, parity transformation, and translation $\mathfrak{S}_\theta : t \mapsto t + \theta/\mu_0$ interact non-trivially with each other and with the action of a phase vector. More precisely, $\mathbb{Z}_N$ acts on $T^{N-1} \subset SU(N)$ via

$$\rho \cdot P(\vec{\varphi}) = S_N^{-1} P(\vec{\varphi}) S_N, \tag{3.10}$$

where S_N is the $N \times N$ **standard shift matrix**

$$S_N = \left(\begin{array}{ccc|c} 0 & \cdots & 0 & 1 \\ \hline & & & 0 \\ & \mathbb{1}_{N-1} & & \vdots \\ & & & 0 \end{array}\right), \tag{3.11}$$

the parity transformation σ acts on $T^{N-1} \rtimes \mathbb{Z}_N$ via

$$\sigma \cdot \rho = \rho^{-1}, \tag{3.12}$$

$$\sigma \cdot P\left((\varphi_1, \ldots, \varphi_N)\right) = P\left((\varphi_N, \ldots, \varphi_1)\right), \tag{3.13}$$

and the translation $\mathfrak{S}_\theta$ acts on $T^{N-1} \rtimes \mathbb{Z}_N$ as

$$\mathfrak{S}_\theta \cdot \rho = \mathfrak{S}_\theta^* \rho, \tag{3.14}$$

$$\mathfrak{S}_\theta \cdot P(\vec{\varphi}) = P(\vec{\varphi}). \tag{3.15}$$

Remark 3.2.1 *It is clear from the above relationships that the contribution of the rotation map ρ, and the parity transformation σ, make up an N-fold dihedral group. However, we choose to present the isometry group $\mathcal{S}$ as (3.9) to highlight the distinction between the euclidean isometries, and the gauge transformation type isometries.*

Also note that the relationship (3.14) is equivalent to saying that a translation by θ/μ_0 in S^1 affects the rotation map by right-multiplication of the overall phase vector

$$(\theta(1/N-1), \theta/N, \ldots, \theta/N).$$

The main purpose of this chapter is find 'symmetric calorons', that is, fixed points under the action of subgroups of $\mathcal{S}$. More formally:

Definition 3.2.2 *Let $H \subset \mathcal{S}$ be a subgroup. A caloron $D^A \in \mathcal{C}_k^N$ is called H-**symmetric** if its connection 1-form satisfies $[h \cdot A] = [A]$ for all $h \in H$, where $[\cdot]$ denotes the framed gauge equivalence classes. We denote by $\mathcal{C}_k^N(H)$ the set of all H-symmetric calorons.*

3.3 Group actions on Nahm data and monads

Much of the historical success in constructing symmetric monopoles and instantons utilised indirect methods, for example the ADHM and Nahm constructions, and analogues to monad matrix data [3, 43, 55, 83]. This motivates us to look to the Nahm and monad data in order to construct symmetric calorons. This has been done before in the context of caloron Nahm data [49, 90, 122]. Until a recent publication [30], which is ours, the caloron monad matrices had not been employed for the purpose of symmetric constructions.

Of course, in order to use the Nahm and monad data for finding fixed points, we need to understand the corresponding actions of the generators of $\mathcal{S}$ on these data. These generators are summarised as follows.

1. The **translations** in $S^1 \times \mathbb{R}^3$ are generated by $(\mathfrak{S}_\theta, \vec{v}) \in SO(2) \times \mathbb{R}^3$, representing the euclidean isometry $(t, \vec{x}) \mapsto (t + \theta/\mu_0, \vec{x} + \vec{v}) \in S^1 \times \mathbb{R}^3$.

2. The **rotations** in $\mathbb{R}^3$ are generated by $(\mathbb{1}, \mathfrak{R}(\vec{n}, \phi)) \in SO(2) \times SO(3)$, where $\mathfrak{R}(\vec{n}, \phi)$ represents a rotation by angle ϕ around a fixed unit axis $\vec{n} = (n_1, n_2, n_3) \in \mathbb{R}^3$. This generator is a euclidean isometry, and acts on $S^1 \times \mathbb{R}^3$ by $(t, x^j) \mapsto \left(t, \sum_{k=1}^3 \mathfrak{R}_{jk} x^k\right)$, where the components $\mathfrak{R}_{jk}$ may be written as

$$\mathfrak{R}_{jk} = \begin{cases} \cos^2 \frac{\phi}{2} + \sin^2 \frac{\phi}{2} \left(2n_j^2 - 1\right), & \text{if } j = k, \\ 2n_j n_k \sin^2 \frac{\phi}{2} + \epsilon_{jkl} n_l \sin \phi, & \text{if } j \neq k. \end{cases}$$

3. The **parity transformation** $\sigma \in (O(2) \times O(3))_+$, represented by the element $\sigma = \left(\begin{pmatrix} 1 & 0 \\ 0 & -1 \end{pmatrix}, \begin{pmatrix} -1 & 0 & 0 \\ 0 & -1 & 0 \\ 0 & 0 & -1 \end{pmatrix} \right)$. This is the final euclidean isometry, and acts on $S^1 \times \mathbb{R}^3$ via $(t, \vec{x}) \mapsto (-t, -\vec{x})$.

4. The **phase vectors** $P(\vec{\varphi}) \in T^{N-1}$.

5. The **rotation map** $\rho \in \mathbb{Z}_N$.

6. The translation $\mathfrak{S}_\theta$ may be used to define the **circle translation** S_θ, which is the composition of $\mathfrak{S}_\theta$ with the parallel transport along the t-direction from $t = 0$ to $t = \theta/\mu_0$. That is $S_\theta = \mathfrak{S}_\theta \circ P(\vec{\varphi}_\theta)$, where

$$\vec{\varphi}_\theta = \left(\frac{\theta}{\mu_0} \mu_1, \ldots, \frac{\theta}{\mu_0} \mu_N \right),$$

where μ_p are set as in (3.8). This transformation has the advantage over $\mathfrak{S}_\theta$ that it commutes with the rotation map.

The actions of these generators on Nahm data and monads are given in tables 3.1 and 3.2.[1] As with calorons, we have really only described them as actions on the configuration spaces, but they are again able to be lifted to the respective moduli spaces. Importantly, we are only able to derive actions on monad matrices for euclidean subsets of $\mathcal{S}$ which

[1]The action of $\mathfrak{S}_\theta$ may be easily extracted by the formula $\mathfrak{S}_\theta = S_\theta \circ P(\vec{\varphi}_\theta)^{-1}$.

fix the x^1-axis, and for further simplicity, we have only stated the actions for euclidean subgroups of $SO(2) \times E(2)$. The simple reason for this restriction is due to the nature of the isomorphism between Nahm data and Nahm complexes – it reduces the structure of the data to be holomorphic, and as such, the actions we describe are the only ones which are immediately compatible with this holomorphic structure. This is analogous to the restriction of Donaldson rational maps [33] for monopoles. Nevertheless, it still remains an important open problem to derive the full $SO(3)$ action on such objects, or better, to derive analogous data which has such an action, for example an analogue of the Jarvis rational map [67, 68].

Element of $\mathcal{S}$	Action on $\mathcal{N}_k^N$ via $(T_p^\lambda, (u_p, w_p)) \mapsto \star$
$(S_\theta, \vec{v})$	$\left(T_p^0 + \imath\frac{\theta}{\mu_0}, T_p^j + \imath v^j, (u_p, w_p)\right)$
$(\mathbb{1}, \mathfrak{R}(\vec{n}, \phi))$	$\left(T_p^0, \sum_{k=1}^3 \mathfrak{R}_{jk} T_p^k, \left(\overline{a}u_p - bw_p, \overline{b}u_p + aw_p\right)\right)$
σ	$\left(-T_{N-p}^\lambda(-s), (u_{N-p+1}, w_{N-p+1})\right), p = 1, \ldots, N-1,$ $\left(-T_0^\lambda(\mu_0 - s), (u_1, w_1)\right), p = 0$
$P(\vec{\varphi})$	$\left(T_p^\lambda, e^{\imath\varphi_p}(u_p, w_p)\right), p = 1, \ldots, N-1$ $\left(T_0^\lambda, e^{\imath\varphi_N}(u_0, w_0)\right), p = 0$
ρ	$(T_0(s + (N-1)\mu_0/N), (u_0, w_0)), p = N-1,$ $\left(T_{p+1}^\lambda(s - \mu_0/N), (u_{p+1}, w_{p+1}\right), p = 0, \ldots, N-2$

Table 3.1: The actions of the various generators of $\mathcal{S}$ on the moduli space $\mathcal{N}_k^N$.

In the tables, we have introduced the following shorthands:

$$\begin{gathered} a = \cos\tfrac{\phi}{2} + \imath n_1 \sin\tfrac{\phi}{2}, \quad b = \sin\tfrac{\phi}{2}\,(n_2 + \imath n_3)\,, \\ \sigma_\theta = \operatorname{diag}\left\{e^{\imath\frac{\theta(N+1-2p)}{2N}}\right\}_{p=0}^{N-1}, \quad \widetilde{\sigma}_\theta = \operatorname{diag}\left\{e^{\imath\frac{\theta(N-1+2p)}{2N}}\right\}_{p=0}^{N-1}, \\ q_{\vec{\varphi}} = \operatorname{diag}\{\varphi_N, \varphi_1, \ldots, \varphi_{N-1}\}. \end{gathered} \tag{3.16}$$

It is straightforward to see via the construction (2.65) and (2.53) that the actions on monad matrices correspond precisely to those on Nahm data, up to gauge transformations.

Element of $\mathcal{S}$	Action on $\mathcal{M}_k^N$ via $(A,B,C,D)\mapsto\star$
$(S_\theta,(v^1,0,0))$	$\left(e^{\imath\theta-v^1}A,B,C\sigma_{\theta+\imath v^1},\widetilde{\sigma}_{\theta+\imath v^1}D\right)$
$(\mathbb{1},\mathfrak{R}(\vec{x^1},\phi))$	$\left(A,e^{-\imath\phi}B,e^{-\imath\frac{\phi}{2}}C,e^{-\imath\frac{\phi}{2}}D\right)$
$P(\vec{\varphi})$	$\left(A,B,Cq_{\vec{\varphi}},q_{\vec{\varphi}}^{-1}D\right)$
ρ	$\left(A,B-\sum_{q=1}^{N-1}C_qD_qA^{-1},AC_{p+1},C_0,D_{p+1}A^{-1},D_0\right),p=0,\dots,N-2$

Table 3.2: The actions of the various compatible generators of $\mathcal{S}$ on the moduli space $\mathcal{M}_k^N$

Understanding how these actions relate to the actions on calorons requires analysing their effect on the Nahm operator (2.36). For the rotation map and phases, this has been discussed in section 2.4.2. For the euclidean isometries, it is best to break it down by generator. The standard technique is to view the $SO(3)$ rotations of $\mathbb{R}^3$ as elements of $SU(2)$, via the double covering

$$\begin{array}{rccc} \chi: & SU(2) & \longrightarrow & SO(3) \\ & h & \mapsto & h: \begin{array}{ccc}\mathbb{R}^3 & \longrightarrow & \mathbb{R}^3 \\ x & \mapsto & hxh^{-1},\end{array}\end{array} \tag{3.17}$$

where $h\in SU(2)$ is viewed as a unit quaternion, and $x\in\mathbb{R}^3$ as an imaginary quaternion. Similarly, for the parity transformation σ, we may first view it as an element of $SO(4)$, and then as the element $(\imath\sigma^3,\imath\sigma^3)\in SU(2)\times SU(2)$ via the analogous double covering

$$\begin{array}{rccc} \eta: & SU(2)\times SU(2) & \longrightarrow & SO(4) \\ & (h,h') & \mapsto & (h,h'): \begin{array}{ccc}\mathbb{R}^4 & \longrightarrow & \mathbb{R}^4 \\ x & \mapsto & hxh',\end{array}\end{array} \tag{3.18}$$

where here $x\in\mathbb{R}^4$ is viewed as a quaternion. Using these, it is straightforward to see that the actions we have described on Nahm data correspond to the correct actions on calorons, up to automorphisms of $V\cong S^1\times\mathbb{R}^3\times\mathrm{Ker}(\not{D})$.

For most of the euclidean isometries, it is clear that the actions are equivalent modulo framed gauge transformations. However, for the parity transformation σ, and the circle

translation S_θ, it is only clear that these actions agree up to some, not necessarily framed, gauge transformation. Regardless of this, we shall always be considering actions which include a generic phase vector, and so this discrepancy does not remove any generality, and we have chosen the actions as described simply for later notational convenience. With this in mind, from this point forward, whenever we are referring to an element of $(O(2) \times O(3))_+$, we will replace the euclidean generator $\mathfrak{S}_\theta \in SO(2)$ with the circle translation $S_\theta \in SO(2)$.

A further remark is to recognise that the action of ρ on monad matrices is rather complicated in comparison to the action of ρ^{-1}, given by

$$(A, B, C, D) \mapsto \left(A, B - C_{N-1}D_{N-1}A^{-1}, AC_{N-1}, C_{p-1}, D_{N-1}A^{-1}, D_{p-1}\right),$$

for $p = 1, \ldots, N-1$. Since the $\mathbb{Z}_N$ action on the moduli space is generated equivalently by ρ^{-1}, we may without loss of generality consider this generator when we act with the rotation map on monad matrices.

3.4 Hunting for invariants

In section 3.5, we shall construct examples of symmetric calorons with cyclic symmetries. Before we do that, it is worthwhile discussing some preliminary results and conventions regarding which of the isometries described in the previous sections may have fixed points, and which do not. One immediate result is that there are no fixed points in $\mathcal{C}_k^N$ under any translations of $\mathbb{R}^3$. This is obvious, as if such a symmetric caloron existed, it would not have finite action. For the circle translations, it is possible that there are fixed points, however there are restrictions:

Proposition 3.4.1 *Let $H \subset \mathcal{S}$ contain a non-trivial contribution of the euclidean action $\mathfrak{S}_\theta : t \mapsto t + \theta/\mu_0$, or the circle translation S_θ. Then $\mathcal{C}_k^N(H) \neq \emptyset$ only if $\theta = 2r\pi/k$, for some $r \in \mathbb{Z}$.*

Proof

The action of $\mathfrak{S}_\theta$ on monad matrices is the same as the action of $S_\theta \circ P(\vec{\varphi}_\theta)^{-1}$, and both this and S_θ affect the matrix $A \in GL(k,\mathbb{C})$ via $A \mapsto e^{\imath\theta}A$. This is invariant in $\mathcal{M}_k^N$ only if the eigenvalues of A are preserved. In particular, since $\det A \neq 0$, we must have $e^{\imath k\theta} = 1$, that is, there exists $r \in \mathbb{Z}$ such that $\theta = 2r\pi/k$. □

What Proposition 3.4.1 says is that the only translations of S^1 that may yield fixed points are those of finite cyclic type. However, there is more subtlety at play that this result does not reveal. In order to have true invariant solutions, these circle translations must be considered along with non-trivial transformations of $\mathbb{R}^3$. Indeed, if a $(k,\ldots,k)$-caloron were seen to be invariant under the action $S_{2r\pi/k}$ alone, then, up to the action of a phase vector, this is the same as saying it has r/k times its expected period, i.e. we would be studying calorons with period $2r\pi/k\mu_0$. Such a caloron is more efficiently described by a lower charge caloron when $r/k \in \mathbb{Z}$, or simply one with a different value of μ_0.

3.4.1 The role of the rotation map

Up until now, no study of symmetric calorons has ever asked if groups containing the rotation map have fixed points, but it is an interesting consideration that we would like to address. Besides the fact that nobody has done it before, a good motivation is due to the kinship between calorons and monopoles. From the loop group perspective, we see that $SU(N)$ calorons may be viewed as N constituent $SU(2)$ monopoles[2], and the rotation map is a way of relating these monopoles to each other. Therefore, calorons which are symmetric with respect to a group containing the rotation map may in some way be interpreted as consisting of N identical symmetric monopoles. Another benefit of considering the rotation map has perhaps already been observed, but not commented on, and that is that its corresponding map on monad matrices (seen in table 3.2), to the best

[2]Strictly speaking this only applies to calorons with maximal symmetry breaking, but this is okay as all of our discussions have generally assumed this.

of the author's knowledge, has never before been noticed as a symmetry of the monad equations (2.60).[3] Due to the role and interest of these equations in related subjects [32, 125], considering this symmetry may shed light on otherwise overlooked properties of this integrable system.

In order to study the rotation map's role in the topic of symmetric calorons, it is beneficial to understand any restrictions on the types of symmetry groups to consider.

Proposition 3.4.2 *Let $H \subset \mathcal{S}$ be such that $P(\vec{\varphi})\rho^r \in H$, for some phase vector $\vec{\varphi}$ and $r \in \{1, \dots, N-1\}$. Then $\mathcal{C}_k^N(H) = \emptyset$.*

Proof

Let $g_{\vec{\varphi}} = P(\vec{\varphi})\rho^r \in H$, and suppose that $\mathcal{C}_k^N(H) \neq \emptyset$. Recalling the action of the rotation map (2.26), this means there exists a framed bundle isomorphism $\eta : V \otimes L^r \longrightarrow V$ such that the restriction $\eta_\infty : V_\infty \otimes L_\infty^r \longrightarrow V_\infty$ is an isomorphism. The notion of 'framed' in this context means that

$$g_{\vec{\varphi}} \cdot f = f \circ \eta_\infty, \tag{3.19}$$

where f is the framing (2.1), and $g_{\vec{\varphi}} \cdot f$ is the transformed framing from the action of the phase and the rotation map (2.26). We also require that the connection A is fixed, which means

$$g_{\vec{\varphi}} \cdot A = \eta^* A. \tag{3.20}$$

With respect to a global trivialisation of V, η may be described by a gauge transformation $h : \mathbb{R} \times \mathbb{R}^3 \longrightarrow SU(N)$ which satisfies

$$h\left(t + \frac{2\pi}{\mu_0}, \vec{x}\right) = \exp\left(\frac{2r\pi\imath}{N}\right) h(t, \vec{x}), \quad \forall\ (t, \vec{x}) \in \mathbb{R} \times \mathbb{R}^3.$$

Now, (3.20) implies that $h^{-1}P(\vec{\varphi})$ is covariantly constant (parallel) with respect to the connection $A \otimes 0 \otimes \cdots \otimes 0$. This in turn implies that the eigenvalues of $h^{-1}P(\vec{\varphi})$ must

[3] This is of course, only true in the case that the monad matrix A is invertible.

be constant, and hence the eigenvalues of h must be everywhere constant, including on $\mathbb{R} \times S^2_\infty$. But from (3.19), and the formulae (2.22)-(2.23) and (3.7), it is straightforward to see that the eigenvalues of h_∞ are

$$\lambda_p = \begin{cases} e^{-\imath\varphi_p} \exp\left(\imath \frac{(r-N)}{N} t\mu_0\right), & 1 \leq p \leq r, \\ e^{-\imath\varphi_p} \exp\left(\imath \frac{r}{N} t\mu_0\right), & r+1 \leq p \leq N, \end{cases}$$

which, since $r \neq N$, are clearly not constant. □

The upshot is, the rotation map (along with a phase contribution) cannot be a generator; in order to include the rotation map in the symmetry group, it must appear as part of a generator of the form

$$h = K_m \circ P(\vec{\varphi}) \circ \rho^r, \tag{3.21}$$

where $K_m \in SO(2) \times SO(3)$ generates a group of order $m \in \mathbb{Z}^+ \cup \{\infty\}$, and $r \in \{1, \ldots, N-1\}$. The contribution K_m must be suitably chosen so that the conditions discussed above are met. Along with various constraints on the combination of circle translations and spatial rotations (which are too many to discuss in full generality here), this in particular constrains the order m of the element K_m in (3.21).

Proposition 3.4.3 *Let $H \subset \mathcal{S}$ contain a generator of the form (3.21) for some order $m \in \mathbb{Z}^+$ element K_m, and let $r \in \{1, \ldots, N-1\}$. Then $\mathcal{C}^N_k(H) \neq \emptyset$ only if*

$$m = \frac{Nn}{\gcd(r, N)},$$

for some $n \in \mathbb{Z}^+$.

Proof

If $\mathcal{C}^N_k(H) \neq \emptyset$, then by definition there exists a caloron fixed by every element of H, so in particular is fixed by the element

$$h^m = \left(P(\vec{\varphi}) S_N^{-r}\right)^{m-1} \circ P(\vec{\varphi}) S_N^{(m-1)r} \circ \rho^{mr}. \tag{3.22}$$

Note that this equality holds by (3.10) and the straightforward result that K_m commutes with the rotation map and unframed gauge transformations.[4] If m is not as stated, then by (3.22), H contains an element of the form $h' = P(\vec{\varphi}')\rho^{r'}$, with $r' \in \{1, \ldots, N-1\}$, so there cannot be any such invariant caloron by Proposition 3.4.2. □

3.5 Cyclic calorons

The work of Braden and Sutcliffe on cyclically symmetric monopoles [14, 116] was very influential in furthering the understanding of monopole moduli spaces, and so it is certainly worthwhile studying cyclic calorons, that is, calorons invariant under various cyclic subgroups of $\mathcal{S}$. As discussed in the previous section, of particular interest are those groups which incorporate a non-trivial action of the rotation map. Our main results are showing existence of non-trivial fixed point sets in some special cases, and some explicit constructions of monad matrix and Nahm data in even more specific cases.

This section reproduces results published in [30], here in the more general context of $SU(N)$ calorons, with some additional results not found in [30].

3.5.1 Cyclic groups and rotation cyclic symmetries

The euclidean isometries that we shall be considering are generated from cyclic subgroups of $S^1 \times \mathbb{R}^3$, which act temporally as well as in space. Since we shall be utilising the monad matrix data to construct fixed points, we may only choose subgroups which preserve the chosen holomorphic structure, namely those which fix the x^1 axis. To this end, let

[4] This is true as we are considering S_θ as the $SO(2)$ generator, not $\mathfrak{S}_\theta$.

$K_m^i \in SO(2) \times SO(3)$ be defined by

$$K_m^i := \left(S_{\frac{2i\pi}{m}}, \begin{pmatrix} 1 & 0 & 0 \\ 0 & \cos\left(\frac{2\pi}{m}\right) & \sin\left(\frac{2\pi}{m}\right) \\ 0 & -\sin\left(\frac{2\pi}{m}\right) & \cos\left(\frac{2\pi}{m}\right) \end{pmatrix} \right), \tag{3.23}$$

for $m \in \mathbb{Z}^+$ and $i \in \mathbb{Z}_m$. This generates an order m cyclic subgroup of $SO(2) \times SO(3)$. From this, we may form the **rotation cyclic groups**[5]

$$\rho(C_{Nn}^{j,\vec{\varphi}}) := \left\langle K_{Nn}^{Nj} \circ P(\vec{\varphi}) \circ \rho^{-1} \right\rangle \subset \mathcal{S}, \tag{3.24}$$

for $n \in \mathbb{Z}^+$, $j \in \mathbb{Z}_n$, and $\vec{\varphi}$ a phase vector. It is straightforward to see that $\rho(C_{Nn}^{j,\vec{\varphi}})$ is a cyclic group of order Nn for all choices of $j, \vec{\varphi}$. Note that there are two possible avenues for generalisation, namely replacing ρ by ρ^r in (3.24), and replacing $Nj \in \mathbb{Z}_{Nn}$ by $i \in \mathbb{Z}_{Nn}$. However, we conjecture that the second of these considerations only yields solutions in the cases that we are already considering, that is $i = Nj$. This conjecture is certainly true in the the case $n = k$ as a result of Proposition 3.4.1, and it is straightforward to show by results in [30] that this also holds in general for the case $N = 2$.

Remark 3.5.1 *We have chosen to study cyclic groups involving the rotation map, but there are cyclic groups of the form*

$$C_n^{j,\vec{q}} = \left\langle K_n^j \circ P(2\vec{q}\pi/n) \right\rangle, \tag{3.25}$$

where $\vec{q} \in \mathbb{Z}^N$ such that $q_1 + \cdots + q_N = 0$, which do not include the rotation map. The work of Furuta and Hashimoto in [43] may be implicitly applied to study such cyclic calorons (at least in the case $N = 2$) by picking out the solutions for which the monad matrix $A \in GL(k, \mathbb{C})$. Importantly, the cyclic groups considered in [43] did not consider the rotation map.

[5] We have decided to act with ρ^{-1} due to the simpler form of its action on monad matrices. This is equivalent to acting with ρ in the case $N = 2$, as is the convention in [30].

To study the rotation cyclic symmetric calorons, we shall investigate $\rho(C_{Nn}^{j,\vec{\varphi}})$-invariant monad matrices, that is, $(A,B,C,D) \in \mathcal{M}_k^N$ such that

$$A = e^{\imath\frac{2j\pi}{n}} gAg^{-1}, \tag{3.26}$$

$$B = e^{-\imath\frac{2\pi}{Nn}} g\left(B - C_{N-1}D_{N-1}A^{-1}\right)g^{-1}, \tag{3.27}$$

$$C_0 = e^{-\imath\frac{\pi}{Nn}} e^{\imath\frac{j\pi}{Nn}(N+1)} e^{\imath\varphi_N} gAC_{N-1}, \tag{3.28}$$

$$C_p = e^{-\imath\frac{\pi}{Nn}} e^{\imath\frac{j\pi}{Nn}(1+N-2p)} e^{\imath\varphi_p} gC_{p-1}, \tag{3.29}$$

$$D_0 = e^{-\imath\frac{\pi}{Nn}} e^{\imath\frac{j\pi}{Nn}(N-1)} e^{-\imath\varphi_N} D_{N-1}A^{-1}g^{-1}, \tag{3.30}$$

$$D_p = e^{-\imath\frac{\pi}{Nn}} e^{\imath\frac{j\pi}{Nn}(N-1+2p)} e^{-\imath\varphi_p} D_{p-1}g^{-1}, \tag{3.31}$$

for some $g = g_{N,n,j,\vec{\varphi}} \in GL(k,\mathbb{C})$, and where $p = 1,\ldots,N-1$. To help solve these equations, it is worth also studying the $C_n^{Nj,0}$-invariant monads:

$$A = e^{\imath\frac{2Nj\pi}{n}} GAG^{-1}, \tag{3.32}$$

$$B = e^{-\imath\frac{2\pi}{n}} GBG^{-1}, \tag{3.33}$$

$$C = e^{-\imath\frac{\pi}{n}} GC\sigma_{2Nj\pi/n}, \tag{3.34}$$

$$D = e^{-\imath\frac{\pi}{n}} \widetilde{\sigma}_{2Nj\pi/n} DG^{-1}, \tag{3.35}$$

for $G \in GL(k,\mathbb{C})$. We denote by $\mathcal{M}_k^N(C_n^{Nj,0})$ the set of matrices in $\mathcal{M}_k^N$ satisfying (3.32)-(3.35), and denote by $\mathcal{M}_k^N(\rho(C_{Nn}^{j,\vec{\varphi}}))$ the set of matrices in $\mathcal{M}_k^N$ satisfying (3.26)-(3.30). We have the inclusion $\mathcal{M}_k^N(\rho(C_{Nn}^{j,\vec{\varphi}})) \subset \mathcal{M}_k^N(C_n^{Nj,0})$ by setting

$$G = e^{\imath\frac{j\pi}{n}(N-1)} g^N A. \tag{3.36}$$

To aid us in solving (3.26)-(3.31), we shall prove some necessary conditions for the existence of fixed points. The most important of these is the result given by Lemma 3.5.4, which translates to say that the matrix $G = e^{\imath\frac{\pi}{n}} g^N A$ may be chosen to be diagonal, with eigenvalues given precisely by set of n-th roots of unity. Using (3.36), this makes solving (3.32)-(3.35) much more manageable, and we may setup an ansatz for $\mathcal{M}_k^N(\rho(C_{Nn}^{j,\vec{\varphi}}))$. Ultimately, we will then only consider the case where $n = k$, which as a result of this statement about G, is the maximal order of a cyclic symmetry group we may consider.

Notation 3.5.2 *Before we embark on studying the symmetric solutions, we will first review, and prescribe our various notational decisions. So, from this point forward in this chapter, we shall always stick to the following notation conventions:* $k \in \mathbb{Z}^+$ *is the instanton number,* $N \geq 2$ *is the rank of the caloron,* $n \in \mathbb{Z}^+$ *defines the order* Nn *of the cyclic group* $\rho(C^{j,\vec{\varphi}}_{Nn})$*,* $j \in \mathbb{Z}_n$ *is the order of the circle translation, furthermore, we denote*

$$\aleph = \gcd(n, Nj), \quad \Gamma = \gcd(n, j), \quad \omega_r = e^{\imath \frac{2\pi r}{n}}, \quad \Omega = e^{\imath \frac{1+(N-1)j}{n}\pi}.$$

In addition, all indices of indexed objects shall be understood to obey their corresponding modular arithmetic, for example, we interpret the product $P = \prod_{p=1}^{3} x_{2p+1}$*, where the* x_r *are taken from the set* $\{x_1, x_2, x_3, x_4\}$*, as* $P = x_1^2 x_3$*. Finally, the letters* a, b, i, m, p, q, r *and* s *will always, unless otherwise specified, be used as dummy indices.*

Before we prove the main 'gauge-fixing' result, we need the following simple lemma.

Lemma 3.5.3 *Let* $(A, B, C, D) \in \mathcal{M}^N_k(\rho(C^{j,\vec{\varphi}}_{Nn}))$*. Then* $C_p, D_p \neq 0$ *for all* $p = 1, \ldots, N$*, furthermore,*

$$\left\{\Omega\omega_{n-(N-p)j}, \Omega\omega_{pj-1} \,:\, p = 0, \ldots, N-1\right\} \subset \mathrm{Eval}(G),$$

with

$$C_p \in \mathrm{Evec}\left(G, \Omega\omega_{n-(N-p)j}\right), \quad D_p \in \mathrm{Ecovec}\left(G, \Omega\omega_{pj-1}\right).$$

Proof

If $C_p = 0$ for some $p \in \{0, \ldots, N-1\}$, then by (3.29) and (3.28), this implies $C_q = 0$ for all q, i.e. $C = 0$. But this violates Corollary 2.5.10. A similar argument applies for D_p. The statement about the eigenspaces follows immediately from equations (3.34) and (3.35). □

Lemma 3.5.4 *For* $(A,B,C,D) \in \mathcal{M}_k^N(\rho(C_{Nn}^{j,\vec{\varphi}}))$, G *is diagonalisable, and the eigenvalues of* $\Omega^{-1}G$ *are the set of* n*-th roots of unity*

$$\mathrm{Eval}(\Omega^{-1}G) = \{\omega_p \,:\, p = 1,\dots,n\}.$$

Moreover, if ω_r *has multiplicity* $m \in \mathbb{N}$*, then so does* ω_q*, for all* q *such that* $q = r \pmod{\aleph}$.

Proof

If $(A,B,C,D) \in \mathcal{M}_k^N(\rho(C_{Nn}^{j,\vec{\varphi}}))$, then we may apply the symmetry equations (3.32)-(3.35) n times to yield

$$A = G^n A G^{-n}, \qquad B = G^n B G^{-n},$$
$$C = -e^{\imath j(N+1)\pi} G^n C, \quad D = -e^{\imath j(N-1)\pi} D G^{-n}.$$

Since the action of gauge transformations is free by Lemma 2.5.11, the above equations imply that $-e^{\imath j(1-N)\pi} G^n = \mathbb{1}$. So G is diagonalisable with eigenvalues λ satisfying $\lambda^n = e^{\imath\pi(1+(N-1)j)} = \Omega^n$. Hence

$$\emptyset \neq X \equiv \mathrm{Eval}(\Omega^{-1}G) \subset \{\omega_r \,:\, r = 1,\dots,n\}.$$

Let $\widetilde{G} = \Omega^{-1}G$. Now, if $\omega_r \in X$, let V_r denote the eigenspace of $\widetilde{G}$ with eigenvalue ω_r, and otherwise set $V_r = 0$. If $\{v_i\}_{i=1}^m \subset \mathbb{C}^k$ is a basis for V_r, by (3.32), we have for any $a \in \mathbb{Z}^+$,

$$\widetilde{G} A^a v_i = (\widetilde{G} A \widetilde{G}^{-1})^a \widetilde{G} v_i = \omega_{r-Nja} A^a v_i,$$

for all $i = 1,\dots,m$. As $A \in GL(k,\mathbb{C})$, $A^a v_i \neq 0$ for all $a \in \mathbb{Z}^+$, so these are eigenvectors with eigenvalues ω_{r-Nja}, for all $a = 1,\dots,n/\aleph$, moreover, $\{A^a v_i\}_{i=1}^m$ is a linearly independent set of non-zero vectors. Hence, the multiplicity of $\omega_r \in X$ is the same for all ω_q such that $q = r \pmod{\aleph}$. In particular, $V_r \neq 0$ if and only if $V_{r+a\aleph} \neq 0$ for all $a = 1,\dots,n/\aleph$. Now define the corresponding modular eigenspaces W_a, $a \in \{1,\dots,\aleph\}$ as

$$W_a := \bigoplus_{r=a \pmod{\aleph}} V_r.$$

By the above observations, the result hence follows if we show that $W_a \neq 0$ for all $a = 1, \ldots, \aleph$. By (3.32), and above $A(W_a) \subset W_a$ for all $a = 1, \ldots, \aleph$. We also have by (3.33) that $B(W_a) \subset W_{a+1}$ for all $a = 1, \ldots, \aleph$. Additionally, Lemma 3.5.3 shows that we have that $W_{pj}, W_{pj-1} \neq 0$ for all $p = 0, \ldots, N-1$.

Now, assume there exists $1 \leq s \leq \aleph$, $s \neq pj, pj-1$, for all $p = 0, \ldots, N-1$, such that $W_s = 0$. Then there exists $p \in \{0, \ldots, N-1\}$, and a pair (q, q') such that

$$pj \leq q < q' \leq (p+1)j - 1,$$

with $W_q, W_{q'} \neq 0$, and $W_r = 0$ for all $q < r < q'$, where all of these inequalities are understood cyclically modulo $\aleph$. Then, by the fact that $B(W_a) \subset W_{a+1}$, and Lemma 3.5.3, we have

$$B(W_q) = D(W_q) = 0.$$

Hence, as $A(W_a) \subset W_a$ for all a, we must have that for all $w \in W_q$ and $\Pi \in \mathcal{I}$,[6] that

$$D\Pi(A, B)w = 0,$$

which violates Lemma 2.5.9. Therefore $W_a \neq 0$ for all $a = 1, \ldots, \aleph$. □

Corollary 3.5.5 *$\mathcal{M}_k^N(\rho(C_{Nn}^{j,\vec{\varphi}})) \neq \emptyset$ only if $n \leq k$.*

Proof

This follows immediately from Lemma 3.5.4 as $n = |\mathrm{Eval}(G)| \leq k$. □

3.5.2 The case $n = k$

By Corollary 3.5.5, the largest rotation cyclic symmetry group we may consider is when $n = k$, and this is the case which we shall now pursue in more detail. In this case, by

[6] Recalling that $\mathcal{I}$ is the space of all non-commuting words in two variables.

Lemma 3.5.4, we may fix a basis so that G takes the **standard form**

$$G = \Omega \mathrm{diag}\{\omega_1, \dots, \omega_k\}, \tag{3.37}$$

where we recall that $\omega_r = e^{\imath \frac{2r\pi}{k}}$ is the r-th k-th root of unity. Letting $\vec{e}_i$ and $\vec{f}_i$ for $i = 1, \dots, k$ denote the standard basis vectors and covectors for $\mathbb{C}^k$ and $(\mathbb{C}^k)^*$ respectively, and S denote the $k \times k$ *standard shift matrix*

$$S = \left(\begin{array}{c|c} \begin{matrix} 0 & \cdots & 0 \end{matrix} & 1 \\ \hline & 0 \\ \mathbb{1}_{k-1} & \vdots \\ & 0 \end{array}\right),$$

we may hence solve (3.32)-(3.35) in this choice of basis to obtain a $C_k^{Nj,0}$-symmetric ansatz for $\mathcal{M}_k^N(\rho(C_{Nk}^{j,\vec{\varphi}}))$:

$$\begin{aligned} A = \mathrm{diag}\{\alpha_1, \dots, \alpha_k\} S^{k-Nj} \quad B = \mathrm{diag}\{\beta_1, \dots, \beta_k\} S, \\ C_p = u_p \vec{e}_{k-(N-p)j}, \qquad\qquad D_p = y_p \vec{f}_{pj-1}, \end{aligned} \tag{3.38}$$

where $\alpha_i, u_p, y_p \in \mathbb{C}^*$, and $\beta_i \in \mathbb{C}$, for $i = 1, \dots, k$, $p = 0, \dots, N-1$.

Remark 3.5.6 *Consider (A, B, C, D) as in (3.38). Then we have*

$$A^m \vec{e}_i = \left(\prod_{r=1}^{m} \alpha_{i-rNj} \right) \vec{e}_{i-mNj}, \tag{3.39}$$

$$B^m \vec{e}_i = \left(\prod_{r=1}^{m} \beta_{i+r} \right) \vec{e}_{i+m}, \tag{3.40}$$

$$\mathrm{Im}(C) = \mathrm{sp}_{\mathbb{C}^*}\{\vec{e}_{(p-N)j} \ : \ p = 0, \dots, N-1\}, \tag{3.41}$$

$$D\vec{e}_i = y_0 \delta_{i,k-1} \vec{b}_N + \sum_{q=1}^{N-1} y_q \delta_{i,qj-1} \vec{b}_q, \tag{3.42}$$

where $\vec{b}_q$ denotes the standard basis for $\mathbb{C}^N$.

The case $n = k$ is particularly nice due to the following important lemma:

Lemma 3.5.7 *Let* $(A, B, C, D) \in \mathcal{M}_k^N(\rho(C_{Nk}^{j,\vec{\varphi}}))$. *Then* $\det B \neq 0$.

Proof

By Lemma 3.5.4, we may write a representative $(A, B, C, D) \in \mathcal{M}_k^N(\rho(C_{Nk}^{j,\vec{\varphi}}))$ in the form as in (3.38). With this data, the monad equations (2.60) imply

$$\beta_i = \frac{\alpha_{i-Nj-1}}{\alpha_{i-Nj}}\beta_{i-Nj}, \quad i \in \{1, \dots, k\} \setminus \{qj \pmod k \,:\, q = 0, \dots, N-1\}. \tag{3.43}$$

We have $\det B \neq 0$ if and only if $\beta_i \neq 0$ for all $i = 1, \dots, k$. So, suppose $\beta_r = 0$ for some $r \in \{1, \dots, k\}$.

Case 1: $r \neq qj \pmod{\aleph}$**, for all** $q = 0, \dots, N-1$**.** From (3.43), this means $\beta_i = 0$ for all $i = r \pmod{\aleph}$. Define the vector spaces

$$E_i^{\aleph} = \mathrm{sp}_{\mathbb{C}}\{\vec{e}_n \,:\, n = i \pmod{\aleph}\}, \quad i \in \{1, \dots, \aleph\}.$$

By (3.39) and (3.40), we have that $A(E_i^{\aleph}) \subset E_i^{\aleph}$ for all i, and $B(E_{s-1}^{\aleph}) = 0$, where $s = r \pmod{\aleph}$. As $r \neq qj$, we also have by (3.42) that $D(E_{s-1}^{\aleph}) = 0$, again where $s = r \pmod{\aleph}$. Therefore, for all $v \in E_{s-1}^{\aleph}$, and $\Pi \in \mathcal{I}$, we have

$$D\Pi(A, B)v = 0,$$

which violates Lemma 2.5.9 since $E_i^{\aleph} \neq 0$ for all i. Hence, $\beta_r \neq 0$ for all $r \neq qj \pmod{\aleph}$, for all $q = 0, \dots, N-1$.

Case 2: $r = qj \pmod{\aleph}$ **for some** $q \in \{0, \dots, N-1\}$**.** Consider $g \in GL(k, \mathbb{C})$ in the form

$$g = \sum_{a=1}^{k} \mathrm{diag}\{\gamma_1^a, \dots, \gamma_k^a\} S^a, \quad \gamma_i^a \in \mathbb{C}. \tag{3.44}$$

Using this g as in (3.44), the symmetry equation (3.26) implies

$$\gamma_i^a = e^{-\imath\frac{2j\pi}{k}} \frac{\alpha_i}{\alpha_{i-a}} \gamma_{i+Nj}^a, \quad \text{for all } a = 1, \dots, k. \tag{3.45}$$

Since $\alpha_i \neq 0$ for all $i = 1, \ldots, k$, (3.45) tells us is that the sets

$$\mathcal{H}^a_m = \{\gamma^a_i \ : \ i = m \ (\text{mod } \aleph)\},$$

for varying $a, m \in \{1, \ldots, k\}$, satisfy $\mathcal{H}^a_m = 0$ or $0 \notin \mathcal{H}^a_m$. Now, by (3.28)-(3.29) we have that in column $k-(N-q)j$, for all $q = 0, \ldots N-1$, there is only one non-zero component, namely $\gamma^j_{k-(N-q)j+j} \neq 0$, and $\gamma^a_{k-(N-q)j+a} = 0$, for all $q = 0, \ldots, N-1$, $a \neq j$. Similarly, equations (3.30)-(3.31) imply that in row $qj-1$, for all $q = 0, \ldots N-1$, there is only one non-zero component, namely $\gamma^j_{qj-1} \neq 0$, and $\gamma^a_{qj-1} = 0$, for all $q = 0, \ldots, N-1$, $a \neq j$. To summarise all of this in the notation of (3.44), letting

$$S_a = \{l, m+a \ : \ l = qj-1, \ m = rj \ (\text{mod } \aleph), \ q, r = 0, \ldots, N-1\},$$

we have

$$\gamma^j_i \neq 0, \ \forall\, i \in S_j, \quad \gamma^a_i = 0 \ \forall\, i \in \{1, \ldots, k\} \setminus S_a, \ \forall a \in \{1, \ldots, k\} \setminus \{j\}. \tag{3.46}$$

With all of this in mind, we now focus our attention to equation (3.27), which, with g as in (3.44), and matrices (3.49) implies (among others) the equations:

$$\gamma^j_m \beta_{m-j} = e^{\imath \frac{2\pi}{Nk}} \gamma^j_{m-1} \beta_m, \quad m = 1, \ldots, k-1, \tag{3.47}$$

$$\gamma^j_k (\beta_{k-j} - u_{N-1} y_{N-1} \alpha^{-1}_{k-j-1}) = e^{\imath \frac{2\pi}{Nk}} \gamma^j_{k-1} \beta_k. \tag{3.48}$$

By (3.46), the coefficients γ^j_m and γ^j_{m-1} are non-zero for $m = qj \ (\text{mod } \aleph)$ for any $q = 0, \ldots, N-1$. So, if $\beta_r = 0$ for some $r = qj \ (\text{mod } \aleph)$, (3.47) implies that $\beta_i = 0$ for all $i = r \ (\text{mod } \Gamma) = 0 \ (\text{mod } \Gamma)$. In particular, this means that $\beta_{k-j} = \beta_k = 0$, which hence implies by (3.48) that either $u_{N-1} = 0$, or $y_{N-1} = 0$, which is a contradiction of corollary 2.5.10 and equations (3.28)-(3.31). So $\beta_r \neq 0$ for all $r = qj \ (\text{mod } \aleph)$, $q = 0, \ldots, N-1$.

Since each case has arrived at a contradiction, we must have that $\beta_r \neq 0$ for all $r = 1, \ldots, k$, i.e. $\det B \neq 0$. □

3.5.3 Existence of cyclically symmetric calorons

We may use the results of the previous sections to construct the parameters of $\mathcal{M}_k^N(\rho(C_{Nk}^{j,\vec{\varphi}}))$, that is, the monad matrices invariant under the action of $\rho(C_{Nk}^{j,\vec{\varphi}})$.

Theorem 3.5.8 *Let $k, N \in \mathbb{Z}^+$, $N \geq 2$, $j \in \mathbb{Z}_k$, and $\vec{\varphi}$ be an arbitrary phase vector. Then $\mathcal{M}_k^N(\rho(C_{Nk}^{j,\vec{\varphi}}))$ is isomorphic to $(\mathbb{C}^*)^2$.*

Proof

Let $(A, B, C, D) \in \mathcal{M}_k^N(\rho(C_{Nk}^{j,\vec{\varphi}}))$. As a result of Lemma 3.5.4, we may fix the form of G, and solve (3.32)-(3.35) so that (A, B, C, D) necessarily take the form as in (3.38). By Lemma 3.5.7, the matrix

$$h = \operatorname{diag}\left\{\prod_{i=2}^{k-1}\beta_i, \prod_{i=3}^{k-1}\beta_i, \ldots, \beta_{k-1}, 1, \prod_{i=1}^{k-1}\beta_i\right\},$$

is invertible, so we may use it as a gauge transformation to further fix the data as in (3.38) to be

$$\begin{aligned} A &= \operatorname{diag}\{\alpha_1, \ldots, \alpha_k\}S^{k-Nj}, \quad B = \operatorname{diag}\{1, \ldots, 1, \beta\}S, \\ C_p &= u_p \vec{e}_{k-(N-p)j}, \qquad\qquad D_p = y_p \vec{f}_{pj-1}. \end{aligned} \tag{3.49}$$

With another gauge transformation, we may also choose to set $y_{N-1} = 1$. After some calculation, we see that this form of the data fully fixes the gauge. Note that by (3.27), we have $\det(B - C_{N-1}D_{N-1}A^{-1}) \neq 0$, which means that $u_{N-1} \neq \alpha_{k-j-1}$ when $j \neq k$, and $u\alpha_{k-1}^{-1} \neq \beta$ when $j = k$.

Consider the general $GL(k, \mathbb{C})$ matrix

$$g = e^{\imath\frac{\pi}{Nk}} \sum_{a=1}^{k} \operatorname{diag}\{\gamma_1^a, \ldots, \gamma_k^a\}S^a.$$

As in the proof of Lemma 3.5.7, equations (3.28)-(3.31) imply that for $a \neq j$

$$\gamma_i^a = 0, \ \forall\, i \notin \{l, m+a \ : \ l = qj - 1, \ m = rj \ (\text{mod } \aleph), \ q, r = 0, \ldots, N-1\}. \tag{3.50}$$

Additionally, equation (3.27) implies

$$\gamma_i^a = \lambda_i^a \gamma_{i-1}^a, \quad \text{for all } i, a = 1, \dots, k,$$

where $\lambda_i^a \neq 0$. In particular,

$$\gamma_i^a = \left(\prod_{r=0}^{i+1} \lambda_{i-r}^a \right) \gamma_{k-1}^a,$$

which is 0 for all $a \neq j$ by (3.50). This means our ansatz for g reduces to

$$g = e^{\imath \frac{\pi}{Nk}} \mathrm{diag}\{\gamma_1, \dots, \gamma_k\} S^j, \tag{3.51}$$

where we have relabelled the components for simplicity. Using this and the form of A, we may solve (3.36) to give

$$\alpha_i = \omega_{i+Nj} \prod_{q=1}^{N} \gamma_{i+qj}^{-1}, \quad i = 1, \dots, k. \tag{3.52}$$

This solution also satisfies (3.26). Equations (3.28)-(3.31) imply

$$C_p = e^{-\imath \frac{(p+1)\pi}{Nk}} e^{\imath \frac{j\pi}{Nk}(p(N-p)+N+1)} e^{\imath \left(\varphi_N + \sum_{q=1}^p \varphi_q\right)} g^{p+1} A C_{N-1}, \tag{3.53}$$

$$D_p = e^{-\imath \frac{(p+1)\pi}{Nk}} e^{\imath \frac{j\pi}{Nk}(p(p+N)+N-1)} e^{-\imath \left(\varphi_N + \sum_{q=1}^p \varphi_q\right)} D_{N-1} A^{-1} g^{-p-1}, \tag{3.54}$$

for $p = 0, \dots, N-1$. Relabelling $u_{N-1} = u$, and using the form of g and A, this, along with (3.28) and (3.30) reduces to the solution

$$u_p = e^{\imath \frac{j\pi}{Nk}(p(N-p)-N+1)} e^{\imath \left(\varphi_N + \sum_{q=1}^p \varphi_q\right)} u \prod_{q=1}^{N-p-1} \gamma_{k-qj}^{-1}, \tag{3.55}$$

$$y_p = e^{-\imath \frac{2(p+1)\pi}{Nk}} e^{\imath \frac{j\pi}{Nk}((2N-1)(1-N)+p(p+N))} \omega_1 e^{-\imath \left(\varphi_N + \sum_{q=1}^p \varphi_q\right)} \prod_{q=p+1}^{N-1} \gamma_{qj-1}, \tag{3.56}$$

for all $p = 0, \dots, N-1$. Note that (3.55) and (3.56) reduce to the trivial equations $u_{N-1} = u$ and $y_{N-1} = 1$ in the case $p = N-1$. The final symmetry conditions to solve are dictated by (3.27). For this we have two cases to consider, namely $j = k$, and $j \neq k$.

Case 1: $j = k$ In this case, (3.27) decomposes as

$$\gamma_m = e^{\imath \frac{2\pi}{Nk}} \gamma_{m-1}, \quad m = 1, \ldots, k-1, \tag{3.57}$$

$$\gamma_k \left(\beta - e^{\imath \frac{2\pi}{k}} u \gamma_{k-1}^N \right) = e^{\imath \frac{2\pi}{Nk}} \gamma_{k-1} \beta, . \tag{3.58}$$

These may be solved to yield the solution

$$\gamma_m = e^{\imath \frac{2m\pi}{Nk}} \gamma_k, \quad m = 1, \ldots, k-1, \tag{3.59}$$

$$\beta = \frac{u \gamma_k^N}{1 - e^{\imath \frac{2\pi}{N}}}, \tag{3.60}$$

which has two free parameters u and $\gamma \equiv \gamma_k$.

Case 2: $j \neq k$ In this case, (3.27) decomposes as

$$\gamma_m = e^{\imath \frac{2\pi}{Nk}} \gamma_{m-1}, \quad m \neq j, k, \tag{3.61}$$

$$\gamma_k \left(1 - u \omega_{k-(N-1)j+1} \prod_{q=0}^{N-1} \gamma_{qj-1} \right) = e^{\imath \frac{2\pi}{Nk}} \gamma_{k-1} \beta, \tag{3.62}$$

$$\gamma_j \beta = e^{\imath \frac{2\pi}{Nk}} \gamma_{j-1}. \tag{3.63}$$

We may straightforwardly solve (3.61) to obtain

$$\gamma_m = \begin{cases} e^{\imath \frac{2m\pi}{Nk}} \gamma_k, & 0 \leq m \leq j-1, \\ e^{\imath \frac{2(m-j)\pi}{Nk}} \gamma_j, & j \leq m \leq k-1, \end{cases} \tag{3.64}$$

where we are, as usual, identifying $m = 0$ as $m = k$. Combining this with (3.63) implies that

$$\beta = e^{\imath \frac{2j\pi}{Nk}} \gamma_k \gamma_j^{-1}. \tag{3.65}$$

Using (3.64) and (3.65), along with (3.62), we conclude that

$$u = \left(1 - e^{\imath \frac{2\pi}{N}} \right) \omega_{(N-1)j-1} \prod_{q=0}^{N-1} \gamma_{qj-1}^{-1}. \tag{3.66}$$

This leaves us with two free parameters $\gamma \equiv \gamma_k$, and $\widetilde{\gamma} = \gamma_j$.

In both cases we have shown that the general solution to equations (3.26)-(3.31) in the moduli space of non-singular monad matrices $\mathcal{M}_k^N$ is necessarily a subset of $(\mathbb{C}^*)^2$. It is straightforward to check that varying over the parameters $(\gamma, u) \in (\mathbb{C}^*)^2$ in the case $j = k$, and $(\gamma, \widetilde{\gamma}) \in (\mathbb{C}^*)^2$ in the case $j \neq k$, always gives different gauge equivalence classes of solutions. Similarly, the full-rank conditions (2.61) certainly hold for this data, as can be easily verified. The final hurdle is to show that for all $(\gamma, u), (\gamma, \widetilde{\gamma}) \in (\mathbb{C}^*)^2$, these solutions satisfy the monad equation (2.60).

To do this, let $M = [A, B] + CD$ for our solutions (A, B, C, D). By the symmetry equations (3.26)-(3.31) (with $n = k$) we thus have that

$$M = e^{\imath \frac{2\pi}{Nk}(Nj-1)} g M g^{-1}. \tag{3.67}$$

Due to the form of the data (3.49), the matrix M is of the form

$$M = \mathrm{diag}\{\chi_1, \ldots, \chi_k\} S^{k-(N-1)j+1}.$$

Therefore, using the definition of g as (3.51), equation (3.67) is equivalent to

$$\chi_m = e^{\imath \frac{2\pi}{Nk}(Nj-1)} \chi_{m-j} \gamma_m \gamma_{m+Nj-1}^{-1}, \quad \forall\, m = 1, \ldots, k. \tag{3.68}$$

This implies that

$$\chi_m = e^{-\imath \frac{2\pi}{N\Gamma}} \chi_m \prod_{q=0}^{k/\Gamma-1} \gamma_{m-qj} \gamma_{m+(N-q)j-1}^{-1}, \tag{3.69}$$

for all $m = 1, \ldots, k$ (where we recall that $\Gamma = \gcd(k, j)$). Using the formulae (3.59) and (3.64) for the γ_i in each case, after a little calculation, we obtain from (3.69) that

$$\chi_k = e^{-\imath \frac{2\pi}{N}} \chi_k,$$

which means, as $N \geq 2$, that $\chi_k = 0$. Thus, by (3.68), we must have that $\chi_m = 0$ for all $m = 0 \pmod{\Gamma}$. For the remaining components, using (3.49) and (3.52), we see that

$$\chi_m = \omega_{m+j} \left(\prod_{q=1}^{N} \gamma_{m+qj}^{-1} - \omega_{k-1} \prod_{q=1}^{N} \gamma_{m+qj-1}^{-1} \right), \quad \text{for } m \neq 0 \pmod{\Gamma}. \tag{3.70}$$

In particular, since $m \neq 0 \pmod{\Gamma}$, the factors γ_k and γ_j never appear in the first product in (3.70), so that by (3.61),[7] (3.70) reduces to

$$\chi_m = \omega_{m+j}\left(e^{-\imath\frac{2\pi}{k}} - e^{\imath\frac{2(k-1)\pi}{k}}\right)\prod_{q=1}^{N}\gamma_{m+qj-1}^{-1} = 0, \quad \text{for } m \neq 0 \pmod{\Gamma}. \tag{3.71}$$

Thus, $M = 0$, and so our solutions belong to $\mathcal{M}_k^N$. □

Corollary 3.5.9 *$\mathcal{C}_k^N(\rho(C_{Nk}^{j,\vec{\varphi}})) \neq \emptyset$ for all $N \geq 2$, $k \in \mathbb{Z}^+$, $j \in \mathbb{Z}_k$, and phase vectors $\vec{\varphi}$. Furthermore, in the case $N = 2$, we have $\mathcal{C}_k^2(\rho(C_{2k}^{j,\vec{\varphi}})) \cong (\mathbb{C}^*)^2$.*

Proof

These follow immediately from Theorem 3.5.8 with the knowledge of Theorems 2.4.4 and 2.5.6, in particular the fact that the Nahm transform is a bijection for $N = 2$. □

Example 3.5.10 *To further illustrate the statement of Theorem 3.5.8, we shall demonstrate a simple example. Consider the case $N = 2$, and $k = 3$. By Theorem 3.5.8, there are 3 cases of these rotation cyclic solutions to write down, for any arbitrary phase vector $\vec{\varphi} = (-\varphi, \varphi)$, dictated by $j = 1, 2, 3$. In each case, $(\gamma, \widetilde{\gamma}), (\gamma, u) \in (\mathbb{C}^*)^2$ in line with the notation in the proof of Theorem 3.5.8.*

For $j = 1$, the symmetric monad matrices are

$$\begin{aligned} A &= \begin{pmatrix} 0 & 0 & e^{-\imath\frac{\pi}{3}}\gamma^{-1}\widetilde{\gamma}^{-1} \\ e^{\imath\frac{2\pi}{3}}\gamma^{-1}\widetilde{\gamma}^{-1} & 0 & 0 \\ 0 & -\widetilde{\gamma}^{-2} & 0 \end{pmatrix}, \quad B = \begin{pmatrix} 0 & 0 & 1 \\ 1 & 0 & 0 \\ 0 & e^{\imath\frac{\pi}{3}}\gamma\widetilde{\gamma}^{-1} & 0 \end{pmatrix}, \\ C &= \begin{pmatrix} 2e^{\imath\frac{7\pi}{6}}e^{\imath\varphi}\gamma^{-1}\widetilde{\gamma}^{-2} & 0 \\ 0 & 2e^{-\imath\frac{\pi}{3}}\gamma^{-1}\widetilde{\gamma}^{-1} \\ 0 & 0 \end{pmatrix}, \quad D = \begin{pmatrix} 0 & e^{-\imath\frac{\pi}{6}}e^{-\imath\varphi}\gamma & 0 \\ 0 & 0 & 1 \end{pmatrix}. \end{aligned} \tag{3.72}$$

[7] Note that this is the same as (3.57) in the case $j = k$.

These solve (3.26)-(3.31) in the case we are considering with accompanying gauge transformation

$$g = \begin{pmatrix} 0 & 0 & e^{\imath\frac{\pi}{6}}\widetilde{\gamma} \\ e^{\imath\frac{\pi}{2}}\widetilde{\gamma} & 0 & 0 \\ 0 & e^{\imath\frac{\pi}{6}}\gamma & 0 \end{pmatrix}. \tag{3.73}$$

For $j = 2$, the symmetric monad matrices are

$$\begin{aligned} A &= \begin{pmatrix} 0 & e^{\imath\frac{4\pi}{3}}\gamma^{-1}\widetilde{\gamma}^{-1} & 0 \\ 0 & 0 & e^{-\imath\frac{\pi}{3}}\gamma^{-2} \\ e^{\imath\frac{\pi}{3}}\gamma^{-1}\widetilde{\gamma}^{-1} & 0 & 0 \end{pmatrix}, \quad B = \begin{pmatrix} 0 & 0 & 1 \\ 1 & 0 & 0 \\ 0 & e^{\imath\frac{2\pi}{3}}\gamma\widetilde{\gamma}^{-1} & 0 \end{pmatrix}, \\ C &= \begin{pmatrix} 0 & 2e^{\imath\frac{\pi}{3}}\gamma^{-1}\widetilde{\gamma}^{-1} \\ 2e^{-\imath\frac{\pi}{3}}e^{\imath\varphi}\gamma^{-2}\widetilde{\gamma}^{-1} & 0 \\ 0 & 0 \end{pmatrix}, \quad D = \begin{pmatrix} 0 & e^{-\imath\frac{\pi}{3}}e^{-\imath\varphi}\gamma & 0 \\ 1 & 0 & 0 \end{pmatrix}. \end{aligned} \tag{3.74}$$

The gauge transformation which completes this data, in order to satisfy (3.26)-(3.31), is

$$g = \begin{pmatrix} 0 & e^{\imath\frac{\pi}{2}}\gamma & 0 \\ 0 & 0 & e^{\imath\frac{\pi}{6}}\widetilde{\gamma} \\ e^{\imath\frac{\pi}{6}}\gamma & 0 & 0 \end{pmatrix}. \tag{3.75}$$

Finally, for $j = 3$, the symmetric monad matrices are

$$\begin{aligned} A &= \begin{pmatrix} \gamma^{-2} & 0 & 0 \\ 0 & \gamma^{-2} & 0 \\ 0 & 0 & \gamma^{-2} \end{pmatrix}, \quad B = \begin{pmatrix} 0 & 0 & 1 \\ 1 & 0 & 0 \\ 0 & \frac{1}{2}u\gamma^2 & 0 \end{pmatrix}, \\ C &= \begin{pmatrix} 0 & 0 \\ 0 & 0 \\ e^{-\imath\frac{\pi}{2}}e^{\imath\varphi}\gamma^{-1}u & u \end{pmatrix}, \quad D = \begin{pmatrix} 0 & e^{\imath\frac{3\pi}{2}}e^{-\imath\varphi}\gamma & 0 \\ 0 & 1 & 0 \end{pmatrix}, \end{aligned} \tag{3.76}$$

with accompanying gauge transformation

$$g = \begin{pmatrix} e^{\imath\frac{\pi}{2}}\gamma & 0 & 0 \\ 0 & e^{\imath\frac{5\pi}{6}}\gamma & 0 \\ 0 & 0 & e^{\imath\frac{\pi}{6}}\gamma \end{pmatrix}. \tag{3.77}$$

We leave it as an exercise for the reader to check that the matrices (3.72), (3.74), and (3.76) are in $\mathcal{M}_3^2(\rho(C_6^{j,\vec{\varphi}}))$ *for each* $j = 1, 2, 3$ *respectively.*

3.6 Nahm data for cyclic calorons

Despite indicating geometric and topological information about calorons, the monad matrix data lacks the accessibility of Nahm data when it comes to reconstructing the associated caloron. Whilst the Nahm transform is in general a hard process, constructing a caloron from monad matrices is harder still – to do this one must settle for either reproducing the Nahm data via a Nahm complex, or obtain the caloron from the holomorphic vector bundles over $(\mathbb{C}P^1)^2$ which arise as quotients of the maps (2.61).[8] Both of these processes require solving several ordinary or partial differential equations.

In contrast, it is significantly more desirable to have Nahm data than monad matrix data when it comes to actually constructing calorons. The Nahm transform has been implemented explicitly and numerically in many cases, especially for monopoles on $\mathbb{R}^3$, in order to reconstruct the object of interest. It would therefore be nice to be able to know the cyclic Nahm data, in particular for our cyclic calorons from Corollary 3.5.9, so we shall hence dedicate this final section to the story of how to study this Nahm data.

3.6.1 Cyclic Nahm data

Constructing fixed points under the action of $\rho(C_{Nn}^{j,\vec{\varphi}})$ in the moduli space $\mathcal{N}_k$ of k-Nahm data, amounts to finding continuous functions $g_p : I_p \longrightarrow U(k)$, and Nahm data T_p^{λ} :

[8] See [22].

$I_p \longrightarrow \mathfrak{u}(k)$, $(u_p, w_p) \in (\mathbb{C}^k \times \mathbb{C}^k) \setminus \{(0,0)\}$, satisfying[9]

$$\begin{aligned}
T^0_p(s) &= \left(g_{p-1} T^0_{p-1} g^{-1}_{p-1} - \frac{dg_{p-1}}{ds} g^{-1}_{p-1} \right) \left(s + \tfrac{\mu_0}{N}\right) + \frac{2\imath j\pi}{n\mu_0} \mathbb{1}, \\
T^1_p(s) &= \left(g_{p-1} T^1_{p-1} g^{-1}_{p-1} \right) \left(s + \tfrac{\mu_0}{N}\right), \\
T^2_p(s) &= \left(g_{p-1} \left(\cos\left(\tfrac{2\pi}{Nn}\right) T^2_{p-1} + \sin\left(\tfrac{2\pi}{Nn}\right) T^3_{p-1} \right) g^{-1}_{p-1} \right) \left(s + \tfrac{\mu_0}{N}\right), \\
T^3_p(s) &= \left(g_{p-1} \left(-\sin\left(\tfrac{2\pi}{Nn}\right) T^2_{p-1} + \cos\left(\tfrac{2\pi}{Nn}\right) T^3_{p-1} \right) g^{-1}_{p-1} \right) \left(s + \tfrac{\mu_0}{N}\right), \\
(u_p, w_p) &= e^{\imath\varphi_p} g_{p-1} \left(\tfrac{3-2p+N}{2N}\mu_0\right) \left(e^{-\imath\frac{\pi}{Nn}} u_{p-1}, e^{\imath\frac{\pi}{Nn}} w_{p-1} \right),
\end{aligned} \tag{3.78}$$

for $p = 1, \ldots, N-1$. For $p = 0$, the above is replaced by shifting all function arguments on the right-hand-side by $-\mu_0$, and replacing the subscript '-1' with the subscript '$N-1$'.

To solve this system, in analogy to the methods for monad matrices outlined and executed in the previous section, we may first consider Nahm matrices on I_{N-1} with $C^{Nj,0}_n$-symmetry that is, such that

$$\begin{aligned}
T^0_{N-1}(s) &= G(s) T^0_{N-1} G(s)^{-1} - \tfrac{dG}{ds}(s) G(s)^{-1} + \tfrac{2\imath Nj\pi}{n\mu_0} \mathbb{1}, \\
T^1_{N-1}(s) &= G(s) T^1_{N-1}(s) G(s)^{-1}, \\
T^2_{N-1}(s) &= G(s) \left(\cos\left(\tfrac{2\pi}{n}\right) T^2_{N-1}(s) + \sin\left(\tfrac{2\pi}{n}\right) T^3_{N-1}(s) \right) G(s)^{-1}, \\
T^3_{N-1}(s) &= G(s) \left(-\sin\left(\tfrac{2\pi}{n}\right) T^2_{N-1}(s) + \cos\left(\tfrac{2\pi}{n}\right) T^3_{N-1}(s) \right) G(s)^{-1},
\end{aligned} \tag{3.79}$$

for some $G : I_{N-1} \longrightarrow U(k)$, and data $T^\lambda_{N-1} : I_{N-1} \longrightarrow \mathfrak{u}(k)$ satisfying Nahm's equations on I_{N-1}. Additionally, the matching data (u_{N-1}, w_{N-1}) at $s = \mu_{N-1} = \frac{3-N}{2N}\mu_0$ are constrained to satisfy

$$(u_{N-1}, w_{N-1}) = G\left(\frac{3-N}{2N}\mu_0\right) \left(e^{-\imath\frac{\pi}{n}} u_{N-1}, e^{\imath\frac{\pi}{n}} w_{N-1} \right). \tag{3.80}$$

This gauge transformation G is to be related to the g_p found in (3.78) via

$$G(s) = \left(\prod_{p=1}^{N-1} g_{N-1-p}\left(s + p\frac{\mu_0}{N}\right) \right) g_{N-1}(s). \tag{3.81}$$

Once we have the Nahm matrices on I_{N-1}, matching data at $s = \mu_{N-1}$, and gauge transformations g_p, we may fix the form of the remaining data to satisfy (3.78) by using

[9] Recalling that the group $\rho(C^{j,\vec{\varphi}}_{Nn})$ incorporates $\rho^{-1} \equiv \rho^{N-1}$.

g_p and this initial Nahm data, via the formulae

$$T_q^\lambda(s) = G_q(s) \cdot \left((K_{Nn}^{Nj})^{q+1} \cdot T_{N-1}^\lambda \left(s + \frac{q+1-N}{N}\mu_0 \right) \right), \tag{3.82}$$

$$(u_q, w_q) = e^{\imath \sum_{p=0}^q \varphi_p} G_q \left(\frac{1+N-2q}{2N}\mu_0 \right) \left(e^{-\imath \frac{(1+q)\pi}{N}} u_{N-1}, e^{\imath \frac{(q+1)\pi}{N}} w_{N-1} \right), \tag{3.83}$$

for $q = 0, \ldots, N-1$, where K_m^i is the euclidean generator (3.23), and we have introduced the short-hand

$$G_q(s) = \left(\prod_{r=1}^q g_{q-r} \left(s + r\frac{\mu_0}{N} \right) \right) g_{N-1} \left(s + \frac{q+1-N}{N}\mu_0 \right),$$

for $q = 0, \ldots, N-1$ (the product is of course ignored in the case $q = 0$). It is straightforward to check that (3.82) and (3.83), along with the T_{N-1}^λ satisfying (3.79), and (u_{N-1}, w_{N-1}) solving (3.80), is a general solution to (3.78).

The final obstruction is solving the matching conditions (2.33) with the symmetric data. This only needs to be performed at $s = \mu_{N-1} = (3-N)\mu_0/(2N)$, as the other conditions are equivalent to this one due to the symmetric form of the data.

3.6.2 The case $k = 1$.

To ease us into studying the symmetric Nahm data, we shall start with a simple case – when the rank of the data is $k = 1$. It is worth remarking that this case is somewhat special since the Nahm transform has been shown to be a hyperkähler isometry for all $SU(N)$ $(1, \ldots, 1)$-calorons [70]. Furthermore, it is this case which we are able to complete the algorithm outlined in the previous section for all N, and hence obtain a full description of the sub-moduli spaces $\mathcal{C}_1^N(\rho(C_N^{j,\vec{\varphi}}))$. We also note that there is only one case to consider here, namely $j = 0$.[10]

[10] Strictly speaking, in the language of section 3.5, we really mean $j = 1$, but this is equivalent to setting $j = 0$, up to the action of an overall phase, by Proposition 2.4.6.

Recall that the Nahm equations in this case take the simple form $dT_p^i/ds = 0$ for all $p = 0, \dots, N-1$, $i = 1, 2, 3$. Using Lemma 2.4.5, we may hence fix the Nahm matrices on I_{N-1} to be of the form

$$\left(T_{N-1}^0, T_{N-1}^1, T_{N-1}^2, T_{N-1}^3\right) = \left(\imath\frac{\theta}{\mu_0}, \imath x, \imath y, \imath z\right), \tag{3.84}$$

with $\theta, x, y, z \in \mathbb{R}$ constants. Note that this data satisfies (3.79) trivially in the case $n = k = 1$, and $j = 0$, for any $G \in U(1)$ constant. This G is further constrained by equation (3.80), from which we deduce that $G = -1$ is the only possibility.

The next ingredients for the symmetric data are the transformations $g_p : I_p \longrightarrow U(1)$ solving (3.81), and so that (3.78) may be satisfied. It is clear that such a set of gauge transformations must be constant, and since $G = -1$, they must satisfy $g^N = -1$, that is $g = e^{\imath\frac{(2r+1)\pi}{N}}$ for some $r \in \{0, \dots, N-1\}$. We may fix $r = 0$ without any loss of generality, since all of the cases give gauge equivalent data via (3.82) and (3.83) due to Proposition 2.4.6. Thus, this choice of g, along with the data (3.84), the matching data $(u_{N-1}, w_{N-1}) = (u, w)$, and the formulae (3.82)-(3.83) determine a general solution to (3.78).

The final hurdle is to solve the matching conditions (2.33). Due to the symmetric form, it is enough to solve one matching condition, namely at $s = \mu_{N-1}$. In this case, since the data are constant, there is no dependence on this point μ_{N-1}, and the matching conditions are equivalent to the equations

$$|u|^2 - |w|^2 = 0, \tag{3.85}$$

$$\left(e^{\imath\frac{2\pi}{N}} - 1\right)(z - \imath y) = u\overline{w}. \tag{3.86}$$

Equation (3.85) implies that $(u, w) = (\lambda e^{\imath\eta}, \lambda e^{\imath\zeta})$, for some $\lambda, \eta, \zeta \in \mathbb{R}$, and we may perform a constant gauge transformation to fix $\eta = 0$. Solving (3.86) in this gauge, we

conclude that the symmetric Nahm data is given by

$$\begin{aligned} T^0_{N-1} &= \imath\tfrac{\theta}{\mu_0}, \quad T^1_{N-1} = \imath x \\ T^2_{N-1} &= \imath\frac{\lambda^2}{2}\frac{\sin\left(\frac{2\pi}{N}\right)\cos\zeta - \left(1-\cos\left(\frac{2\pi}{N}\right)\right)\sin\zeta}{\left(1-\cos\left(\frac{2\pi}{N}\right)\right)}, \\ T^3_{N-1} &= -\imath\frac{\lambda^2}{2}\frac{\sin\left(\frac{2\pi}{N}\right)\sin\zeta + \left(1-\cos\left(\frac{2\pi}{N}\right)\right)\cos\zeta}{\left(1-\cos\left(\frac{2\pi}{N}\right)\right)}, \\ (u_{N-1}, w_{N-1}) &= \left(\lambda, \lambda e^{\imath\zeta}\right), \end{aligned} \tag{3.87}$$

which defines the remaining data via (3.82) and (3.83), with $g_p = e^{\imath\frac{\pi}{N}}$ for all p. The parameters are $\theta \in \mathbb{R}/2N\pi\mathbb{Z}$,[11] $x \in \mathbb{R}$, $\zeta \in \mathbb{R}/2\pi\mathbb{Z}$, and $\lambda \in \mathbb{R}^+$, determining that the moduli space $\mathcal{C}_1^N(\rho(C_N^{j,\vec{\varphi}}))$ is isomorphic to $\mathbb{R}\times\mathbb{R}^+\times\mathbb{R}/2N\pi\mathbb{Z}\times\mathbb{R}/2\pi\mathbb{Z} \cong (\mathbb{C}^*)^2$, in agreement with Theorem 3.5.8 and Corollary 3.5.9.

In the simplest case $N = 2$, the solution simplifies tremendously. In terms of the most general $(1,1)$ Nahm data (2.49), this symmetric data is determined by the subfamily of (2.49) with separation parameters $\lambda_1 = \lambda_0 = \lambda$, and $\beta = \zeta$, phase $\alpha = 0$, and constituent monopole locations $(x, \pm y, \pm z)$ with $y = -\frac{\lambda^2}{2}\sin\zeta$, and $z = -\frac{\lambda^2}{2}\cos\zeta$.

3.6.3 The case $k = 2$

The next example of $\rho(C_{Nn}^{j,\vec{\varphi}})$-symmetric Nahm data we shall consider is the case of charge $k = 2$. To remain parallel to Theorem 3.5.8, we shall restrict to the case $n = k = 2$, and for further simplicity, we shall only consider the case $N = 2$, that is symmetric $SU(2)$-calorons.[12] Much of the content of this section appears published in [30].

In accordance with our conventions, and Proposition 3.4.1, the only actions of the circle translations to consider are $j = 2 \equiv 0$ and $j = 1$. In both cases, we shall need to start

[11] This can be seen by the fact that μ_p are all of the form $r_p/2N$ with $r_p \in \mathbb{Z}$, and applying Proposition 2.4.6.

[12] Alongside a lot more complexity regarding the choices of gauge transformations g_p and G, the other major difference when $N > 2$ is that the matching conditions are significantly harder to tackle.

with solving (3.79) and (3.80), which requires fixing Nahm matrices on I_1, matching data at $s = \mu_1 = \mu_0/4$, and a function $G : I_1 \longrightarrow U(2)$ which fixes the data under the action of $C_2^{2j,0}$. For all $p = 0, 1$, we may fix T_p^0 to be constant, and equal, by Lemma 2.4.5, and by anti-hermicity, we may use a constant gauge transformation so that they are diagonal, i.e. $T_p^0 = \imath(\frac{\theta}{\mu_0}\mathbb{1} + \xi\sigma^3)$. We may further simplify things on I_1 by performing a further transformation $h : I_1 \longrightarrow U(2)$, given by $h(s) = \exp(\imath\xi s\sigma^3)$, which sets a gauge so that $T_1^0 = \imath\frac{\theta}{\mu_0}\mathbb{1}$. The matrices $T_1^i : I_1 \longrightarrow \mathfrak{u}(2)$, for $i = 1, 2, 3$, will be of the form given in (2.50), and are constrained further by the symmetry equations (3.79). Without loss of generality, we may set the Nahm matrices on I_1 to be in the form of the ansatz

$$\begin{aligned} T_1^0 &= \frac{\imath}{\mu_0}\theta\mathbb{1}, \quad T_1^1(s) = \imath\left(\alpha\mathbb{1} + \frac{D}{2}f_1(Ds)\sigma^3\right), \\ T_1^2(s) &= \imath\frac{D}{2}\left(\cos\phi f_2(Ds)\sigma^2 + \sin\phi f_3(Ds)\sigma^1\right), \\ T_1^3(s) &= \imath\frac{D}{2}\left(\cos\phi f_3(Ds)\sigma^1 - \sin\phi f_2(Ds)\sigma^2\right), \end{aligned} \tag{3.88}$$

for some constants θ, D, ϕ, α, and functions $f_i : I_1 \longrightarrow \mathbb{R}$. Nahm's equations hence reduce to $f_1' = -f_2 f_3$ and cyclic permutations, with solution given by the elliptic functions (2.52):

$$\Phi_1(s) = -\frac{\kappa'}{\mathrm{cn}_\kappa(s)}, \quad \Phi_2(s) = \frac{\kappa'\mathrm{sn}_\kappa(s)}{\mathrm{cn}_\kappa(s)}, \quad \Phi_3(s) = \frac{\mathrm{dn}_\kappa(s)}{\mathrm{cn}_\kappa(s)}.$$

The ordering of these functions will be determined later. Additionally, we may fix the matching data (u_1, w_1) as

$$(u_1, w_1) = \left(\begin{pmatrix} u \\ 0 \end{pmatrix}, \begin{pmatrix} 0 \\ w \end{pmatrix}\right), \tag{3.89}$$

with $(u, w) \in \mathbb{C}^2 \setminus \{(0, 0)\}$. It is straightforward to check that (3.88) and (3.89) satisfy (3.79) and (3.80) with the gauge transformation

$$G(s) = e^{\imath\frac{2j\pi\left(s-\frac{\mu_0}{4}\right)}{\mu_0}}e^{\imath\frac{\pi}{2}\sigma^3}. \tag{3.90}$$

At this stage we meet a fork in the road, where we shall explore the cases $j = 0$ and $j = 1$ independently. It turns out that all solutions to (3.78) in the case $N = n = k = 2$,

$j = 0$, are known. These are described by the 'crossed solution' of Nógrádi and coworkers [18, 93]. We will describe this Nahm data in the next section. In the remaining sections we shall construct previously unknown solutions, by looking at the case $N = n = k = 2$, and $j = 1$, which we call the *oscillating solutions*, in detail.

The crossed solutions

In [18, 93], a solution of Nahm's equations and the matching conditions, in the case $N = k = 2$, is described called the 'crossed solution'. This can be seen to contain a subfamily which is $\rho(C_4^{0,\vec{\varphi}})$-symmetric, but with the convention of the cyclic generator fixing the x^2-axis (rather than the x^1-axis which is our convention). This solution may be described within our conventions via the generating data (3.88)-(3.89), and the formulae (3.82)-(3.83). The gauge transformations $g_p : I_p \longrightarrow U(2)$ which are crucial to this process are

$$g_p(s) = e^{\imath\frac{\pi}{4}}\mathrm{diag}\{1, \imath\}.$$

One can straightforwardly check that all of this solves (3.78) in the case $N = n = k = 2$, $j = 0$, and are hence $\rho(C_4^{0,\varphi})$-symmetric, moreover, they describe the Nahm data for all $(2, 2)$-calorons with such symmetry. The matching conditions (2.33) for this data reduce to

$$2D\kappa'\mathrm{sc}_\kappa(D\mu_0/4) = \lambda^2,$$
$$D(\mathrm{dc}_\kappa(D\mu_0/4) - \kappa'\mathrm{nc}_\kappa(D\mu_0/4)) = \lambda^2.$$

The free parameters in this solution are given by $\phi \in \mathbb{R}/2\pi\mathbb{Z}$, $\theta \in \mathbb{R}/4\pi\mathbb{Z}$, $\alpha \in \mathbb{R}$, and $\kappa \in (0, 1)$. One may show that for all $\kappa \in (0, 1)$, there exists a unique solution $(D_\kappa, \lambda_\kappa)$ to the matching conditions in terms of κ (the analysis is similar to the detailed example we present in the next section).

It is worth remarking that this solution family is called 'crossed' as in a particular limit where the caloron becomes abelian [93], the constituent monopoles localise as two crossed ellipses occupying the same plane.

The oscillating solutions

In this and the remaining sections, we construct the Nahm data for $\mathcal{C}_2(\rho(C_4^{1,\vec{\varphi}}))$, which we know by Corollary 3.5.9 should be parameterised by $(\mathbb{C}^*)^2$. Our ansatz is given by the solution (3.88) to (3.79) when $n = 2$ with gauge transformation $G(s) = e^{\imath\frac{2\pi}{\mu_0}s\sigma^3}$.

The first step is to solve the equation (3.81) to obtain the $g_p : I_p \longrightarrow U(2)$ which appear in the symmetry equations (3.78). In general, this factorisation problem is potentially quite hard, however, we can use the form of (3.88), the fact that $N = 2$, and the intended symmetry, to our advantage. Let $\chi \in I_1$, and consider the T^0-parallel transport operator[13] $\Omega(s, \chi)$ solving

$$\frac{d\Omega(s,\chi)}{ds} + T^0\Omega(s,\chi) = 0, \quad \Omega(\chi,\chi) = \mathbb{1},$$

where T^0 is the connection on $[\chi, \mu_0 + \chi]$ formed by T_p^0 via

$$T^0(s) = \begin{cases} T_1^0(s), & s \in [\chi, \mu_0/4], \\ T_2^0(s), & s \in [\mu_0/4, 3\mu_0/4], \\ T_1^0(\mu_0 + \chi - s), & s \in [3\mu_0/4, \mu_0 + \chi]. \end{cases} \tag{3.91}$$

Define $\Omega(s) := \Omega(s,\chi)\Omega(\mu_0 + \chi, \chi)\Omega(s,\chi)^{-1}$. The first equation of (3.78) (with $N = n = 2$ and $j = 1$) implies the existence of a $g : S^1 \longrightarrow U(2)$ such that

$$\Omega(s) = -g(s)\Omega(s)g(s)^{-1}. \tag{3.92}$$

In particular, since the characteristic polynomial is gauge invariant, we must have

$$\mathrm{Eval}(\Omega(s)) = \mathrm{Eval}(-\Omega(s)). \tag{3.93}$$

[13] This is similar, but not precisely the same as the parallel transport operator for $\alpha = T^0 + \imath T^1$ considered in the proof of Theorem 2.5.6, even though we use the same notation.

By definition, we must also have that the eigenvalues of $\Omega(s)$ are constant. Putting this together, since the operator $\Omega(s)$ takes values in $U(2)$, equation (3.93) tells us that

$$\mathrm{Eval}(\Omega(s)) = \{\pm\varrho\}, \quad |\varrho| = 1.$$

We may thus fix a gauge[14] such that $\Omega(s) = \varrho\sigma^3$. In particular, this gauge forces T_p^0 diagonal for each p, and is hence compatible with our earlier choices. Having fixed the form of $\Omega(s)$, we may fix the form of $g(s)$. By (3.92), and the form of the data (3.88) and $G(s)$ in (3.90), a short calculation reveals that

$$g_1(s) = g_2(s) = \begin{pmatrix} 0 & 1 \\ e^{-\imath\psi}e^{\imath\frac{2\pi}{\mu_0}s} & 0 \end{pmatrix} e^{\imath\psi}, \tag{3.94}$$

for some $\psi \in \mathbb{R}$, is the most general choice[15] for such a gauge transformation which makes the data (3.88)-(3.89), along with its generated data (3.82)-(3.83), have $\rho(C_4^{1,\vec{\varphi}})$-symmetry.

Solving the matching conditions

The matching conditions for the data above may be written as

$$-D\left(f_1\left(D\frac{\mu_0}{4}\right) + f_1\left(-D\frac{\mu_0}{4}\right)\right) = |u|^2 = |w|^2, \tag{3.95}$$

$$\frac{D}{2}\left(f_2\left(D\frac{\mu_0}{4}\right) - f_3\left(D\frac{\mu_0}{4}\right) + e^{2\imath\psi}\left(f_2\left(-D\frac{\mu_0}{4}\right) + f_3\left(-D\frac{\mu_0}{4}\right)\right)\right) = e^{\imath\phi}u\overline{w}, \tag{3.96}$$

$$D\left(f_3\left(D\frac{\mu_0}{4}\right) + f_2\left(D\frac{\mu_0}{4}\right) - e^{-2\imath\psi}\left(f_2\left(-D\frac{\mu_0}{4}\right) - f_3\left(-D\frac{\mu_0}{4}\right)\right)\right) = 0. \tag{3.97}$$

[14]Suppose $P \in U(2)$ is such that $P\Omega(\mu_0 + \chi, \chi)P^{-1} = \varrho\sigma^3$, and $\gamma : [\chi, \mu_0 + \chi] \longrightarrow U(2)$ is a continuous path between $\mathbb{1}$ and $\varrho\sigma^3$. Then a gauge transformation $h : S^1 \longrightarrow U(2)$ fixing $\Omega(s)$ in this form may be given by

$$h(s) = \gamma(s)P\Omega(s, \chi)^{-1}, \quad s \in [\chi, \mu_0 + \chi],$$

extended periodically.

[15]That is, up to gauge equivalence.

straightforward analysis of these equations reveals that we may set

$$u = \lambda, \quad w = \lambda e^{\imath(\phi + n\pi)}, \tag{3.98}$$

for $\lambda \in \mathbb{R}^+$ and $n \in \mathbb{Z}$. Now, recall that $\{f_1, f_2, f_3\} = \{\Phi_1, \Phi_2, \Phi_3\}$, where the Φ_i are given in (2.52), with Φ_1, Φ_2 even functions, and Φ_3 an odd function. These matching conditions reveal that f_2 and f_3 must have opposite parity, and f_1 must be even. We may, without loss of generality, fix f_2 even, and f_3 odd, as the opposite case is gauge equivalent. It then follows from (3.96) and (3.97) that $2\psi = 2r\pi$, with different values of $r \in \mathbb{Z}$ giving gauge equivalent data by Proposition 2.4.6. This means that the matching equations (3.96) and (3.97) are reduced to the cases of finding solutions to either of the following equations:

$$(-1)^n \left(\kappa' \mathrm{sc}_\kappa(x) - \mathrm{dc}_\kappa(x)\right) + 2\kappa' \mathrm{nc}\,(x) = 0, \tag{3.99}$$

or

$$(-1)^n \kappa' \left(\mathrm{sc}_\kappa(x) + \mathrm{nc}_\kappa(x)\right) - 2\mathrm{dc}_\kappa(x) = 0, \tag{3.100}$$

where we have relabelled $x \equiv D\mu_0/4$. We must check for which values of x, κ, n these equations have solutions, if any exist at all. In appeal to Corollary 3.5.9, we expect there to be a unique family of solutions. We shall proceed to analyse existence or non-existence of solutions to (3.99) and (3.100).

Note that each of the elliptic functions Φ_i have poles at $x = rK$, for odd integers r, where $K(\kappa) \in \mathbb{R}$ is the *complete elliptic integral of the first kind*

$$K(\kappa) = \int_0^{\frac{\pi}{2}} \frac{1}{\sqrt{1 - \kappa^2 \sin\theta}} d\theta.$$

It is possible, due to the residues of the individual functions, that rK could be a solution to (3.99) or (3.100). However, an important property of Nahm data is that it needs to be bounded and continuous, and hence pole-free across all of I_p. Therefore, we can throw out any solutions which lead to the arguments Ds attaining poles for some $s \in I_1$. A

straightforward calculation reveals that the only values of $x = D\mu_0/4$ which lead to pole-free data are found in $-K < x < K$, hence we shall fix our attention to this interval only.

Lemma 3.6.1 *There are no solutions to equation (3.100) in the range $-K < x < K$, for all κ, n.*

Proof

Multiplying through by $\mathrm{cn}_\kappa(x)$, and rearranging using elliptic function identities, (3.100) implies

$$\left(4 - 3\kappa'^2\right) \mathrm{sn}_\kappa^2(x) + 2\kappa'^2 \mathrm{sn}_\kappa(x) + \kappa'^2 - 4 = 0.$$

Since $\kappa' \in [0, 1]$, we have $4 - 3\kappa'^2 > 0$, so that this is solved if and only if

$$\mathrm{sn}_\kappa(x) = 1, \quad \text{or} \quad \mathrm{sn}_\kappa(x) = \frac{\kappa'^2 - 4}{4 - 3\kappa'^2}. \tag{3.101}$$

Note also

$$\frac{\kappa'^2 - 4}{4 - 3\kappa'^2} \leq \frac{3\kappa'^2 - 4}{4 - 3\kappa'^2} = -1.$$

As $\mathrm{sn}_\kappa(x) \in [-1, 1]$, this means (3.101) is satisfied only when $\mathrm{sn}_\kappa(x) = \pm 1$, that is, when $x = K(\kappa)$ (modulo $4K$), which is not in the interval $(-K, K)$. □

As stipulated above, we may only look for solutions in the interval $(-K, K)$. Thus, by Lemma 3.6.1, the only remaining case to consider is (3.99), which corresponds to

$$f_1(s) = -\kappa' \mathrm{nc}_\kappa(s), \quad f_2(s) = \mathrm{dc}_\kappa(s), \quad f_3(s) = \kappa' \mathrm{sc}_\kappa(s).$$

Solutions to (3.99)

In this section, we consider the equation (3.99). First we shall show that no solutions exist when $n = 1 \pmod 2$, and then show existence of a unique family of solutions in the case

$n = 0 \pmod 2$ within the required range. Consider the functions

$$F_1(x,\kappa) = \kappa' \mathrm{sc}_\kappa(x) - \mathrm{dc}_\kappa(x), \tag{3.102}$$

$$F_2(x,\kappa) = 2\kappa' \mathrm{nc}_\kappa(x). \tag{3.103}$$

It is clear that for $-K < x < K$, the equation $F_1(x,\kappa) = F_2(x,\kappa)$ has no solutions, since we have

$$F_1(x,\kappa) \leq -1 < 2\kappa' \leq F_2(x,\kappa) \quad \forall\, \kappa \in [0,1],\ -K(\kappa) < x < K(\kappa).$$

This rules out the case $n = 1$, and hence we are only left with the case $n = 0$, for which we are interested in finding solutions to $F_1 = -F_2$. We shall soon show that there exists a subset $U \subset [0,1]$ such that there exist solutions $x \in (-K, K)$ to $F_1(x,\kappa) = F_2(x,\kappa)$ for all $\kappa \in U$. However, in order for these solutions to yield Nahm data, they must solve not only this equation, but the complete set of matching conditions. Other than the equation we're considering, the other dependent is (3.95), which in our situation gives the condition

$$x \mathrm{nc}_\kappa(x) > 0. \tag{3.104}$$

As $\mathrm{nc}_\kappa(x) > 0$ for all $-K < x < K$, we easily see that (3.104) is satisfied only if $0 < x < K$. This all leads to the following.

Proposition 3.6.2 *For $0 < x < K$, there exists a unique solution to the equation $F_1(x,\kappa) = -F_2(x,\kappa)$ if and only if $\kappa \in \left(\frac{\sqrt{3}}{2}, 1\right)$.*

Proof

By rearranging and squaring, and using elliptic function identities, it is straightforward to see that any solution to $F_1 = -F_2$ necessarily satisfies

$$\mathrm{sn}^2_\kappa(x) + 4\kappa'^2 \mathrm{sn}_\kappa(x) + 4\kappa'^2 - 1 = 0,$$

which is solved if and only if

$$\mathrm{sn}_\kappa(x) = -1, \quad \text{or} \quad \mathrm{sn}_\kappa(x) = 1 - 4\kappa'^2 = 4\kappa^2 - 3. \tag{3.105}$$

As $\mathrm{sn}_\kappa(x) \in (0,1)$ for all $x \in (0,K)$, and $\kappa \in [0,1]$, (3.105) is solved in this range only if $\kappa \in \left(\frac{\sqrt{3}}{2}, 1\right)$.

Conversely, let $\kappa \in \left(\frac{\sqrt{3}}{2}, 1\right)$, and consider the function $F(x,\kappa) = F_1(x,\kappa) + F_2(x,\kappa)$. As $\kappa \in \left(\frac{\sqrt{3}}{2}, 1\right)$, we have $\kappa' \in \left(0, \frac{1}{2}\right)$, thus

$$F(0,\kappa) = 2\kappa' - 1 < 0. \tag{3.106}$$

Also, F has a simple pole with residue 2 at $x = K$, so $F(K,\kappa) = \infty > 0$. As F is continuous on $(0,K)$, combining this with (3.106), the intermediate value theorem says that there exists $x_0 \in (0,K)$ such that $F(x_0,\kappa) = 0$, that is $F_1(x_0,\kappa) = -F_2(x_0,\kappa)$. Moreover, this solution x_0 will be unique as both $F_1' > 0$ and $F_2' > 0$ for all $0 < x < K$, and hence the same for F. □

The invariant Nahm data

Following the analysis of the matching conditions in the previous section, we may summarise our results in the theorem below.

Theorem 3.6.3 *There is a four-parameter family of $\rho(C_4^{1,\varphi})$-symmetric, charge $k = 2$ caloron Nahm data, given by the Nahm matrices (3.88) on I_1 with the replacements*

$$f_1 = -\kappa' \mathrm{nc}_\kappa, \quad f_2 = \mathrm{dc}_\kappa, \quad f_3 = \kappa' \mathrm{sc}_\kappa, \quad D = D_\kappa, \tag{3.107}$$

which determine the Nahm matrices on I_2 via (3.82) using the gauge transformation (3.94) with $\psi = 0$. The matching data are given by (3.89) and (3.83), with the replacements

$$u = \sqrt{2D_\kappa \kappa' \mathrm{nc}\left(D_\kappa \frac{\mu_0}{4}\right)}, \quad w = \sqrt{2D_\kappa \kappa' \mathrm{nc}\left(D_\kappa \frac{\mu_0}{4}\right)} e^{\imath(\phi+\pi)}. \tag{3.108}$$

The parameter D_κ mentioned in theorem 3.6.3is given implicitly by the solution to the equation

$$\kappa' \mathrm{sc}_\kappa\left(D_\kappa\frac{\mu_0}{4}\right) - \mathrm{dc}_\kappa\left(D_\kappa\frac{\mu_0}{4}\right) + 2\kappa' \mathrm{nc}_\kappa\left(D_\kappa\frac{\mu_0}{4}\right) = 0,$$

which we know exists and is unique for all $\kappa \in \left(\frac{\sqrt{3}}{2}, 1\right)$ by Proposition 3.6.2. As a consistency check with the result of Corollary 3.5.9, we will now look for evidence that our Nahm data coincides with the corresponding monad matrices. Firstly, we see that the free parameters θ, ϕ, α, and κ take values in a diffeomorphic space to $(\mathbb{C}^*)^2$, which agrees with Corollary 3.5.9. A better indicator is to consider the values that $|\det B|$ can take, as this is a gauge invariant quantity. By the construction (2.53) and (2.65), we may identify $B = T_1^2(0) + \imath T_1^3(0)$, and we see from (3.88) and (3.107) that $|\det B| \sim D_\kappa$. The solution (3.49) tells us that for the monads, $|\det B| = |\beta|$, which can take all possible values in $\mathbb{R}^+$. We want this to be the case for D_κ. We know from the proof of Proposition 3.6.2 that D_κ necessarily satisfies (3.105), with $x \equiv D_\kappa\mu_0/4$. Note that $K(1) = \infty$, and when $\kappa \approx 1$, we have the asymptotic formula [1]

$$\mathrm{sn}_\kappa(x) \approx \tanh(x) + \frac{\kappa'^2}{4}\left(\tanh(x) - x\mathrm{sech}^2(x)\right).$$

Therefore, when $\kappa \approx 1$, D_κ must satisfy

$$\frac{4 - 4\tanh\left(D_\kappa\frac{\mu_0}{4}\right)}{4 + \tanh\left(D_\kappa\frac{\mu_0}{4}\right) - D_\kappa\frac{\mu_0}{4}\mathrm{sech}^2\left(D_\kappa\frac{\mu_0}{4}\right)} = \kappa'^2. \tag{3.109}$$

The solutions D_κ to this equation satisfy $D_\kappa \longrightarrow \infty$ as $\kappa' \longrightarrow 0$. Hence, the eigenvalues of $T_1^2 + \imath T_1^3$ diverge as $\kappa \longrightarrow 1$, which agrees with the associated symmetric monad matrix B, as expected.

Up to gauge equivalence, the parameters for this Nahm data are $\theta \in \mathbb{R}/4\pi\mathbb{Z}$, $\phi \in \mathbb{R}/2\pi\mathbb{Z}$, $\alpha \in \mathbb{R}$, and $\kappa \in \left(\frac{\sqrt{3}}{2}, 1\right)$ which determines $D_\kappa \in (0, K(\kappa))$ in line with Proposition 3.6.2. These parameters make up the fixed-point moduli space $\mathcal{C}_2^2(\rho(C_4^{1,\vec{\varphi}})) \cong (\mathbb{C}^*)^2$, in agreement with Corollary 3.5.9. We call this solution space 'oscillating' as it is much like the crossed solution, but the crossing of the monopole constituents is shifted temporally by half the period.

3.7 Summary and open problems

We have introduced the notion of *symmetric calorons*, with particular emphasis on the moduli spaces with equal monopole masses and charges. This emphasis is due to the incorporation of the rotation map, which is an automorphic isometry of these moduli spaces. To this end, we have proven various necessary conditions for the existence of symmetric calorons, particularly in the case of cyclic groups of order Nn involving the rotation map. When $n = k$, we have provided a classification of fixed point sets of these cyclic groups of order Nk, in the moduli space $\mathcal{C}_k^N$ of $SU(N)$ calorons with all monopole masses and charges equal to μ_0/N and k respectively. Our work has made use of the monad matrix data, an approach which to date has not been utilised before in this context. Additionally, in the case $N = k = 2$, we have derived a new solution to Nahm's equations and the matching conditions for one family of these symmetric calorons, and in doing so, this has completed the list of rank 2, charge 2 Nahm data with these symmetries.

We suspect that a similar result may be obtained analogously for Nahm data of charge 2 in the general case of $SU(N)$, but the hard work is in solving the corresponding matching conditions. Other generalisations would be to also consider values of $k > 2$. As we have already seen in section 2.4.2, increasing the charge of the caloron increases the complexity of solving Nahm's equations. For this reason, even describing the Nahm data for $k > 2$ in the case $N = 2$ is tricky. In [116], Sutcliffe gives an ansatz for monopole Nahm data with C_k symmetry, and this may be able to be exploited and adapted for our purposes to solve (3.79) in general. However, it still remains to solve the matching conditions, and derive the gauge transformations satisfying (3.81) in order to have a full set of $\rho(C_{Nk}^{j,\vec{\varphi}})$-symmetric caloron Nahm data.

Regarding the main classification result (Theorem 3.5.8), it still remains open whether this result can be interpreted as a classification of the moduli spaces of calorons. We know that this is certainly true in the case $N = 2$, as expressed by Corollary 3.5.9, since the Nahm

transform is bijective in this case. An interesting observation is that the geometry of the fixed point sets is not dependent on k, indeed they are all equal to $(\mathbb{C}^*)^2$, and it would be interesting if this is the case for smaller cyclic groups with $n < k$. Going even further into generalisation, using the recent work by Cherkis and Hurtubise [26] on monads for Taub-NUT instantons, the next step in studying these symmetries would be to try and reproduce these results in the case of Taub-NUT instantons.

Another question that is left open is how these calorons relate to other solitons, for example, their large parameter limits (for example as considered in [49, 75, 122]). In particular, in the next chapter we shall discuss how calorons are related to skyrmions, and it would be interesting to see how these calorons fit into that picture. In line with the work in [51], one expects some of these calorons to provide approximations to symmetric periodic skyrmions by taking holonomies along a line in $\mathbb{R}^3$. However, in order to do this properly would require the implementation of the Nahm transform on the Nahm data constructed, which we are currently working on with some collaborators.

Finally, a broader understanding of which symmetry groups yield symmetric calorons is still largely unknown, and in particular, what the full symmetry groups[16] of the calorons from Theorem 3.5.8 are for each N, k. Unfortunately, the methods involving the monad matrices, presented in this chapter, can only divulge information in the case where the Euclidean actions fix the x^1 axis, and not generically, and so the only remaining symmetries that may be investigated in this manner are the parity transformation and dihedral symmetries.

[16] That is, stabiliser subgroup of $\mathcal{S}$.

Chapter 4

Calorons and skyrmions

[1]

4.1 Skyrme models

An $SU(2)$ Skyrme model is a 3-dimensional field theory, concerned with an $SU(2)$-valued function $U : X \longrightarrow SU(2)$ called the **Skyrme field**, where (X, η) is a riemannian 3-manifold. The simplest form of a static energy for the Skyrme model is given by

$$E = \int_X \left(c_0 |U^{-1} dU|^2 + c_1 |U^{-1} dU \wedge U^{-1} dU|^2 \right) \mathrm{Vol}_\eta, \tag{4.1}$$

where $\langle \zeta, \eta \rangle \mathrm{Vol}_\eta = -\mathrm{tr}\,(\zeta \wedge \star_3 \eta)$, with $\star_3$ denoting the Hodge-star on (X, η), $c_1, c_2 \in \mathbb{R}^+$ are arbitrary constants, and Vol_η is a choice of volume form on X. The most commonly studied example of a Skyrme model is the case where $X = \mathbb{R}^3$ with the usual euclidean flat metric, and this is the case that we shall consider. Various generalisations of Skyrme models can be considered by including other terms, for example the sextic term and the

[1] Since the submission of this thesis, the results of this chapter have been written up in the author's preprint [29], which also contains additional results.

'pion mass' term. Other terms are also considered when dealing with higher rank Skyrme fields (e.g. $SU(N)$, for $N > 2$).

The $SU(2)$ Skyrme model described by the energy functional (4.1) aims to describe nuclear physics, and in particular, is a theory of pions. The pion fields are manifested as a vector valued field $\vec{\pi} : \mathbb{R}^3 \longrightarrow \mathbb{R}^3$ seen in the Skyrme field's $SU(2)$ expansion:

$$U(\vec{x}) = \sigma(\vec{x})\mathbb{1} + \imath\vec{\pi}(\vec{x}) \cdot \vec{\sigma}. \tag{4.2}$$

The function $\sigma : \mathbb{R}^3 \longrightarrow \mathbb{R}$ is a scalar field which has less physical significance than the pion fields.

4.1.1 Skyrmions

Critical points of the energy functional (4.1) are given by $U : \mathbb{R}^3 \longrightarrow SU(2)$ satisfying the *Skyrme field equation*

$$\sum_{i,j} \partial_i \left(c_0 U^{-1}\partial_i U + c_1 \left[U^{-1}\partial_j U, [U^{-1}\partial_i U, U^{-1}\partial_j U] \right] \right) = 0. \tag{4.3}$$

The boundary condition $U \longrightarrow \text{const}$ on S^2_∞ is usually imposed, and since E is invariant under left multiplication of U by constant $SU(2)$ matrices, the stricter boundary condition $U \longrightarrow \mathbb{1}$ as $|\vec{x}| \longrightarrow \infty$ may be chosen without loss of generality.[2] Whilst this boundary condition alone is not sufficient for finite energy, it is suspected that the condition of finite energy implies this boundary condition, but this is yet to be proven. Critical points with this boundary condition are called **skyrmions**. The boundary condition implies that a skyrmion descends to a map $U : S^3 \longrightarrow SU(2)$, which is characterised by an integer degree $\mathcal{B} \in \pi_1(SU(2)) \cong \mathbb{Z}$, called the *Skyrme charge*, and is physically identified as the **baryon number**. This has the integral formula

$$\mathcal{B} = \frac{1}{24\pi^2} \int \text{tr}\,(U^{-1}dU \wedge U^{-1}dU \wedge U^{-1}dU). \tag{4.4}$$

[2] Another reason for this boundary condition is for consistency with an extended Skyrme model which includes the 'mass term' $\text{tr}\,(\mathbb{1} - U)d^3x$ in the energy.

The Skyrme field equation (4.3) is a non-linear second order differential equation for U, and is highly 'non-integrable', at least in the sense that writing down exact solutions is close to impossible. In fact, besides in the case of $|\mathcal{B}| = 1$ [37, 38], it is still unknown in general whether any solutions exist within each baryon number homotopy class. There has however been significant work in constructing numerical solutions, whose margins of error are negligible enough that there is a high likelihood that the solutions do exist, and it is expected that there are solutions for all $\mathcal{B} \in \mathbb{Z}$. The Faddeev bound derived in the introduction as (1.20) in the context of the functional (4.1) may be straightforwardly shown to be

$$E_S \geq 48\pi^2\sqrt{c_0 c_1}|\mathcal{B}|. \tag{4.5}$$

For the same reason as outlined in the introduction, the Skyrme model is not a BPS theory, that is, its critical points cannot attain the energy bound.

4.1.2 Symmetries

The symmetries of the Skyrme energy are given by the euclidean isometries of $\mathbb{R}^3$, and the 'chiral symmetry group' given by the isometries of $SU(2) \cong S^3$, namely $O(4)$. However, the boundary condition $U \longrightarrow \mathbb{1}$ breaks this symmetry to $O(3)$. The euclidean group $E(3)$ acts via

$$\mathfrak{R} \cdot U = U \circ \mathfrak{R}, \tag{4.6}$$

for $\mathfrak{R} : \mathbb{R}^3 \longrightarrow \mathbb{R}^3$. The chiral symmetry group $O(3)$ is generated by the $SO(3)$ subgroup of *iso-rotations*, and the parity transformation $\widetilde{\sigma} \in O(3)$, given by the matrix

$$\widetilde{\sigma} = \begin{pmatrix} -1 & 0 & 0 \\ 0 & -1 & 0 \\ 0 & 0 & -1 \end{pmatrix}.$$

The *iso-rotations* act as

$$O \cdot U = \mathfrak{O} U \mathfrak{O}^{-1}, \tag{4.7}$$

where $\mathfrak{O} \in SU(2)$ is a choice of preimage under the double covering (3.17) of the element $O \in SO(3)$, and

$$\widetilde{\sigma} \cdot U = U^{-1}. \tag{4.8}$$

A Skyrme field which is invariant under the action (4.6) for all $\mathfrak{R} \in H \subset O(3)$, modulo chiral symmetries (4.7)-(4.8), is known as H**-symmetric**. Much of the success in numerically constructing skyrmions has been with regards to finding the symmetric solutions, for example in [10, 13]. These symmetric examples are important within their physical interpretations, especially those which appear as clusters of symmetric examples, seen in [40]. Symmetry is also an important consideration when it comes to quantization.

4.1.3 The Atiyah-Manton-Sutcliffe construction

In 1989, Atiyah and Manton [8] proposed a method of approximating skyrmions by using instantons on $\mathbb{R}^4$. The candidate for the Skyrme field is taken to be the holonomy of the gauge field along all lines in one of the directions in $\mathbb{R}^4$ (which may be arbitrarily chosen to be x^0), namely

$$U(\vec{x}) = \mathcal{P} \exp\left(- \int_{-\infty}^{\infty} A_0(z, \vec{x}) dz \right), \tag{4.9}$$

where $\mathcal{P}$ denotes path ordering. This is not an unreasonable consideration. Firstly, since A_0 is $\mathfrak{su}(2)$-valued, the holonomy is a map $U : \mathbb{R}^3 \longrightarrow SU(2)$. Furthermore, since $x^0 = \pm\infty$ correspond to the same point in S^4, namely the point at infinity in $\mathbb{R}^4$, this means that the holonomy (4.9) is taken along a closed loop in S^4, and so any gauge transformation $g : S^4 \longrightarrow SU(2)$ has the effect of transforming U via conjugation by $g(\infty) \in SU(2)$, which leaves the energy invariant. Such a transformation corresponds

to an iso-rotation (4.7), as introduced in the previous section. U also satisfies the correct boundary conditions to be a Skyrme field since in the limit $|\vec{x}| \longrightarrow \infty$, the holonomy (4.9) is taken around a constant loop (namely at the point ∞), and so $U \longrightarrow \mathbb{1}$ in this limit. The topological structure of instantons also translates over to the Skyrme field: if A has instanton number k, this corresponds directly to U having baryon number $\mathcal{B} = k$.

The Skyrme fields U that are obtained from instantons on $\mathbb{R}^4$ via this construction are certainly not exact solutions to the Skyrme field equation (4.3), nevertheless, as approximations to skyrmions, this construction has proven to be remarkably good. Indeed, when compared to the numerical solutions, the energies of the instanton Skyrme fields typically lie within 1% of the 'true energy' given by the numerical solutions. Moreover, many of the symmetric examples of skyrmions that have been found numerically have been reproduced and confirmed by this instanton construction [8, 76, 81, 111, 117]. Another major benefit and motivation of this approximation scheme is in studying low-energy interactions between nucleons. To do this within the Skyrme model, one needs to be able to choose a finite-dimensional manifold of Skyrme fields (with physically relevant coordinates). Since charge k instantons have a moduli space $\mathcal{I}_k$, which is known to be an $8k$-dimensional connected manifold, this approximation generates a connected $(8k-1)$-dimensional manifold of approximate charge k Skyrme fields, given by $\mathcal{I}_k/\mathbb{R}$. We additionally remark that modifications to this approximation have also been considered for more generalised Skyrme models [5, 74], skyrmions defined on different manifolds [80], and skyrmions from generalisations of instantons [35, 103].

For quite some time, nobody had been able to provide a good explanation as to why this construction appeared to approximate skyrmions so well. It wasn't until 2010 that Sutcliffe provided the answer [113]. The key idea was inspired by a Skyrme model introduced by Sakai and Sugimoto [108] in the context of holographic QCD. This Sutcliffe construction utilises a 'mode expansion' of the instanton gauge field in the x^0-direction, by expanding the fields in terms of a complete, orthonormal basis of $L^2(\mathbb{R})$ – the square

integrable functions on $\mathbb{R}$. The correct choice of functions are the **Hermite functions** $\psi_n : \mathbb{R} \longrightarrow \mathbb{R}$, $n \in \mathbb{N}$, defined in [1] by

$$\psi_n(x) = \frac{(-1)^n}{\sqrt{n!2^n\sqrt{\pi}}} e^{\frac{x^2}{2}} \frac{d^n}{dx^n} e^{-x^2}. \tag{4.10}$$

In a gauge where $A_\mu \longrightarrow 0$ as $|x^0| \longrightarrow \infty$, we may perform a subsequent gauge transformation given by the inverse of

$$\Omega(x^0, \vec{x}) = \mathcal{P} \exp\left(- \int_{-\infty}^{x^0} A_0(z, \vec{x}) dz \right). \tag{4.11}$$

Under this, the instanton A transforms such that $A_0 = 0$, and the remaining components satisfy the boundary condition $A_j \longrightarrow U^{-1}\partial_j U$ as $x^0 \longrightarrow +\infty$, where $U(\vec{x}) = \Omega(\infty, \vec{x})$ is the holonomy. These components may be expanded in terms of the Hermite functions as

$$A_j = U^{-1}\partial_j U \psi_+(x^0) + \sum_{n=0}^{\infty} V_j^n(\vec{x}) \psi_n(x^0), \tag{4.12}$$

where $\psi_+ : \mathbb{R} \longrightarrow \mathbb{R}$ is an additional basis function introduced in order to include the holonomy into the expansion. This is defined as

$$\psi_+(x^0) = \frac{1}{\sqrt{2\sqrt{\pi}}} \int_{-\infty}^{x^0} \psi_0(z) dz = \frac{1}{2} + \frac{1}{\sqrt{\pi}} \int_0^{x^0/\sqrt{2}} e^{-w^2} dw, \tag{4.13}$$

and the normalisation given guarantees that $\psi(-\infty) = 0$, and $\psi(\infty) = 1$. The additional fields that appear in the expansion (4.12) are the one-forms V^n, which physically are interpreted as (an infinite number of) *vector mesons*.

The emergence of the Skyrme model is made apparent when the vector mesons are artificially set to be 0. Recall that the Yang-Mills action for the connection D^A is given by

$$S_{YM} = - \int \mathrm{tr}\,(F^A \wedge \star_4 F^A),$$

where $\star_4$ denotes the Hodge-star on $\mathbb{R}^4$. After calculating the curvature F^A of A with respect to the expansion (4.12) in the case that $V^n = 0$, one may perform the integration

$$-\frac{1}{2} \int \left(\int_{-\infty}^{\infty} \mathrm{tr}\ (F_{\mu\nu} F_{\mu\nu})\, dx^0 \right) d^3x$$

corresponding to the contribution of the Yang-Mills lagrangian integrated along the x^0-axis. The resulting integral over $\mathbb{R}^3$ is precisely the energy for a static Skyrme model (4.1), with the coefficients c_0 and c_1 determined explicitly by integrating the Hermite function ψ_+ (4.13):

$$c_0 = \int_{-\infty}^{\infty} \left(\frac{d\psi_+}{dx^0}\right)^2 dx^0 = \frac{1}{2\sqrt{\pi}}, \quad c_1 = \int_{-\infty}^{\infty} \psi_+^2(1-\psi_+)^2 dx^0 \approx 0.099. \tag{4.14}$$

Remark 4.1.1 *The inclusion of the vector mesons in the expansion (4.12) has the fortunate advantage that it makes the derived Skyrme model a BPS theory, and even the inclusion of a finite number reduces the binding energies, leading to more realistic theories [114]. The unfortunate pay-off is that their inclusion is a numerically taxing problem, although some important progress has been made in this area [92].*

4.1.4 Approximating skyrmions with calorons

Very soon after Atiyah and Manton suggested approximating Skyrme fields with instantons (and prior to Sutcliffe's construction), some attempts to compare calorons to Skyrmions were made by calculating caloron holonomies in the S^1 direction [36, 96]. This again showed to be a good approximation of skyrmions. However, there is a problem with using calorons to approximate skyrmions in this way. Apart from the spherically symmetric cases, performing a gauge transformation of the caloron is not a symmetry of the resulting Skyrme field. In fact, this *gauge variance* is a general feature of trying to construct skyrmions from instanton holonomies around circles, for example as seen in [80]. As we shall see in the next section, reassessing this work in light of Sutcliffe's model shows that this problem of missing gauge invariance is no longer apparent when we incorporate an $SU(2)$ gauge field into the model. This means that in reality, the authors of [36, 96] should have been investigating *gauged skyrmions*.

Other interesting applications of the Atiyah-Manton construction involving calorons have been considered in [51], where caloron holonomies have been taken along a line in $\mathbb{R}^3$, resulting in periodic skyrmions, also known as *Skyrme chains*. This in particular shed light on Skyrme chains with symmetries reminiscent of those considered in section 3.6.3, and this suggests that the calorons in Corollary 3.5.9 provide a systematic way of obtaining such symmetric skyrmions.

4.2 Skyrme models from periodic Yang-Mills

In line with our conventions throughout this thesis, let $(t, \vec{x})$ be coordinates on $S^1 \times \mathbb{R}^3$ with the flat product metric, where we identify $t \sim t + \beta$, for some $\beta > 0$.[3] Let A be an $SU(2)$ connection one form on $S^1 \times \mathbb{R}^3$ with components A_μ satisfying

$$A_\mu(t + \beta, \vec{x}) = A_\mu(t, \vec{x}). \tag{4.15}$$

The parallel transport operator of A along S^1 from $-\beta/2$ to t is

$$\Omega(t, \vec{x}) = \mathcal{P} \exp\left(- \int_{-\frac{\beta}{2}}^{t} A_t(z, \vec{x}) dz \right), \tag{4.16}$$

where $\mathcal{P}$ denotes path-ordering. We may choose a gauge such that $\partial_t A_t = 0$, and in this gauge (4.16) becomes

$$\Omega(t, \vec{x}) = \exp\left(- (t + \beta/2)\, A_t(\vec{x}) \right). \tag{4.17}$$

The function $U : \mathbb{R}^3 \longrightarrow SU(2)$ defined by $U(\vec{x}) = \Omega(\beta/2, \vec{x})$, that is, the holonomy, is the candidate for a Skyrme field. This transforms via gauge transformations of the caloron as

$$U(\vec{x}) \mapsto g(\beta/2, \vec{x}) U(\vec{x}) g(-\beta/2, \vec{x})^{-1},$$

and when g is periodic, this hence defines a gauge transformation $g(\vec{x}) := g(\beta/2, \vec{x})$ on $\mathbb{R}^3$.

[3] For notational convenience, we have adopted the notation $\beta = 2\pi/\mu_0$ for the period of a caloron.

We may further transform the connection A with a non-periodic gauge transformation, given by the inverse of the parallel transport operator:

$$A \mapsto \Omega^{-1} A \Omega + \Omega^{-1} d\Omega. \tag{4.18}$$

The transformed gauge potential satisfies

$$A_t = 0, \tag{4.19}$$

$$A_j(t + \beta/2, \vec{x}) = U^{-1} A_j(t - \beta/2, \vec{x}) U + U^{-1} \partial_j U, \tag{4.20}$$

that is, the $\mathbb{R}^3$ components are only periodic up to a gauge transformation by U^{-1}. Now consider an $SU(2)$ connection one form B on $\mathbb{R}^3$ defined via the transformed connection one-form A as $B_j(\vec{x}) = A_j(-\beta/2, \vec{x})$. Let $D^B = d + B$ be the connection covariant derivative defined by B. Then the boundary conditions above for the components A_j imply

$$\begin{aligned} A_j(\beta/2, \vec{x}) - A_j(-\beta/2, \vec{x}) &= U^{-1} D_j^B U, \\ \partial_t \mid_{t=\beta/2} A_j &= U^{-1} \partial_t \mid_{t=-\beta/2} A_j U. \end{aligned} \tag{4.21}$$

We wish to perform a mode expansion of A_j in an analogous way to (4.12), in such a way that respects these boundary conditions. To do this, we shall consider a complete set of L^2-orthogonal functions $\{\varphi_+, \varphi_n \ : \ n \in \mathbb{N}\}$, which span the space $L^2[-\beta/2, \beta/2]$, such that

$$\varphi_+(-\beta/2) = 0, \quad \varphi_+(\beta/2) = 1, \quad \text{and} \quad \varphi_n(\pm\beta/2) = 0, \ \forall \ n \in \mathbb{N}.$$

The function φ_+ is to be defined as

$$\varphi_+(t) = \frac{1}{\mathcal{N}} \int_{-\frac{\beta}{2}}^{t} \varphi_0(s) ds, \tag{4.22}$$

where $\mathcal{N}$ is chosen in such a way that $\varphi_+(\beta/2) = 1$.

There are various choices that we can make here for the functions φ. One obvious choice would be for the mode expansion to be a Fourier expansion, that is, the basis is that of

the trigonometric functions $(-1)^n \cos((n+1)\pi x/\beta)$. Another choice is to consider the *ultra-spherical functions* $\phi_n^{(\alpha,\beta)}$ defined in [1] by[4]

$$\phi_n^{(\alpha,\beta)}(x) = B_n^{(\alpha,\beta)} \left(1 - \left(\frac{2x}{\beta}\right)^2\right)^{\alpha} C_n^{\alpha}\left(\frac{2x}{\beta}\right), \tag{4.23}$$

for all $\alpha > -\frac{1}{2}$, where

$$B_n^{(\alpha,\beta)} = \sqrt{\frac{2}{\beta}}\sqrt{\frac{n!(n+2\alpha+\frac{1}{2})\Gamma(2\alpha+\frac{1}{2})^2}{\pi 2^{-4\alpha}\Gamma(n+4\alpha+1)}}, \quad \alpha \neq -\frac{1}{4}, \quad B_n^{(-\frac{1}{4},\beta)} = \frac{n}{\sqrt{\pi\beta}},$$
$$C_n^{\alpha}(x) = \frac{(-1)^n}{2^n n!}\frac{\Gamma(2\alpha+1)\Gamma(n+4\alpha+1)}{\Gamma(4\alpha+1)\Gamma(n+2\alpha+1)}(1-x^2)^{-2\alpha}\frac{d^n}{dx^n}(1-x^2)^{n+2\alpha},$$

with Γ the usual gamma function

$$\Gamma(x) = \int_0^{\infty} t^{x-1}e^{-t}dt.$$

Ultimately we shall only be considering the ultra-spherical functions in our constructions, and not the Fourier expansion, for reasons outlined later in section 4.2.2.

Expanding A_j in terms of any of these choices of functions, we obtain

$$A_j(t,\vec{x}) = \varphi_+(t)L_j(\vec{x}) + B_j(\vec{x}) + \sum_{n=0}^{\infty} V_j^n(\vec{x})\varphi_n(t), \tag{4.24}$$

where the one form $L = U^{-1}D^B U$ is the left-invariant Maurer-Cartan current on $\mathbb{R}^3$, and the fields V^n represent an infinite tower of vector mesons, in analogy to Sutcliffe's expansion of instantons (4.12). In general, the one-forms V^n may be subject to some additional constraints in order for (4.21) to hold. If we set $V^n = 0$ for all n, then the expanded gauge field (4.24) certainly satisfies the boundary conditions (4.21) regardless of the choice of basis. The curvature F^A of A may be easily calculated in this basis in the case where $V^n = 0$ as

$$F^A = -\frac{d}{dt}\varphi_+(t)L \wedge dt + (1-\varphi_+(t))\left(F^B - \varphi_+(t)L\wedge L\right) + \varphi_+(t)U^{-1}F^B U, \tag{4.25}$$

[4]For the purposes of later simplicity, we have changed the conventions in [1] as $\alpha \mapsto 2\alpha + \frac{1}{2}$.

where $F^B = dB + B \wedge B$ is the curvature of B.

Recall that the Yang-Mills action for the connection D^A is given by

$$S_{YM} = -\int \mathrm{tr}\,(F^A \wedge \star_4 F^A),$$

where $\star_4$ denotes the Hodge-star on $S^1 \times \mathbb{R}^3$. Using (4.25), and integrating over the interval $[-\beta/2, \beta/2]$, we may write an energy functional over $\mathbb{R}^3$ as the contribution of the Yang-Mills lagrangian integrated over this interval:

$$\begin{aligned} E = \int \big(\lambda_0 |L|^2 + \lambda_1 |L \wedge L|^2 + \lambda_2 |F^B|^2 + \lambda_3 \langle F^B, U^{-1} F^B U\rangle \\ -\lambda_4 \left\langle F^B, L \wedge L\right\rangle - \lambda_5 \left\langle U^{-1} F^B U, L \wedge L\right\rangle\big)\, d^3x. \end{aligned} \tag{4.26}$$

The coefficients λ_p are determined by the φ_+-dependent integrals

$$\begin{aligned} &\lambda_0 = \textstyle\int_{-\frac{\beta}{2}}^{\frac{\beta}{2}} \left(\frac{d\varphi_+}{dt}\right)^2 dt, && \lambda_1 = \textstyle\int_{-\frac{\beta}{2}}^{\frac{\beta}{2}} (1-\varphi_+)^2 \varphi_+^2 dt, \\ &\lambda_2 = \textstyle\int_{-\frac{\beta}{2}}^{\frac{\beta}{2}} \left(1 - 2\varphi_+ + 2\varphi_+^2\right) dt, && \lambda_3 = 2\textstyle\int_{-\frac{\beta}{2}}^{\frac{\beta}{2}} (1-\varphi_+)\varphi_+ dt, \\ &\lambda_4 = 2\textstyle\int_{-\frac{\beta}{2}}^{\frac{\beta}{2}} (1-\varphi_+)^2 \varphi_+ dt, && \lambda_5 = 2\textstyle\int_{-\frac{\beta}{2}}^{\frac{\beta}{2}} (1-\varphi_+)\varphi_+^2 dt. \end{aligned} \tag{4.27}$$

The energy (4.26) describes an $SU(2)$ Skyrme model on $\mathbb{R}^3$ coupled to a gauge field B, that is, a *gauged Skyrme model*. Moreover, the energy is invariant under gauge transformations induced by transforming the periodic connection D^A.

There have been various previous considerations of static gauged Skyrme models [4, 16, 17, 102]. In the cases where the gauge transformations take values in $SU(2)$ [4, 16], the terms in the energies considered are $|L|^2$, $|L \wedge L|^2$, and $|F|^2$. The model (4.26) that we have derived contains additional 'cross terms' which have not been considered in the context of of any gauged Skyrme model before, but nevertheless are gauge-invariant, and seem to be natural terms to include due to their appearance from this construction.

4.2.1 A family of gauged Skyrme energies

Recall the ultraspherical functions $\phi_n^{(\alpha,\beta)}$ defined for $\alpha > -1/2$ and $\beta > 0$ by (4.23). We shall now consider the expansion (4.24) in terms of these functions. Since we are only interested at this time in the case where $V^n = 0$, the only function that contributes to the energy (4.26) is the additional function $\phi_+^{(\alpha,\beta)}$, given by

$$\begin{aligned}\phi_+^{(\alpha,\beta)}(t) &= \frac{2^{\frac{1}{2}-2\alpha}\Gamma\left(\alpha+\frac{3}{2}\right)}{\Gamma\left(\alpha+1\right)\sqrt{(2\alpha+\frac{1}{2})\beta}}\sqrt{\frac{\Gamma(4\alpha+1)}{\Gamma(2\alpha+\frac{1}{2})^2}}\int_{-\frac{\beta}{2}}^{t}\phi_0^{(\alpha,\beta)}(z)dz \\ &= \frac{2t}{\beta}\frac{\Gamma(\alpha+\frac{3}{2})}{\sqrt{\pi}\Gamma(\alpha+1)}\,{}_2F_1\left(\frac{1}{2},-\alpha;\frac{3}{2};\frac{4t^2}{\beta^2}\right)+\frac{1}{2}. \qquad (4.28)\end{aligned}$$

Here ${}_2F_1(a,b;c;z)$ denotes the hypergeometric function[5], and the normalisation has been chosen so that $\phi_+^{(\alpha,\beta)}(-\beta/2) = 0$, and $\phi_+^{(\alpha,\beta)}(\beta/2) = 1$. These identities may be straightforwardly checked by utilising the integral formula for the 'beta function'

$$\frac{\Gamma(z)\Gamma(w)}{\Gamma(z+w)} = 2\int_0^{\frac{\pi}{2}}\sin^{2z-1}(x)\cos^{2w-1}(x)dx, \quad \text{for } \Re(z),\Re(w) > 0.$$

The hypergeometric function (4.28) has a power series expansion given by (see [1])

$$\phi_+^{(\alpha,1)}(t) = \frac{1}{2} + \mathcal{K}\sum_{k=0}^{\infty}\frac{1}{2k+1}\frac{(-1)^k}{k!}\left(\prod_{r=0}^{k-1}(\alpha-r)\right)(2t)^{2k+1}, \qquad (4.29)$$

where $\mathcal{K}$ is a constant dependent only on α, which is well-defined when $\alpha > -\frac{1}{2}$. Letting

$$x_k = \frac{1}{2k+1}\frac{(-1)^k}{k!}\left(\prod_{r=0}^{k-1}(\alpha-r)\right)(2t)^{2k+1},$$

note that

$$\lim_{k\longrightarrow\infty}\left|\frac{x_{k+1}}{x_k}\right| = 4|t|^2.$$

Therefore this series converges for all $|t| < \frac{1}{2}$. Since $\phi_+^{(\alpha,\beta)}(t) = \phi_+^{(\alpha,1)}(t/\beta)$, this means the function $\phi_+^{(\alpha,\beta)}$ is well-defined, and clearly continuous on $[-\frac{1}{2},\frac{1}{2}]$, for all $\alpha > -\frac{1}{2}$, and $\beta > 0$.

[5] See [1].

The next step is to compute the coefficients λ_p appearing in the energy (4.26). These are determined by the formulae (4.27) and require the evaluation of the integrals

$$I_r(\alpha) = \int_{-\frac{1}{2}}^{\frac{1}{2}} \left(\phi_+^{(\alpha,1)}(t)\right)^r dt, \tag{4.30}$$

for all $r = 0, \ldots, 4$. For $r = 0, 1$, the integrals I_r are easy to calculate, namely

$$I_0(\alpha) = 1, \quad I_1(\alpha) = \frac{1}{2}. \tag{4.31}$$

Additionally, for $r = 3$, we can use the symmetry of the interval $[-1/2, 1/2]$, and the fact that the non-constant term of (4.28) is an odd function, to obtain

$$I_3(\alpha) = \frac{3}{2} I_2(\alpha) - \frac{1}{4}. \tag{4.32}$$

Evaluating I_r for $r = 2, 4$ is a harder problem, and it seems that for $r = 4$ it cannot even be done analytically[6] in general. Nevertheless, we may use (4.26) and (4.27), and formulate a family of gauged Skyrme energies

$$\begin{aligned} E_{\alpha,\beta} = \int \Bigg(& \frac{\kappa_0}{\beta}|L|^2 + \frac{\beta}{2}\kappa_1 |L \wedge L|^2 + \beta |F^B|^2 \\ & + \beta\kappa_2 \left(\left\langle U^{-1} F^B U, F^B \right\rangle - \frac{1}{2} \left\langle F^B + U^{-1} F^B U, L \wedge L \right\rangle - |F^B|^2 \right) \Bigg) d^3x, \end{aligned} \tag{4.33}$$

where we have introduced the notation

$$\kappa_0(\alpha) = \frac{2}{\sqrt{\pi}} \frac{\Gamma(2\alpha+1)\Gamma(\alpha+\frac{3}{2})^2}{\Gamma(2\alpha+\frac{3}{2})\Gamma(\alpha+1)^2}, \tag{4.34}$$

$$\kappa_1(\alpha) = 1 + 2I_4 - 4I_2, \tag{4.35}$$

$$\kappa_2(\alpha) = 1 - 2I_2. \tag{4.36}$$

As already stipulated, calculating κ_1 and κ_2 explicitly is generally not possible, and numerical integration techniques must be employed. In the case that $\alpha = m \in \mathbb{Z}$, the

[6] That is, cannot be expressed in closed form in terms of elementary functions of α. A recently calculated formula for I_2 appears in [29].

hypergeometric function (4.28) takes the form of a degree $2m+1$ polynomial with rational coefficients:

$$\phi_+^{(m,\beta)}(t) = \frac{1}{2} + \frac{\Gamma(m+\frac{3}{2})}{m!\sqrt{\pi}} \sum_{k=0}^{m} \binom{m}{k} \frac{(-1)^k}{(2k+1)} \left(\frac{2t}{\beta}\right)^{2k+1}. \tag{4.37}$$

In these special cases, the coupling constants κ_p are rational, and may be explicitly calculated for any $m \in \mathbb{Z}$. However, as can be seen in table 4.1, these coefficients grow to be dramatically unwieldy as m increases.

m	0	1	2	3	4
κ_0	1	$6/5$	$10/7$	$700/429$	$4410/2431$
κ_1	$1/15$	$243/5005$	$38750/969969$	$\frac{506611}{14593293}$	$\frac{5496461712}{176684241305}$
κ_2	$1/3$	$9/35$	$50/231$	$245/1287$	$\frac{7938}{46189}$

Table 4.1: The coupling coefficients in the energy $E_{m,\beta}$ for $m = 0, 1, 2, 3, 4$.

4.2.2 The instanton/un-gauged limit

Expanding the caloron gauge field (4.24) in terms of the complete, orthonormal basis of $L^2([-\beta/2, \beta/2])$, given by the ultra-spherical functions, has revealed a family of gauged Skyrme energies parameterised by the period $\beta > 0$ of the caloron, and the ultraspherical parameter $\alpha > -1/2$. Other more complicated models may also be obtained by including some of the vector mesons V^n in (4.24), resulting in extensions to the family of energies we already have. This choice of functions already has an advantage over considering a different basis of $L^2([-\beta/2, \beta/2])$, for example the trigonometric functions, since we may vary the parameter α to explore different properties of the energy (4.33). Another advantage of this choice is the relationship between the ultraspherical functions and the Hermite functions (4.10) and (4.13). Indeed, consider a limit where $\alpha, \beta \longrightarrow \infty$, such

that $\alpha/\beta^2 \longrightarrow 1/8$. In this limit, the weight function for the ultraspherical functions satisfies

$$\left(1-\left(\frac{2x}{\beta}\right)^2\right)^{\alpha} \longrightarrow e^{-\frac{x^2}{2}}. \tag{4.38}$$

Also, for all $z > 0$ sufficiently large, we have [1] that for all $a > 0$, $b \in \mathbb{R}$

$$\Gamma(az+b) \sim \sqrt{2\pi}e^{-az}(az)^{az+b-\frac{1}{2}}. \tag{4.39}$$

From the formula (4.23), and using both (4.38) and (4.39), we therefore have that for $\alpha, \beta > 0$ large:

$$\begin{aligned}
\phi_n^{(\alpha,\beta)}(x) &\sim (-1)^n \sqrt{\frac{2^{\frac{3}{2}-2n}}{\beta n!\sqrt{\pi}\alpha^{n-\frac{1}{2}}}} \left(1-\left(\frac{2x}{\beta}\right)^2\right)^{-\alpha} \left(\frac{\beta}{2}\right)^n \frac{d^n}{dx^n}\left(1-\left(\frac{2x}{\beta}\right)^2\right)^{2\alpha} \\
&= (-1)^n \sqrt{\frac{(\beta^2/8\alpha)^{n-\frac{1}{2}}}{n!2^n\sqrt{\pi}}} \left(1-\left(\frac{2x}{\beta}\right)^2\right)^{-\alpha} \frac{d^n}{dx^n}\left(1-\left(\frac{2x}{\beta}\right)^2\right)^{2\alpha} \\
&\xrightarrow{\alpha,\beta\longrightarrow\infty} \frac{(-1)^n}{\sqrt{n!2^n\sqrt{\pi}}} e^{\frac{x^2}{2}} \frac{d^n}{dx^n} e^{-x^2},
\end{aligned}$$

which is the formula (4.10) for the Hermite functions ψ_n. As ψ_+ and $\phi_+^{(\alpha,\beta)}$ are defined as normalised integrals (over $\mathbb{R}$ and $[-\beta/2, \beta/2]$) of ψ_0 and $\phi_0^{(\alpha,\beta)}$ respectively, it hence follows that the limit $\phi_+^{(\alpha,\beta)} \longrightarrow \psi_+$ also holds.

The main consequence of this limiting behaviour is that any gauged Skyrme model derived from the ultraspherical functions in the mode expansion (4.24) of a caloron (with any number of vector mesons included) reduces, in a particular limit as $\alpha, \beta \longrightarrow \infty$, to the Sutcliffe model derived from an instanton mode expansion (4.12), with the same number of vector mesons included. In particular, in the case that $V^n = 0$, we have that the energy for an ordinary Skyrme model is made manifest in this limit as a part of the gauged Skyrme energy (4.33). Since the limit $\beta \longrightarrow \infty$ corresponds to an infinitely periodic caloron, which may in many cases be recognised as an instanton on $\mathbb{R}^4$, we shall hence call the limit $\alpha, \beta \longrightarrow \infty$ with $\alpha/\beta^2 \longrightarrow 1/8$ the *instanton* or *un-gauged limit* of the gauged Skyrme energy (4.33).

4.2.3 Scaling and parameter fixing

It is straightforward to show that under a re-scaling of the spatial coordinates via $\vec{x} \mapsto \frac{1}{\beta}\vec{x}$, the energy (4.33) transforms as

$$E_{\alpha,\beta} \mapsto \frac{1}{\beta^3} E_{\alpha,1}.$$

What this means is that as far as the functional $E_{\alpha,\beta}$ is concerned, the parameter β only affects it up to a re-scaling of the energy and length units. Therefore, in order to make things simpler, we may without loss of generality choose to set $\beta = 1$, which we shall do from now on. For notational brevity, we shall also introduce the notation $E_\alpha = E_{\alpha,1}$ and henceforth consider the energies

$$\begin{aligned} E_\alpha = \int \Big(& \kappa_0 |L|^2 + \frac{\kappa_1}{2} |L \wedge L|^2 + |F^B|^2 \\ & + \kappa_2 \left(\left\langle U^{-1} F^B U, F^B \right\rangle - \frac{1}{2} \left\langle F^B + U^{-1} F^B U, L \wedge L \right\rangle - |F^B|^2 \right) \Big) \, d^3x. \end{aligned} \tag{4.40}$$

4.3 Topological charge and energy bounds

Recall that the topological charge for a Yang-Mills field is given by the formula (1.7):

$$Q_{YM} = \frac{1}{8\pi^2} \int \mathrm{tr} \left(F^A \wedge F^A \right).$$

Similarly to the energy, we may calculate the topological charge for our gauged Skyrme model (4.33) by inserting the expansion (4.24) with $V^n = 0$ into (1.7) and integrating over $[-\beta/2, \beta/2]$. We hence obtain the formula

$$\mathcal{B} = \frac{1}{8\pi^2} \int \mathrm{tr} \left(\frac{1}{3} L \wedge L \wedge L - L \wedge \left(F^B + U^{-1} F^B U \right) \right), \tag{4.41}$$

which is precisely the usual topological charge for a gauged Skyrme model [4, 16, 102], and reduces to the topological charge (4.4) for the ordinary Skyrme model when $B = 0$. The Yang-Mills topological bound (1.6) $S_{YM} \geq 8\pi^2 |Q_{YM}|$ may be applied in the context

of our gauged Skyrme models, and we immediately have the energy bound

$$E_\alpha \geq 8\pi^2|\mathcal{B}| \tag{4.42}$$

for all $\alpha > -\frac{1}{2}$. For analogous reasons to why ordinary skyrmions cannot attain the energy bound, any minimisers of (4.33) will not attain the energy bound (4.42) either. However, the model which includes all of the vector mesons will be BPS, in as much as minimisers can obtain the topological bound (4.42), simply because they are a completion of the caloron mode expansion, and calorons *are* BPS.

For the model which we are concerned with, that is, the one with no vector mesons, described by the family of energies (4.33), there is no reason why the bound (4.42) is the best bound that can be found for all $\alpha > -\frac{1}{2}$. In fact, we suspect the following to hold:[7]

Conjecture 4.3.1 *The gauged Skyrme energy E_α satisfies the topological bound*

$$E_\alpha \geq 8\pi^2 C(\alpha)|\mathcal{B}|, \tag{4.43}$$

where $C(\alpha)$ is given by

$$C(\alpha) = \sqrt{\frac{9\kappa_0\left(2\kappa_1 - \kappa_2^2\right)}{1 + 18\kappa_1 - 6\kappa_2}}. \tag{4.44}$$

Moreover, this bound is the best bound that may be obtained by completing the square.

Proving this conjecture in general is an analytically hard problem, as it requires proving many different inequalities for the coefficients κ_p. A general approach of how to prove this would be the following argument.

Consider the quadratic forms on $\mathbb{R}^4$:

$$\omega_E = \kappa_0 x^2 + \frac{\kappa_1}{2}y^2 + I_2 z^2 + I_2 w^2 + \kappa_2 zw - \frac{\kappa_2}{2}y(w+z), \tag{4.45}$$

$$\omega_{\mathcal{B}} = \frac{1}{3}xy - x(w+z). \tag{4.46}$$

[7] Following the submission of this thesis, we have arrived at a proof of this conjecture, using an argument that is different to that outlined below. This may be found in [29].

It is straightforward to see from (4.40) and (4.41) that determining an optimal bound of the form

$$E_\alpha \geq 8C\pi^2|\mathcal{B}|$$

is equivalent to finding the maximal value of C such that the quadratic form

$$\Omega_C = \omega_E - C\omega_{\mathcal{B}} \tag{4.47}$$

is positive definite. The associated symmetric matrix to this quadratic form has characteristic polynomial

$$\chi(\Omega_C)(\lambda) = \frac{1}{144}\left(2\kappa_2 - 1 + 2\lambda\right)\left(C^2\left(1 + 18\kappa_1 - 6\kappa_2 - 38\lambda\right)\right.$$
$$\left. +9(\kappa_0 - \lambda)(\kappa_2^2 - 2\kappa_1 + 4(1+\kappa_1)\lambda - 8\lambda^2)\right).$$

The eigenvalues of Ω_C are given by the roots of $\chi(\Omega_C)$, which are $\lambda_0 = \frac{1}{2}(1-2\kappa_2)$, and $\lambda_{1,2,3}$ determined by the roots of the polynomial P_C:

$$P_C(\lambda) = C^2\left(1 + 18\kappa_1 - 6\kappa_2 - 38\lambda\right) + 9(\kappa_0 - \lambda)(\kappa_2^2 - 2\kappa_1 + 4(1+\kappa_1)\lambda - 8\lambda^2).$$

Note that by the formula (4.28), the integral I_2 (4.30) satisfies

$$I_2 = \int_{-\frac{1}{2}}^{\frac{1}{2}} \left(\frac{1}{2} + \eta(t)\right)^2 dt = \int_{-\frac{1}{2}}^{\frac{1}{2}} \left(\frac{1}{4} + \eta(t)^2\right) dt,$$

where $\eta(t)$ is the non-constant term in (4.28), which is clearly an odd function. Hence, $\frac{1}{4} < I_2$, which means that $\kappa_2 < \frac{1}{2}$. Thus $\lambda_0 \geq 0$. Therefore, we only need to maximize C such that the roots of P_C are non-negative. When $C = C_{\max}$ where

$$C_{\max}^2 = \frac{9\kappa_0\left(2\kappa_1 - \kappa_2^2\right)}{1 + 18\kappa_1 - 6\kappa_2},$$

we have

$$P_{C_{\max}}(\lambda) = 9\lambda\left(2\kappa_1 - \kappa_2^2 + 4\kappa_0(1+\kappa_1) - \frac{38\kappa_0\left(2\kappa_1 - \kappa_2^2\right)}{1 + 18\kappa_1 - 6\kappa_2} - 4\left(1 + \kappa_1 + 2\kappa_0\right)\lambda + 8\lambda^2\right)$$

The roots of this polynomial are given by $\lambda_1 = 0$ and

$$\lambda_\pm = \frac{1}{4}\left(1 + 2\kappa_0 + \kappa_1 \pm \Xi\right),$$

where

$$\Xi = \sqrt{1 + 4\kappa_0^2 - 2\kappa_1 + \kappa_1^2 + 2\kappa_2^2 - \frac{4\kappa_0\left(1 + 18\kappa_1^2 - 6\kappa_2 + 19\kappa_2^2 - \kappa_1(19 + 6\kappa_2)\right)}{1 + 18\kappa_1 - 6\kappa_2}}.$$

In order to guarantee that this choice of $C_{\max}$ gives a true lower bound, we need to show two things: that $C_{\max}^2 > 0$, namely $C_{\max} \in \mathbb{R}^+$, and that $\lambda_\pm$ are distinct and non-negative for all $\alpha > -\frac{1}{2}$. For the latter, it suffices to show that the $\Xi^2 > 0$, that is, the discriminant is positive. Both of these conditions have been checked and shown to be true for several values of $-\frac{1}{2} < \alpha < 100$.[8]

If these conditions are met for all $\alpha > -\frac{1}{2}$, it is straightforward to see why this is the maximum value that can be obtained in this way, as the following argument shows. If $C > C_{\max}$, it is clear that $\chi(\Omega_C)(0) > 0$, and furthermore

$$\lim_{\lambda \longrightarrow -\infty} \chi(\Omega_C)(\lambda) = -\infty < 0.$$

Therefore by the intermediate value theorem, there exists $-\infty < \lambda_0 < 0$ such that $\chi(\Omega_C)(\lambda_0) = 0$, i.e. a negative eigenvalue. Thus $C_{\max}$ would be the most optimal.

In figure 4.1, we plot the function $C(\alpha)$ given in conjecture 4.3.1, and in each case plotted, the conditions of the above argument have been checked to be true. For $\alpha \geq 0$, the bound is observed to be relatively stable, with $C \sim 1$ for all α, whereas, for $\alpha < 0$, the bound becomes extremely large – whilst it cannot be seen in the plot, we found that $C(-0.499) \approx 8.29811$. This suggests that the model is far more well-behaved for $\alpha \geq 0$. Due to the analysis in section 4.2.2, from the formulae (4.5) and (4.14), we expect the limit

$$\lim_{\alpha \longrightarrow \infty} C(\alpha) = 6\sqrt{c_0 c_1} \approx 1.0027 \tag{4.48}$$

to hold. Interestingly, the minimum value of C that we have found is given uniquely by $\alpha = 0$, where $C(0) = 1$, i.e. the topological bound for $\alpha = 0$ agrees with the Yang-Mills bound, whereas in all other cases, we have a stronger bound.

[8] To be completely transparent, this has only been done analytically for $\alpha \in \mathbb{Z}$, and all other cases had to be checked numerically.

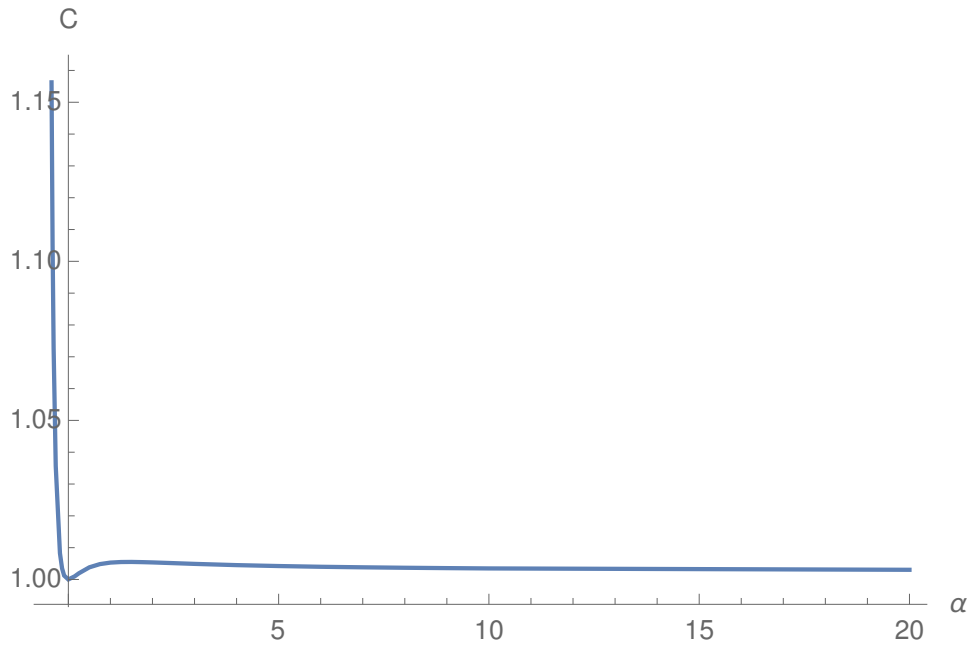

Figure 4.1: The function $C(\alpha)$ appearing in the topological bound $E_\alpha \geq 8\pi^2 C(\alpha)|\mathcal{B}|$.

4.4 Numerical gauged skyrmions and their caloron approximations

4.4.1 The hedgehog ansatz

The group $O(3)$ of spherical rotations and reflections has a natural action on the space of gauged Skyrme configurations given in analogy to (4.6) by

$$\mathfrak{R} \cdot (U, B) = (U \circ \mathfrak{R}, \mathfrak{R}^* B)\,, \tag{4.49}$$

where $\mathfrak{R} : \mathbb{R}^3 \longrightarrow \mathbb{R}^3$ represents an element of $O(3)$. As usual, a gauged skyrmion (U, B) will be called H**-symmetric** if for all $\mathfrak{R} \in H \subset O(3)$, it is invariant under (4.49), up to gauge transformations, and parity transformations (4.8) of the Skyrme field. These actions combined leave the energy (4.40) invariant, so are symmetries of the field theory. It is well-known that the most general representative (U, B) of a gauged Skyrme configuration

which is $O(3)$-symmetric is given by the fields in the *hedgehog ansatz*[9]

$$U = \exp\left(\imath f(r)\frac{\vec{x}\cdot\vec{\sigma}}{r}\right), \quad B = \frac{\imath}{2}\left(g(r)-1\right)\frac{\vec{x}\times\vec{\sigma}}{r^2}\cdot d\vec{x}, \tag{4.50}$$

where $f, g : (0,\infty) \longrightarrow \mathbb{R}$ are functions in the radial direction $r = |\vec{x}|$. Imposing this spherically symmetric form, the family of energies (4.40) reduce to the one-dimensional integral

$$\begin{aligned} E_\alpha^H =& 8\pi\int_0^\infty \left(\kappa_0\left(r^2 f'^2 + 2g^2\sin^2 f\right) + \frac{1}{4r^2}\left(1-g^2\right)^2 + \frac{g'^2}{2}\right. \\ &+\kappa_2\left(\sin^2 f\left(\frac{g^2}{r^2}\left(1-g^2\right) - g'^2\right) - f'gg'\sin 2f\right) \\ &\left.+2\kappa_1\left(\frac{g^4}{r^2}\sin^4 f + 2f'^2 g^2\sin^2 f\right)\right) dr. \end{aligned} \tag{4.51}$$

Similarly, we may calculate the topological charge for the fields in the hedgehog ansatz as

$$\begin{aligned} \mathcal{B}^H &= \frac{1}{\pi}\int_0^\infty \left(f'(1-g^2) - gg'\sin 2f + 2f'g^2\sin^2 f\right) dr \\ &= \frac{1}{\pi}\int_0^\infty \frac{d}{dr}\left(f - \frac{1}{2}g^2\sin 2f\right) dr \\ &= \frac{1}{\pi}\left[f - \frac{1}{2}g^2\sin 2f\right]_0^\infty . \end{aligned} \tag{4.52}$$

[9]The name hedgehog is in reference to the pion fields, which here take the form

$$\vec{\pi} = \sin f\frac{\vec{x}}{r},$$

that is, they point radially outwards from 0 at all points in $\mathbb{R}^3$, which bears resemblance to a hedgehog's spines.

It is straightforward to derive the equations which govern the critical points of (4.51). These are the coupled non-linear second-order $ODEs$ given by

$$2\kappa_0\left(r^2f''+2rf'-g^2\sin 2f\right)-\kappa_2\left(gg''+\frac{g^2}{r^2}\left(1-g^2\right)\right)\sin 2f \tag{4.53}$$
$$+4\kappa_1\left(f'^2g^2\sin 2f+\left(2f''g^2+4f'gg'-\frac{g^4}{r^2}\sin 2f\right)\sin^2 f\right)=0,$$

$$g''+\frac{g}{r^2}\left(1-g^2\right)-4\kappa_0 g\sin^2 f-8\kappa_1\left(\frac{g^2}{r^2}\sin^2 f+f'^2\right)g\sin^2 f \tag{4.54}$$
$$-\kappa_2\left(2f'^2g\cos 2f+\left(f''g+2f'g'\right)\sin 2f+2\left(g''+\frac{g}{r^2}\left(1-2g^2\right)\right)\sin^2 f\right)=0.$$

4.4.2 Skyrme-monopoles

Unlike ordinary skyrmions, the Skyrme field for a gauged Skyrme model does not have to satisfy the boundary condition $U \longrightarrow \mathbb{1}$ as $r \longrightarrow \infty$. This is made apparent by considering BPS[10] monopoles as approximate gauged skyrmions. Indeed, recall that $SU(2)$ BPS monopoles are the $(m,0)$-calorons, whose gauge field A_t is identified with the Higgs field Φ. These satisfy the boundary condition

$$-\frac{1}{2}\mathrm{tr}\left(\Phi^2\right)\longrightarrow\nu^2 \tag{4.55}$$

for some $\nu\in(0,\pi]$.[11] The corresponding Skyrme field given by the holonomy of the monopole hence satisfies the boundary condition

$$\frac{1}{2}\mathrm{tr}\,U\longrightarrow\cos\nu. \tag{4.56}$$

There is hence no reason why we cannot consider boundary conditions like (4.56) for gauged skyrmions. A gauged skyrmion satisfying boundary conditions including the condition (4.56) will be called a **Skyrme-monopole** parameterised by $\nu\in(0,\pi]$. Note that the baryon number of an ordinary skyrmion is always integer valued. In contrast, the

[10] We adopt the term 'BPS' monopoles for the remainder of this chapter to describe monopoles on $\mathbb{R}^3$.

[11] We are still sticking to the convention that $\beta=1$, that is, $\mu_0=2\pi$.

charge (4.41) for fields satisfying (4.56) can potentially be any real number, moreover, there is no reason why such a U should be constant on S^2_∞. This highlights a key difference between ordinary skyrmions and gauged skyrmions.

At the moment, we are concerned with the spherically symmetric configurations. We hence consider the following boundary conditions for the profile functions within the spherically symmetric ansatz (4.50):

$$\begin{aligned} f(0) &= 0, \quad g(0) = 1, \\ f(\infty) &= \nu, \quad g(\infty) = 0, \end{aligned} \tag{4.57}$$

for some constant $\nu \in (0, \pi]$. These conditions are chosen so that (4.56) holds, U and B are well-defined at $r = 0$, and so that $D^B U, F^B \longrightarrow 0$ as $r \longrightarrow \infty$ ensuring finite energy. Immediately, from (4.52), we see that such a Skyrme-monopole has topological charge $\mathcal{B}^H = \nu/\pi$. We remark that boundary conditions of this type have previously been investigated for $SU(2)$ gauged Skyrme models in [16].

The gauged Skyrme fields derived from the charge $m = 1$ BPS monopole with spherical symmetry have the profile functions

$$f(r) = \nu \coth(2\nu r) - \frac{1}{2r}, \tag{4.58}$$

$$g(r) = \frac{2\nu r}{\sinh(2\nu r)}, \tag{4.59}$$

and these are seen to satisfy the boundary conditions (4.57). We may therefore compare gauged skyrmion configurations satisfying the field equations (4.53)-(4.54), with the boundary conditions (4.57), to this monopole.

Solving the equations (4.53)-(4.54) explicitly is not so simple, so we shall approximate solutions numerically. In order to do this, we must understand the limiting behaviour of the functions f and g near the boundaries. For $r << 1$, the linearisations of the field

equations are

$$r^2 f'' + 2rf' + 2(1-2g)f = 0, \tag{4.60}$$

$$g'' + \frac{2}{r^2}(1-g) = 0. \tag{4.61}$$

Equation (4.61) has general solution satisfying (4.57) given by

$$g(r) = 1 - cr^2, \tag{4.62}$$

for some $c \in \mathbb{R}^+$.[12] Substituting this into (4.60), we obtain the equation

$$r^2 f'' + 2rf' + \left(4cr^2 - 2\right) f = 0. \tag{4.63}$$

This is a spherical Bessel equation of order 1. A general spherical Bessel equation of order $n \in \mathbb{Z}^+$ is of the form

$$r^2 f'' + 2rf' + (r^2 - n(n+1))f = 0,$$

with solutions

$$j_n(r) = (-r)^n \left(\frac{1}{r}\frac{d}{dr}\right)^n \frac{\sin r}{r}, \quad y_n(r) = -(-r)^n \left(\frac{1}{r}\frac{d}{dr}\right)^n \frac{\cos r}{r},$$

where and $j_n(z)$ and $y_n(z)$ are the spherical Bessel functions of the first and second kind. These functions satisfy the conditions $j_1(0) = 0$ and $y_1(0) = \infty$. Hence, (4.63) has solutions satisfying (4.57) given by

$$f(r) = aj_1\left(2\sqrt{c}r\right), \tag{4.64}$$

where $a \in \mathbb{R}$.

For r large, the equation (4.53) for f linearises simply to

$$\left(r^2 f'\right)' = 0. \tag{4.65}$$

[12] We expect $c \in \mathbb{R}^+$ as g should be a monotonically decaying function.

Solving (4.65) with the boundary condition $f(\infty) = \nu$ gives the large r form of f as

$$f(r) = \nu - \frac{b}{r}, \tag{4.66}$$

for some constant $b \in \mathbb{R}$. This constant has a physical interpretation, namely the **scalar charge** of the Skyrme-monopole. To understand the asymptotics of g, we need to study equation (4.54) with knowledge of the form of f. The linearisation is (up to order r^{-1}) given by

$$g'' - 4\kappa_0 \left(\frac{\sin^2 \nu}{1 - 2\kappa_2 \sin^2 \nu} - \frac{\sin 2\nu}{\left(1 - 2\kappa_2 \sin^2 \nu\right)^2} \frac{b}{r} \right) g + O(r^{-2}) = 0. \tag{4.67}$$

Drawing inspiration from the Frobenius method [42], we expect an asymptotic form for g of the form

$$g(r) = \sum_{j,k=0}^{\infty} e^{\chi_j r} r^{p_{jk}}, \tag{4.68}$$

where $\chi_0 > \chi_1 > \ldots$, and $p_{j0} > p_{j1} > \ldots$ are real numbers for all $j \in \mathbb{N}$. In practice we only need to consider the leading term, so that $g(r) = e^{\chi r} r^p$. Plugging this into (4.67), we may set the leading and sub-leading terms equal to 0 and solve for χ and p. Choosing the decaying solution, we therefore have the asymptotic form for g as

$$g(r) = d \exp\left(-2 \sin \nu \sqrt{\frac{\kappa_0}{1 - 2\kappa_2 \sin^2 \nu}} r \right) r^{2b \cos \nu \sqrt{\kappa_0} \left(\frac{1}{1 - 2\kappa_2 \sin^2 \nu} \right)^{\frac{3}{2}}}, \tag{4.69}$$

for some constant $d \in \mathbb{R}$ to be determined. It is important to note that the asymptotic formula (4.69) for g near $r = \infty$ may only be applied for $\nu \neq \pi$, since when $\nu = \pi$, this formula does not decay unless $d = 0$, which is not a reasonable choice for the asymptotics.

To find a suitable asymptotic form for g when $\nu = \pi$, we shall need to include more terms in the expansion (4.67). Consider now

$$f(r) \sim \pi - \frac{b}{r},$$

for some $b \in \mathbb{R}$. With this, we may expand (4.54) with $g \sim 0$ to obtain

$$g'' + \frac{4\kappa_2 b^2}{r^3} g' + \left(1 - 4b^2\kappa_0\right) \frac{g}{r^2} + O(r^{-4}) = 0. \tag{4.70}$$

Again we expect the asymptotic solution to take the form $g = de^{\chi r} r^p$. Substituting this ansatz into (4.70), and setting the leading coefficients to 0, we find a decaying solution given by

$$g(r) \sim dr^{\frac{1}{2}\left(1-\sqrt{1+4(4b^2\kappa_0-1)}\right)}, \tag{4.71}$$

again with $d \in \mathbb{R}$ constant. This is only decaying when

$$4b^2\kappa_0 - 1 > 0, \tag{4.72}$$

and if we do not have this condition, we expect no solutions to exist. This is in contrast to the case where $\nu \neq \pi$, where no such condition is required.

Numerical algorithm

Using the asymptotic formulae for the profile functions f and g of a Skyrme-monopole, we may produce numerical solutions to the field equations (4.53)-(4.54). Our approach is to determine the constants (a, b, c, d) in the asymptotic formulae by performing a 'shooting algorithm'. More precisely, using Mathematica's inbuilt numerical differential equation solver (the 'NDSolve' function), for each $\alpha > -1/2$ and $\nu \in (0, \pi]$, we may solve the field equations on a finite interval $[\epsilon, K]$, with boundary conditions at $r = \epsilon \sim 0$, and separately at $r = K \sim \infty$. The boundary conditions are taken by the asymptotic formulae for f and g which depend on the constants $(a, b, c, d) \in \mathbb{R}^4$. This gives a set of four functions $f_s(a, c), f_l(b, d), g_s(a, c), g_l(b, d) : [\epsilon, K] \longrightarrow \mathbb{R}$ describing numerical solutions to the field equations with the 'small r' (subscript s) and 'large r' (subscript l) boundary conditions.

The next step is to determine the values of the constants $(a, b, c, d) \in \mathbb{R}^4$ so that

$$F(a, b, c, d)(r) = (f_s - f_l, f_s' - f_l', g_s - g_l, g_s' - g_l')\,(r) = 0,$$

for some choice of $r \in [\epsilon, K]$. In other words, we desire the numerical solutions, and their derivatives, with 'small r' boundary conditions to match those with 'large r' boundary conditions. To do this, we can employ the multi-variable Newton-Raphson algorithm. In general, an n variable Newton-Raphson algorithm solves the equation $F_j(\vec{x}) = 0$ for all $j = 1, \ldots, n$ with the iteration

$$\vec{x}_{k+1} = \vec{x}_k - \left(\begin{pmatrix} \frac{\partial F_1}{\partial x^1} & \cdots & \frac{\partial F_1}{\partial x^n} \\ \vdots & \ddots & \vdots \\ \frac{\partial F_n}{\partial x^1} & \cdots & \frac{\partial F_n}{\partial x^n} \end{pmatrix}^{-1} F \right)(\vec{x}_k). \tag{4.73}$$

To do this, we need the derivatives with respect to a, b, c, and d of the numerical solutions and their derivatives. These may be well-approximated by taking the linear derivative

$$\frac{df}{da} \approx \frac{f(a+h) - f(a)}{h}, \tag{4.74}$$

for some $h << 1$, which we will fix to be 10^{-9} in all calculations. To further minimise the numerical error, we may repeat this algorithm on a new interval $[\epsilon', K']$, for $\epsilon' \leq \epsilon$ and $K \leq K'$, and with the new initial guesses for (a, b, c, d) determined by the result of the Newton-Raphson step on $[\epsilon, K]$.

The energy for the numerical solutions may also be calculated using numerical integration techniques. For this we will utilise a modified Simpson's rule, with a sufficiently large number of intervals. Again, to minimise the error, we may use the numerical solutions with 'small r' boundary conditions to calculate the integral on $[\epsilon, r_0]$, and the solutions with 'large r' boundary conditions to calculate the integral on $[r_0, K]$, where r_0 is the chosen 'matching point'. In addition to the numerical integration, the value of the energy on $(0, \epsilon) \cup (K, \infty)$ may be calculated analytically by inserting the asymptotic formulae for f and g into a linearised version of the energy functional (4.51).

Whenever any numerics are performed, it is important to have consistency checks in place in order to be sure that we can trust the numerical results. The main check in this case is that increasing the interval size should not vary the values of the constants (a, b, c, d)

or the value of the energy E_α. Another check that can be performed are to calculate the topological charge numerically (in an analogous way to the energy), and see how close it is to the true charge ν/π. Since we are dealing with skyrmions, we have an even better check, and that is to see if the *Virial theorem* holds (which we have adapted for our purposes):

Theorem 4.4.1 *Let E^2 and E^4 correspond to the terms in E_α which are quadratic and quartic respectively in spatial derivatives. Then any minimiser (U, B) of E_α must satisfy*

$$E^2(U, B) = E^4(U, B).$$

Proof

Under a re-scaling of space $\vec{x} \mapsto \mu\vec{x}$, the energy becomes

$$E_\alpha(\mu) = \frac{1}{\mu}E^2 + \mu E^4.$$

Any minimiser of E_α should not depend on this scale, and therefore should satisfy

$$\left.\frac{d}{d\mu}\right|_{\mu=1} E_\alpha(\mu)(U, B) = 0.$$

This equation implies the equation in the statement of the theorem. □

In all of the subsequent statements of numerical results, all numbers and figures have been through these checks, and have been deemed reliable if the accuracy is correct to at least 2 decimal places.

Numerical results and comparison to monopoles

In light of the results given in section 4.2.2, that as $\alpha \longrightarrow \infty$, the gauged Skyrme energy E_α reduces to the ordinary Skyrme energy, it would be most interesting to study the behaviour at the other extreme, namely α small. The smallest value of $\alpha > -\frac{1}{2}$ for which we may explicitly calculate the coefficients in the energy is when $\alpha = 0$, and so this is

the case in which we shall study the general Skyrme-monopoles in detail. This is also a particularly interesting extreme case due to the apparent behaviour of the topological bound, conjectured in conjecture 4.3.1, as a function of α.

We find numerical solutions exist for all $\nu \in (0, \pi]$, and as an example, the profile functions in the case $\nu = \pi/3$ are plotted in figure 4.2. We also would like to compare the

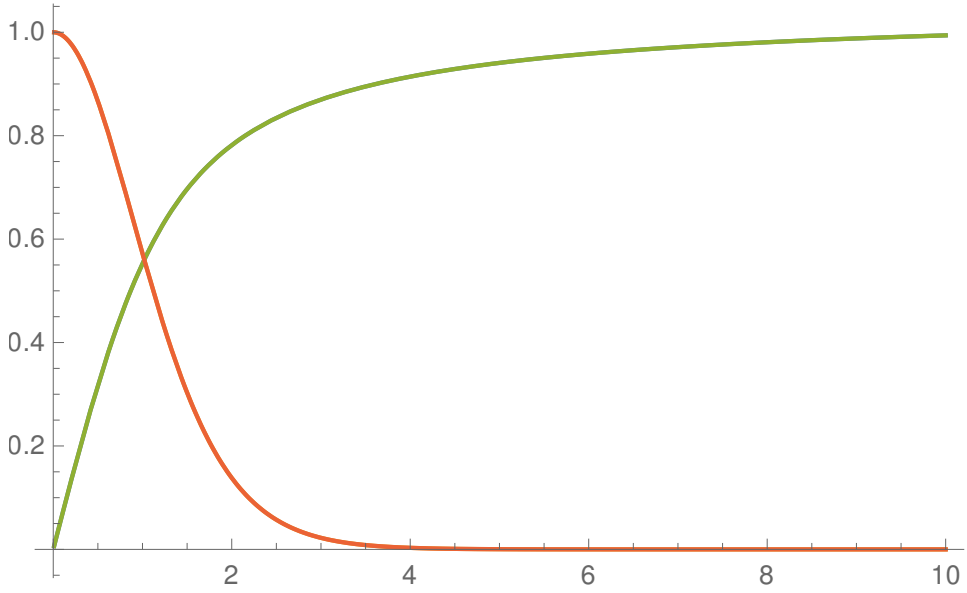

Figure 4.2: The profile functions (f green, g orange) for the Skyrme-monopole with $\nu = \pi/3$ in the energy E_0.

solutions to that of the BPS monopole. The energy data for both the numerical solutions and BPS monopole approximation are plotted in figure 4.3 along with the theoretical energy given by the topological bound. As can be seen, the approximation is really good, with less than a 1% difference in the energies for $0 < \nu < 7\pi/15$, and negligible difference near $\nu = 0$. As ν approaches π, the approximation is seen to be worse, but still within a reasonable degree of accuracy, with the percentage difference at $\nu = \pi$ only 12.6%.

Another good measure of how the Skyrme-monopoles agree with the BPS monopoles is the scalar charge b. For the BPS monopole, this is a topological quantity, namely, it is

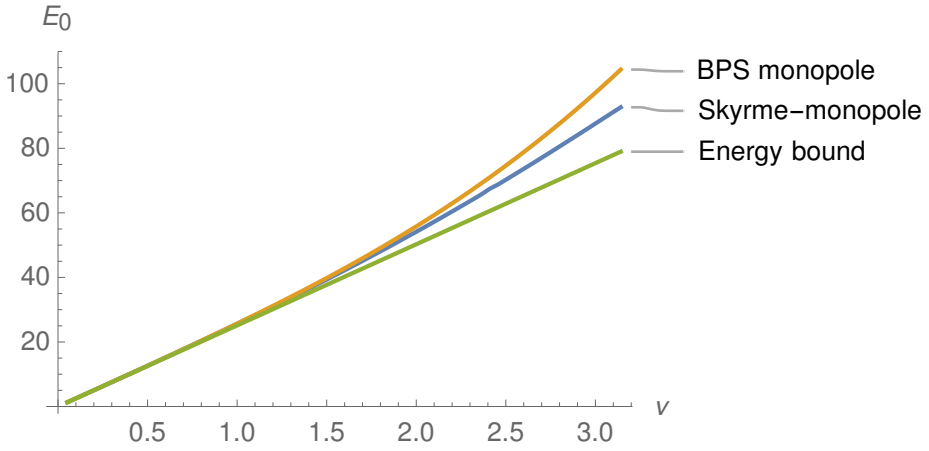

Figure 4.3: The energies of the Skyrme-monopole (blue), monopole approximation (orange), and the topological absolute minimum (green), for $\nu \in (0, \pi]$.

exactly half the magnetic charge, i.e. $b = 1/2$, as seen by the profile function (4.58). The value of b for the Skyrme-monopole solutions is plotted in figure 4.4. As with the energy, this constant is seen to be close to that of the BPS monopole for $\nu \approx 0$, and deviates further away from that of the BPS monopole as $\nu \longrightarrow \pi$.

Varying α

Having studied in some detail the Skyrme-monopole solutions for $\alpha = 0$, it would be interesting to see what occurs as α varies. Doing this for general $\nu \in (0, \pi]$ is quite a laborious task, so instead we have considered three distinctly separated cases: $\nu = \pi$, $\nu = 2\pi/3$, and $\nu = \pi/3$. The case $\nu = \pi$ is particularly interesting for two reasons. Firstly, the asymptotic behaviour for the profile function g is explicitly different to that for $\nu \neq \pi$, and in particular the condition $4b^2\kappa_0(\alpha) - 1 > 0$ must hold in order for solutions to exist. Secondly, the topological charge of such a Skyrme-monopole is $\mathcal{B} = 1$, which is the same as the configurations which we consider in section 4.4.3. We may hence compare these Skyrme-monopoles with these other configurations, and this we shall also explore in section 4.4.3.

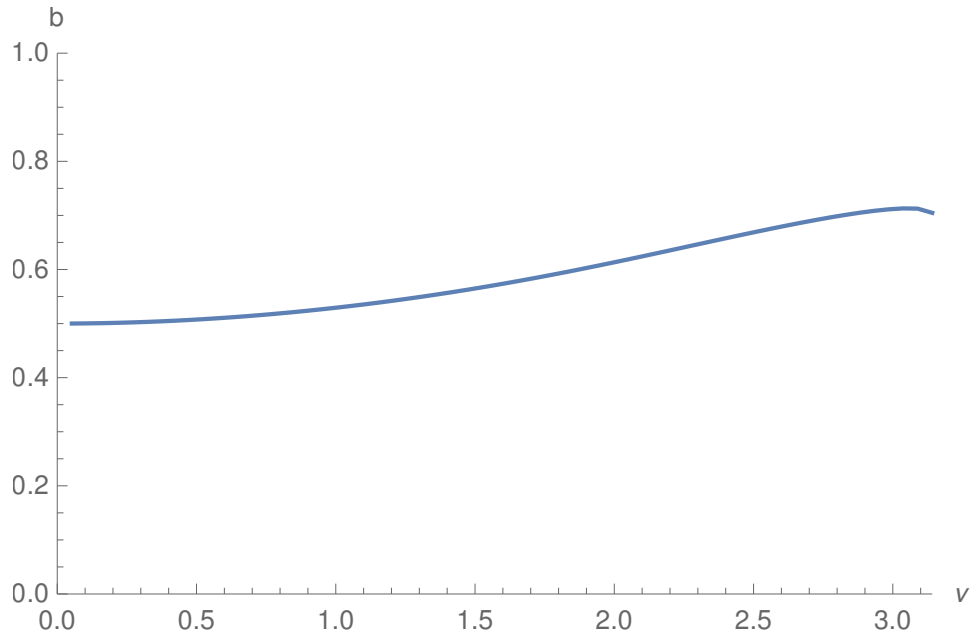

Figure 4.4: The scalar charge of the Skyrme-monopoles for $\nu \in (0, \pi]$.

The phase diagrams of the energies E_α for these Skyrme-monopoles, compared to the BPS monopole energies, for varying $0 \leq \alpha \leq 1$, are plotted in figures 4.6-4.7. A similar observation occurs as with the detailed analysis of the case $\alpha = 0$, namely, the BPS monopole approximation is significantly better for ν close to 0 compared to ν close to π. It is also noticeable that as α increases, whilst the approximation improves in each case, the energies also increase. This seemingly monotone behaviour in the Skyrme-monopole energies is in contrast to the topological energy bound (4.3.1), which remains essentially constant for $\alpha > 0$.

Specifically in the case $\nu = \pi$, we find that for $-\frac{1}{2} < \alpha \leq \frac{1}{2}$[13] there are numerical solutions which satisfy Theorem 4.4.1. However, we were not able to generate such solutions for $\alpha > \frac{1}{2}$. In figure 4.8, we plot the quantity $4b^2\kappa_0 - 1$ for the $\nu = \pi$ Skyrme-monopoles, and it is observed that $4b^2\kappa_0(0.5) - 1 \approx 0$,[14] which may explain why our numerics did not behave well for $\alpha > 0.5$. This aligns with the necessary condition

[13] We have only plotted for $\alpha \geq 0$ for the sake of clarity.

[14] The actual value we obtained numerically was 0.0036 to two significant figures.

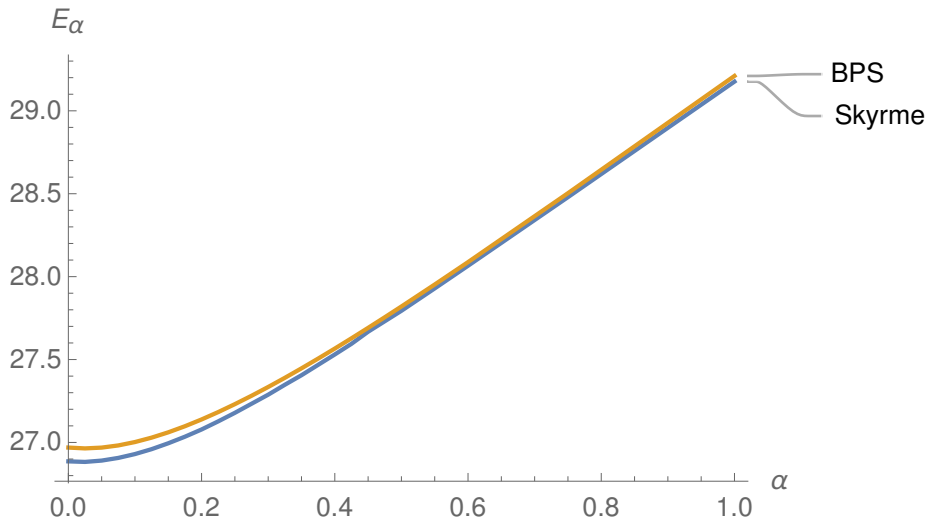

Figure 4.5: The phase diagram for the energies of Skyrme and BPS monopoles with $\nu = \frac{\pi}{3}$, for varying $0 \leq \alpha \leq 1$.

(4.72). Having said this, there is no reason to believe that the quantity $4b^2\kappa_0 - 1$ does not become positive again, and hence that additional Skyrme-monopoles with $\nu = \pi$ could exist, for some value of $\alpha > \frac{1}{2}$. This we are yet to investigate.

Rather intriguingly, for some value of $\alpha \sim 0$ we observe that $4b^2\kappa_0 - 1 = 1$. From (4.71), this means that for this value of α, g behaves like $r^{-1/\varphi}$, where

$$\varphi = \frac{1+\sqrt{5}}{2}$$

is the golden ratio. It is unclear whether any meaning should be taken from this numerological observation, nevertheless, it is certainly rather curious.

4.4.3 Skyrme-instantons

$SU(2)$ calorons with zero magnetic charge are the (k,k)-calorons that much of this thesis has concentrated on. The Skyrme field constructed from the holonomy of a (k,k)-caloron

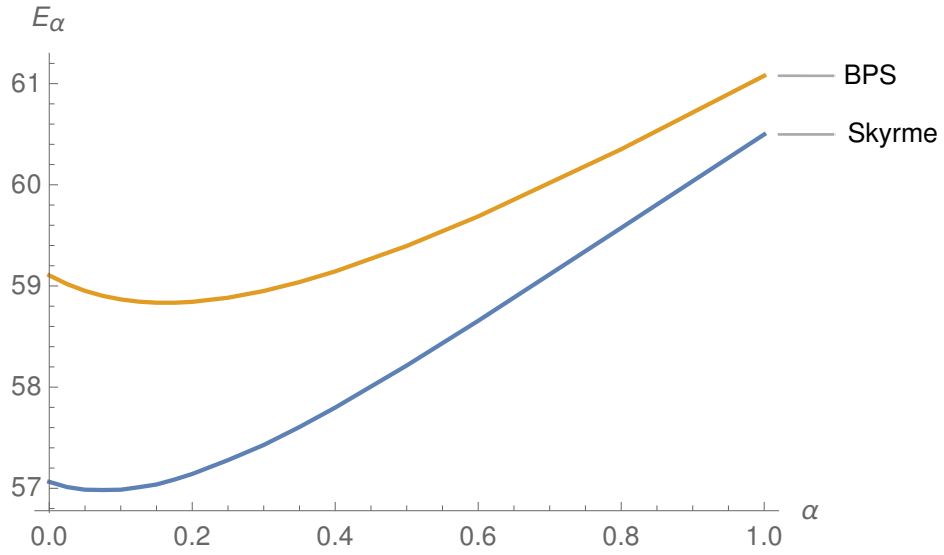

Figure 4.6: The phase diagram for the energies of Skyrme and BPS monopoles with $\nu = \frac{2\pi}{3}$, for varying $0 \leq \alpha \leq 1$.

satisfies the boundary condition

$$U \longrightarrow \begin{pmatrix} e^{-\imath\mu} & 0 \\ 0 & e^{\imath\mu} \end{pmatrix}, \tag{4.75}$$

with $\mu \in [0, \pi]$, and has topological charge $\mathcal{B} = k$. A gauged skyrmion satisfying boundary conditions including the condition (4.75) for any $\mu \in [0, \pi]$ will be called a **Skyrme-instanton** of degree k, where $k = \deg(U)$.

For the time-being, we are interested in the spherically symmetric examples. There is a one-parameter family of $(1,1)$-calorons which possess $O(3)$-symmetry.[15] These are found within the family of Harrington-Shepard calorons from section 2.2.1 which are $(1,1)$ calorons with $\mu = 0$ (i.e. they have trivial holonomy). The components of the caloron gauge field may be written more explicitly. Indeed,

$$A_t(t, \vec{x}) = \imath f(t,r) \frac{\vec{x} \cdot \vec{\sigma}}{r}, \quad A_j(t, \vec{x}) = \frac{\imath}{2} \left((g(t,r) - 1) \frac{\epsilon_{jkl} x^k \sigma^l}{r^2} + h(t,r) \sigma^j \right), \tag{4.76}$$

[15] The $O(3)$ subgroup of $(O(2) \times O(3))_+$ is precisely $(\{e, T\} \times O(3))_+$, where T is the map $t \mapsto -t$ in S^1.

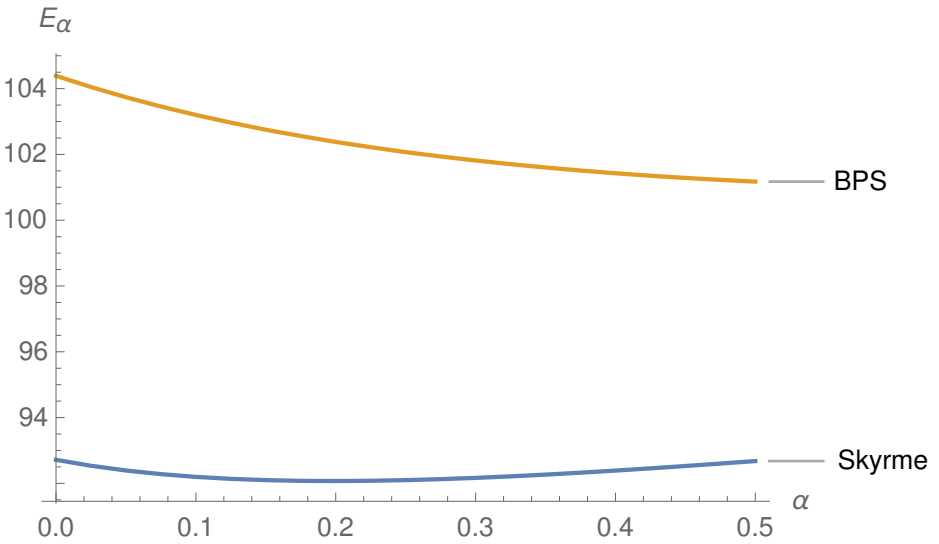

Figure 4.7: The phase diagram for the energies of Skyrme and BPS monopoles with $\nu = \pi$, for varying $0 \leq \alpha \leq \frac{1}{2}$.

where

$$f = -\frac{\partial_r \phi}{2\phi}, \quad g = 1 + \frac{r\partial_r \phi}{\phi}, \quad h = \frac{\partial_t \phi}{\phi}, \tag{4.77}$$

with $\phi : S^1 \times \mathbb{R}^3 \longrightarrow \mathbb{R}$ given by

$$\phi = 1 + \frac{\lambda^2}{2r} \frac{\sinh(2\pi r)}{\cosh(2\pi r) - \cos(2\pi(t-\theta))}, \tag{4.78}$$

which is (2.16) with $k = 1$, spatial position $\vec{a} = 0$, and $\mu_0 = 2\pi$ to match our scaling conventions. At the moment, (4.76) only has $SO(3)$-symmetry, due to the appearance of the function $h(t, r)$. In order to obtain $O(3)$-symmetry we need to fix the parameter θ. Setting $\theta = \pm\frac{1}{2}$, or $\theta = 0$ makes $h(-t, r) = -h(t, r)$, and then we have full spherical symmetry. In these cases, the functions f and g take the forms[16]

$$f_0(t, r) = \frac{\lambda^2}{4r^2} \frac{\sinh(2\pi r)(\cosh(2\pi r) - \cos(2\pi t)) - 2\pi r\,(1 - \cosh(2\pi r)\cos(2\pi t))}{(\cosh(2\pi r) - \cos(2\pi t))(\cosh(2\pi r) - \cos(2\pi t) + \frac{\lambda^2}{2r}\sinh(2\pi r))},$$
$$g_0(-\frac{1}{2}, r) = \frac{\pi\lambda^2 + 1 + \cosh(2\pi r)}{\cosh(2\pi r) + 1 + \frac{\lambda^2}{2r}\sinh(2\pi r)},$$

[16] We have evaluated g at $t = -\frac{1}{2}$ as this is the requirement to define the skyrmion gauge field B.

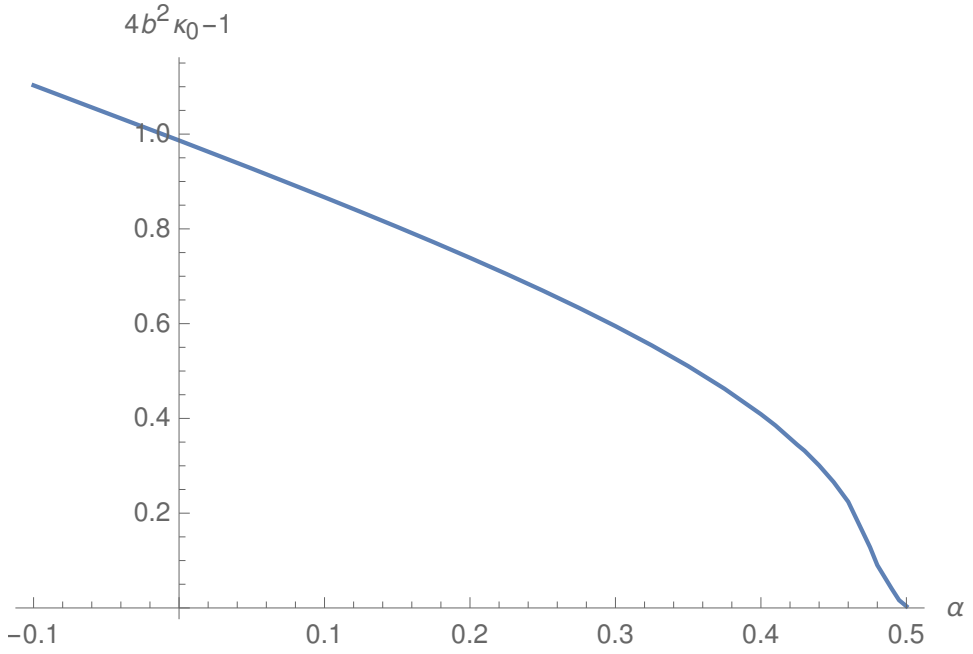

Figure 4.8: The value of the 'cut-off variable' $4b^2\kappa_0 - 1$ plotted as a function of α.

when $\theta = 0$, and

$$f_{\pm}(t,r) = \frac{\lambda^2}{4r^2}\frac{\sinh(2\pi r)(\cosh(2\pi r)+\cos(2\pi t)) - 2\pi r\,(1+\cosh(2\pi r)\cos(2\pi t))}{(\cosh(2\pi r)+\cos(2\pi t))(\cosh(2\pi r)+\cos(2\pi t)+\frac{\lambda^2}{2r}\sinh(2\pi r))},$$
$$g_{\pm}(-\frac{1}{2},r) = \frac{\cosh(2\pi r)) - 1 - \pi\lambda^2}{\cosh(2\pi r) - 1 + \frac{\lambda^2}{2r}\sinh(2\pi r)},$$

when $\theta = \pm\frac{1}{2}$. Note that since $\lambda \neq 0$, we have $g_{\pm} \longrightarrow -1$ as $r \longrightarrow 0$, so the constructed skyrme gauge field B would have a singularity at $r = 0$, as seen by the formula (4.50). This is problematic. However, no such singularity exists for the case $\theta = 0$, since $g_0 \longrightarrow 1$ as $r \longrightarrow 0$, so we shall from now on only consider this case.

After a short calculation, we find that the resulting profile functions for the corresponding Skyrme fields are

$$f_\lambda(r) = \frac{\pi\sinh(2\pi r) - \frac{\lambda^2}{4r^2}(\sinh(2\pi r) - 2\pi r\cosh(2\pi r))}{\sqrt{\left(\frac{\lambda^2}{2r}\sinh(2\pi r)+\cosh(2\pi r)-1\right)\left(\frac{\lambda^2}{2r}\sinh(2\pi r)+\cosh(2\pi r)+1\right)}} - \pi,$$
$$g_\lambda(r) = 1 + \frac{\lambda^2\pi - \frac{\lambda^2}{2r}\sinh(2\pi r)}{\frac{\lambda^2}{2r}\sinh(2\pi r)+1+\cosh(2\pi r)},$$

where the *scale* $\lambda > 0$ is the only remaining parameter. This parameter λ may be optimised for each α so that E_α is minimised. We denote by $\lambda_{\min}$ this optimal value of λ for each $\alpha > -\frac{1}{2}$. These optimal values are plotted for $\alpha > 0$ in figure 4.9.

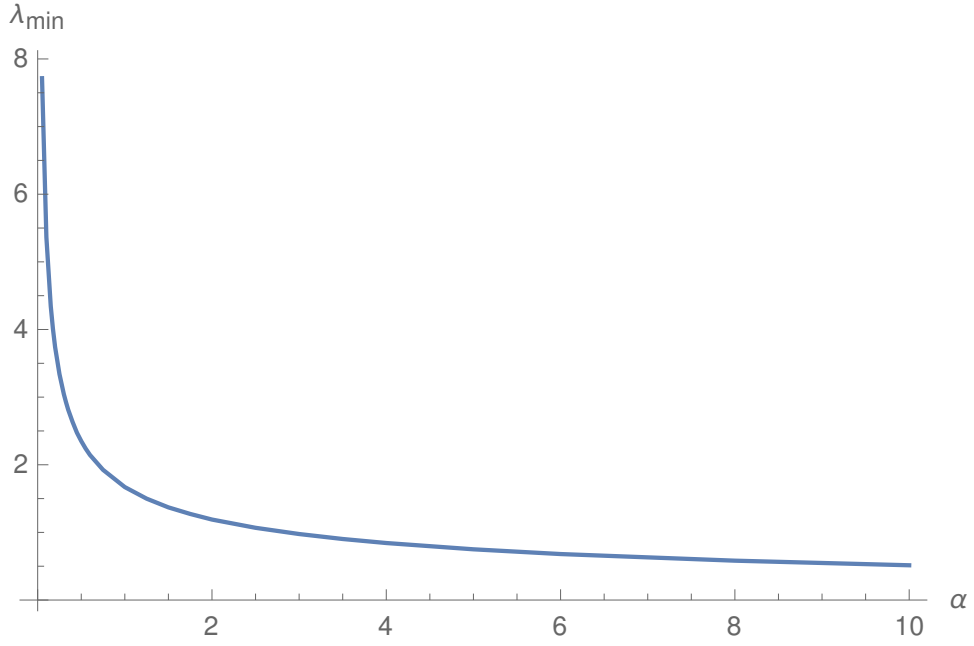

Figure 4.9: The optimal value $\lambda_{\min}(\alpha)$ of the Harrington-Shepard scale parameter such that E_α is minimised.

A noticeable property of this is that for $\alpha \sim 0$, $\lambda_{\min}$ is very large. In fact, our numerics suggest that $\lambda_{\min}(0) = \infty$. Now, the functions f_λ and g_λ both have well-defined limits as $\lambda \longrightarrow \infty$, given by

$$f_\infty(r) = \pi \coth(2\pi r) - \frac{1}{2r} - \pi, \tag{4.79}$$

$$g_\infty(r) = \frac{2\pi r}{\sinh(2\pi r)}. \tag{4.80}$$

These are remarkably similar to the profile functions of the $\nu = \pi$ BPS monopole (4.58)-(4.59), with the difference $f_\infty = f_{\text{BPS}} - \pi$. This is of course not a coincidence, but merely a consequence of the fact that the limit $\lambda \longrightarrow \infty$, the $(1,1)$ Harrington-Shepard caloron is the image under the rotation map of the charge 1 BPS monopole, as discussed in section 2.2.4 and in [107]. This observation, in light of figure 4.9, suggests that the energy E_α

prefers 'monopole-like' boundary conditions near $\alpha = 0$, and these become less preferred as $\alpha \longrightarrow \infty$. This can also be seen by plotting the energy $E_\alpha(\lambda_{\min})$ against the energy $E_\alpha(\mathrm{BPS})$, which we do in figure 4.10.

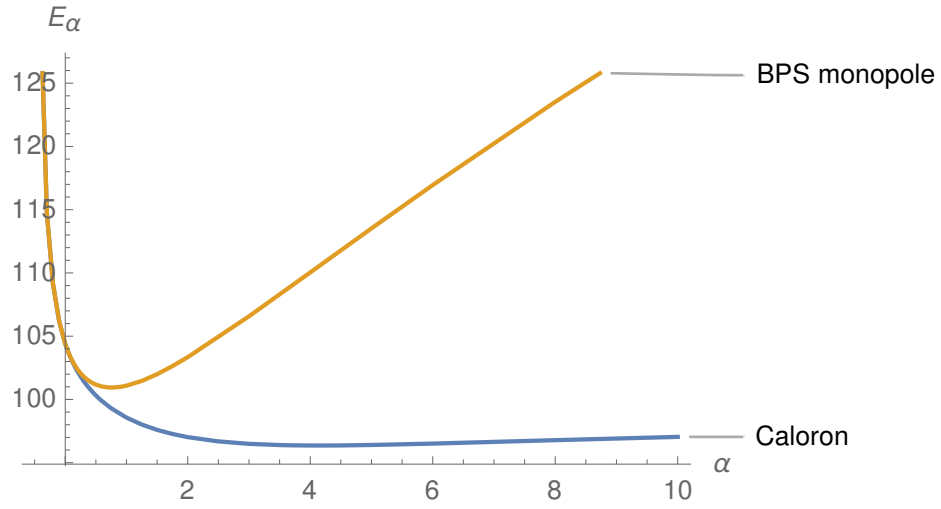

Figure 4.10: The energies E_α, for $-\frac{1}{2} < \alpha \leq 10$, of the optimal Harrington-Shepard caloron and the $\nu = \pi$ BPS monopole.

Having studied the behaviour of the caloron approximations to Skyrme-instantons, we would now like to see how this compares to the behaviour of the 'true' Skyrme-instantons. We consider the following boundary conditions for the hedgehog profile functions:

$$\begin{aligned} f(0) &= -\pi, \quad g(0) = 1, \\ f(\infty) &= 0, \quad g(\infty) = 1. \end{aligned} \tag{4.81}$$

These boundary conditions make (4.50) a Skyrme-instanton in the sense that the boundary condition (4.75) holds. In particular, they are comparable to the Harrington-Shepard caloron, whose profile functions also obey these boundary conditions. From (4.52), the topological charge of such a Skyrme-instanton is $\mathcal{B}^H = 1$. We also remark that the boundary conditions (4.81) are similar to those considered in [4].

In a similar way to the asymptotic analysis of the Skyrme-monopoles, we may linearise the field equations (4.53) and (4.54) to obtain formulae for the asymptotic behaviour of

the Skyrme-instanton. We obtain

$$f_s(r) = ar - \pi, \quad \text{for } r \sim 0, \tag{4.82}$$

$$f_l(r) = -\frac{b}{r^2}, \quad \text{for } r \sim \infty, \tag{4.83}$$

and

$$g_s(r) = 1 - cr^2, \quad \text{for } r \sim 0, \tag{4.84}$$

$$g_l(r) = 1 - \frac{d}{r}, \quad \text{for } r \sim \infty, \tag{4.85}$$

where the numbers $a, b, c, d \in \mathbb{R}$ may be determined using a Newton-Raphson shooting algorithm, analogously to the case of Skyrme-monopoles.

Numerical results and comparison to calorons

For $\alpha > 0$, and sufficiently not close to 0, we find that there are numerical Skyrme-instanton solutions, and we plot their energies against the energies of the optimal caloron approximation in figure 4.11, up to $\alpha = 10$. It would appear from this plot that the caloron approximation gets better as α increases. The behaviour near $\alpha = 0$ is interesting. In the case of Skyrme-monopoles with $\nu = \pi$, we found that there was a cut-off for which our numerics no longer returned valid solutions. For the Skyrme-instantons, our numerics reveal that near $\alpha = 0$, the same absence of solutions occurs. However, in contrast to the case of the Skyrme-monopoles, here we do not have a reasonable hypothesis akin to (4.72) which explains this. What we do have is the caloron approximation. This struggle to find solutions near $\alpha = 0$ was actually predicted by the analysis of the Harrington-Shepard caloron, which suggested that monopole boundary conditions are preferred for $\alpha \sim 0$. It would seem that this is the case for the actual solutions too.

As an illustrative example, implementing the algorithm at $\alpha = 0$ for the Skyrme-instanton boundary conditions (4.81), we observed that the constant d, appearing in the asymptotic

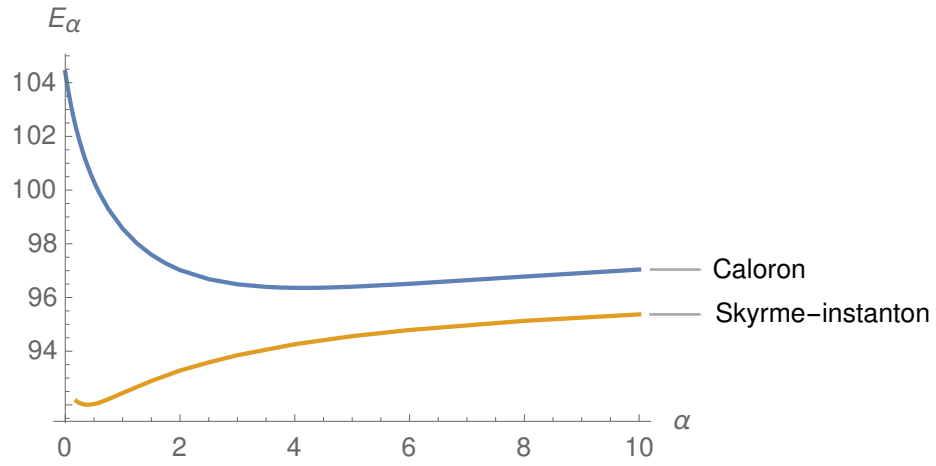

Figure 4.11: The energies E_α for the optimal Harrington-Shepard caloron and the numerical Skyrme-instanton minimisers.

formula (4.85), was not converging as the size of the interval $[\epsilon, K]$ was increased. This can be seen in figure 4.12: as K increases, the profile function g for the gauge field B does not converge to a function satisfying the boundary condition $g(\infty) = 1$. Rather, it appears to become less and less localised, and more comparable to that of a Skyrme-monopole, satisfying $g \longrightarrow 0$ as $r \longrightarrow \infty$. This is manifested in the constant $d = d(K)$ found in (4.85), which satisfies $d(20) \approx 8.16$, and $d(100) \approx 46.93$, suggesting that $g(\infty)$ would prefer to be 0. In contrast, the profile function f for the Skyrme field U does appear to converge (see figure 4.13), which is expected since the boundary conditions are the same as the Skyrme-monopole under the replacement $f \mapsto f - \pi$, which is a symmetry of the field equations.

The energy calculated for this Skyrme-instanton is $E \approx 92.74$, which is extremely close to that of the $\nu = \pi$ Skyrme-monopole, which has energy $E \approx 92.72$. Importantly, this Skyrme-instanton configuration does not satisfy Theorem 4.4.1, with $E^2 \approx 46.35$ and $E^4 \approx 46.39$. We suspect that if we were to continue for $K > 100$, then the energy of the Skyrme-instanton will lower, converging on the energy of the Skyrme-monopole, and with Theorem 4.4.1 satisfied to an acceptable degree of accuracy.

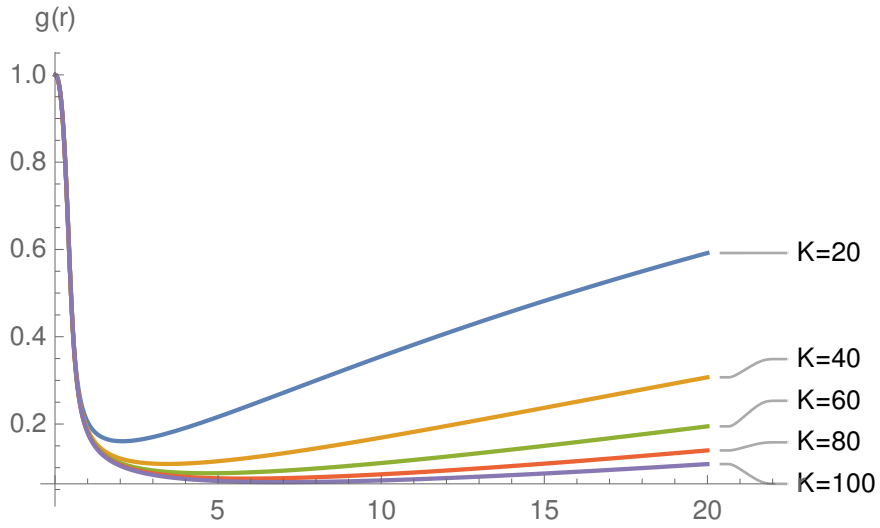

Figure 4.12: The profile functions g for the Skyrme-instanton minimiser of E_0 on the finite intervals $[0.01, K]$, for $K = 20, 40, 60, 80, 100$.

A similar pattern in the numerics is observed for all $0 \leq \alpha < 0.1953$, that is, the algorithm did not converge, and Theorem 4.4.1 was not reasonably satisfied. One hypothesis as to why this is the case for the small values of $\alpha \neq 0$ is that the Skyrme-instanton actually does exist, but it is extremely large, and to construct it would require considering values of K which are far greater than 100, where we usually stopped the process. This is evidenced by considering the behaviour of the optimal Harrington-Shepard caloron profile functions, for which g_λ, for λ large, does not get near to 1 until r is very large. Another idea is that our numerical algorithm is not robust enough to find all of the solutions. One alternative method is to use *pseudo-arclength continuation* alongside our usual shooting algorithm, which means we also vary α, changing the shooting map to a function $\widetilde{F} : \mathbb{R}^5 \longrightarrow \mathbb{R}^4$, $\widetilde{F} = \widetilde{F}(\alpha, a, b, c, d)$. This method has been used for similar purposes, namely to pick out seemingly absent solutions to field equations which depend on a parameter, for example in [41]. Of course, it is also possible that the algorithm did not converge because no solution with those boundary conditions exists.

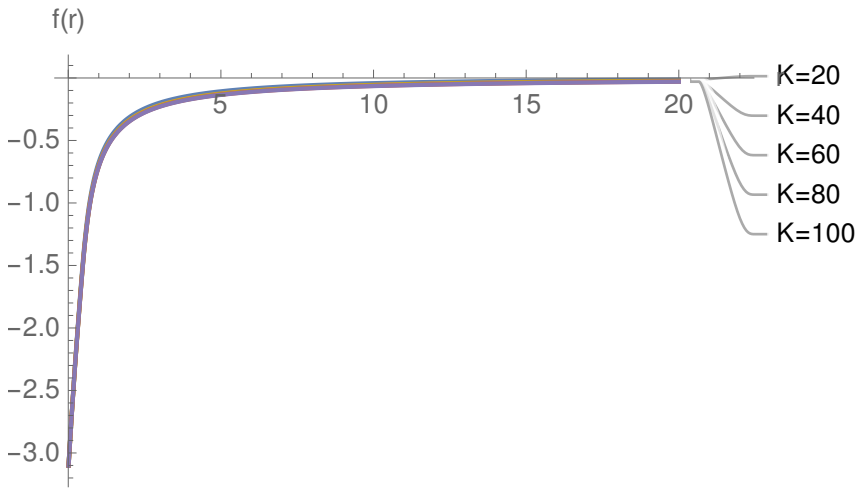

Figure 4.13: The profile functions f for the Skyrme-instanton minimiser of E_0 on the finite intervals $[0.01, K]$, for $K = 20, 40, 60, 80, 100$.

Comparison to Skyrme-monopoles

The main conclusion of studying the spherically-symmetric Skyrme-instantons and Skyrme-monopoles is that the energy (4.51) appears to favour certain boundary conditions as α varies. To test this idea further, we will make another comparison. The Skyrme-monopoles with $\nu = \pi$, and the Skyrme-instantons, both have topological charge $\mathcal{B}^H = 1$, so it is reasonable to compare them as solitons. In fact, we have observed that when $\alpha \approx 0$, these configurations may even be the same, in analogy with the $\lambda \longrightarrow \infty$ limit of the Harrington-Shepard caloron.

Consider the phase diagram in figure 4.14. There we have plotted the value of the energy E_α for both the numerical Skyrme-monopoles and Skyrme-instantons for $\alpha \in [0, 1]$. Clearly, for $\alpha \approx 0$, the Skyrme-monopole boundary conditions dominate since there are no Skyrme-instanton solutions. Extrapolating the curve for the Skyrme-instantons in such a way that the two curves meet at $\alpha = 0$, it is easy to convince oneself that this is also true with regards to minimising the energy. Likewise, the Skyrme-instanton solutions dominate away from $\alpha = 0$.

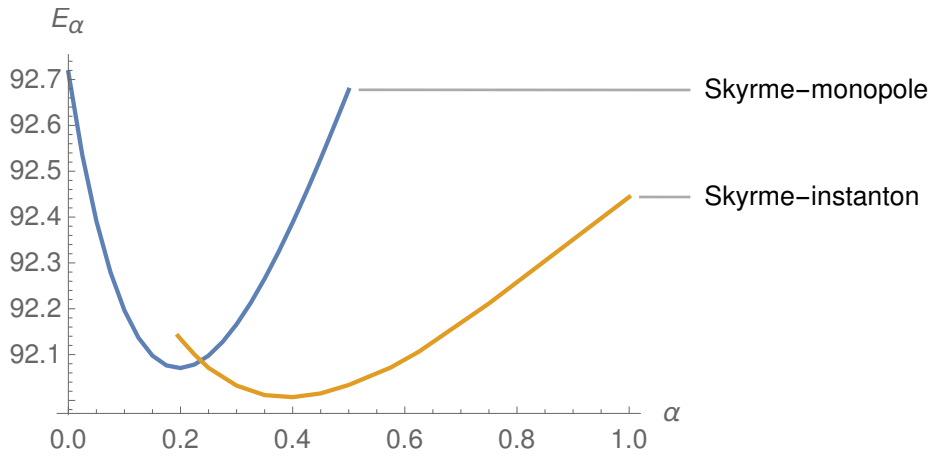

Figure 4.14: A phase diagram of the energies of Skyrme-monopoles and Skyrme-instantons for varying $\alpha \in [0, 1]$.

4.5 Approximating skyrmions with gauged skyrmions

An energy of the form (4.26) describing an $SU(2)$ gauged Skyrme model is a functional $E(U, B)$ of fields (U, B), where $U : \mathbb{R}^3 \longrightarrow SU(2)$, and B is a connection 1-form on $\mathbb{R}^3$. This naturally induces an ordinary Skyrme model in the case that $B = 0$, with energy

$$E^o = \int \left(\lambda_0 |U^{-1}dU|^2 + \lambda_1 |U^{-1}dU \wedge U^{-1}dU|^2\right) d^3x. \tag{4.86}$$

This functional describes a bona-fide $SU(2)$ Skyrme model, whose critical points satisfy the Skyrme field equation (4.3) with $\lambda_p = c_p$. However, unlike the gauged model, this induced model is not invariant under gauge transformations $G : \mathbb{R}^3 \longrightarrow SU(2)$, since here we have

$$U^{-1}dU \mapsto G\left(U^{-1}dU + U^{-1}L_G U - L_G\right)G^{-1},$$

where $L_G = G^{-1}dG$. Letting $\mathcal{L} = U^{-1}(dU + [L_G, U])$, the Skyrme energy (4.86) thus transforms as $E^o(U) \mapsto E(G, U)$, where

$$E(G, U) = \int \left(\lambda_0 |\mathcal{L}|^2 + \lambda_1 |\mathcal{L} \wedge \mathcal{L}|^2\right) d^3x. \tag{4.87}$$

In each gauge equivalence class of gauged skyrmions (U, B) (that is, critical points of (4.26)), it is not unreasonable to ask whether there is a representative $G \cdot (U, B)$ such that GUG^{-1} approximates a critical point of (4.86). This is equivalent to saying (G, U) approximates a critical point of (4.87). Such a pair (G, U) must satisfy the asymptotic boundary conditions $G, U \longrightarrow \mathbb{1}$ as $|\vec{x}| \longrightarrow \infty$, in line with the usual boundary conditions imposed on the Skyrme field.

The important variable that needs to be optimised here is the choice of gauge. Varying $E(G, U)$ with respect to G gives the equations

$$\sum_{i,j} \partial_i \left(G \left[\lambda_0 \mathcal{L}_i + \lambda_1 \left[\mathcal{L}_j, \left[\mathcal{L}_i, \mathcal{L}_j \right] \right], U \right] U^{-1} G^{-1} \right) = 0, \tag{4.88}$$

which is a second order partial differential equation for G. So for any gauged skyrmion (U, B), the representative U' which minimises (4.86) is hence given by $U' = GUG^{-1}$, where (G, U) solves (4.88).

Imposing a symmetric form on the Skyrme field U simplifies this condition. For example, when (U, B) is spherically symmetric, i.e. of the form in (4.50), the gauge transformations which preserve this are those of the same 'hedgehog' form:

$$G(\vec{x}) = \exp\left(\imath \mu(r) \frac{\vec{x} \cdot \vec{\sigma}}{r} \right), \tag{4.89}$$

for some function $\mu : (0, \infty) \longrightarrow \mathbb{R}$. In this scenario, G acts trivially on U, that is $GUG^{-1} = U$, and so (4.88) is obsolete. In other words, the energy (4.86) is invariant under gauge transformations of spherically-symmetric gauged skyrmions.

With this in mind, we may automatically compare the minimisers of (4.86), to the Skyrme-instantons and Skyrme-monopoles found in the previous section, without having to consider a preferred choice of gauge. We set $\lambda_0 = \kappa_0$, and $\lambda_1 = \frac{\kappa_1}{2}$ so that (4.86) aligns with (4.40). Within the hedgehog ansatz, the field equation for (4.86) reduces to the ODE

$$\left(\kappa_0 r^2 + 4\kappa_1 \sin^2 f \right) f'' + 2\kappa_0 r f' + \sin 2f \left(2\kappa_1 f'^2 - \kappa_0 - 2\kappa_1 \frac{\sin^2 f}{r^2} \right) = 0. \tag{4.90}$$

The usual boundary conditions imposed for a spherically-symmetric skyrmion are [82] $f(0) = \pi$ and $f(\infty) = 0$. We shall instead consider the boundary conditions $f(0) = -\pi$ and $f(\infty) = 0$ so that by the formula (4.52), the skyrmion $U = \exp\left(\imath f(r)\frac{\vec{x}\cdot\vec{\sigma}}{r}\right)$ satisfying (4.90) has topological charge $\mathcal{B}^H = 1$. This boundary condition is also comparable to the Skyrme fields of the Skyrme-instantons, and the Skyrme-monopoles with $\nu = \pi$, from the previous section.[17] It is worthwhile noting that even though equation (4.90) appears to depend on the couplings κ_0, κ_1, that is, the parameter α, this dependence is only the case up to a re-scaling of length and energy units. It follows that all solutions of (4.90) with these boundary conditions are the same up to this re-scaling, and will hence all be called *the* spherically-symmetric skyrmion. Linearising (4.90) with these boundary conditions gives a Cauchy-Euler type equation, and we obtain the asymptotic formulae

$$f_s(r) = ar - \pi, \quad r \sim 0, \tag{4.91}$$

$$f_l(r) = -\frac{b}{r^2}, \quad r \sim \infty, \tag{4.92}$$

for some $a, b \in \mathbb{R}^+$ to be determined numerically for each $\alpha > -\frac{1}{2}$.

We are particularly interested in comparing this ordinary skyrmion to the *gauged skyrmions* considered in the previous sections, that is, the Skyrme-monopoles and Skyrme-instantons. The most enlightening comparison in this situation is how much the profile functions agree (or disagree) with each other. To measure this, we will calculate $\Xi = \max_r |f - f_{\text{Sky}}|$, where f is the profile function of the gauged skyrmion Skyrme fields, to be varied over the different types, and f_{Sky} is the ordinary skyrmion (scaled accordingly to solve (4.90) for the correct value of α). We will also use the same measure when we come to compare the ordinary skyrmion to the optimal Harrington-Shepard calorons, and the BPS monopoles, in the next section. Of course, for the monopoles, we consider instead $f - \pi$.

[17] We remark that $f \mapsto f + n\pi$ is a symmetry of the energy and topological charge for all $n \in \mathbb{Z}$, so the boundary condition $f(0) = 0$, and $f(\infty) = \pi$ for the Skyrme-monopoles is essentially equivalent to this.

In figures 4.15-4.16, we plot this measure of difference between the ordinary skyrmion, against the Skyrme fields of the Skyrme-monopoles (with $\nu = \pi$) and Skyrme-instantons respectively.

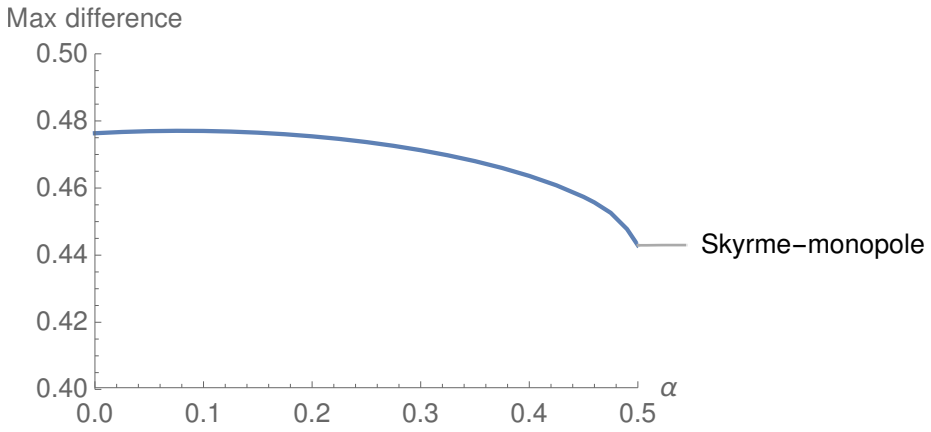

Figure 4.15: The maximum difference between the Skyrme-monopole Skyrme field, and ordinary Skyrme field, as a function of α.

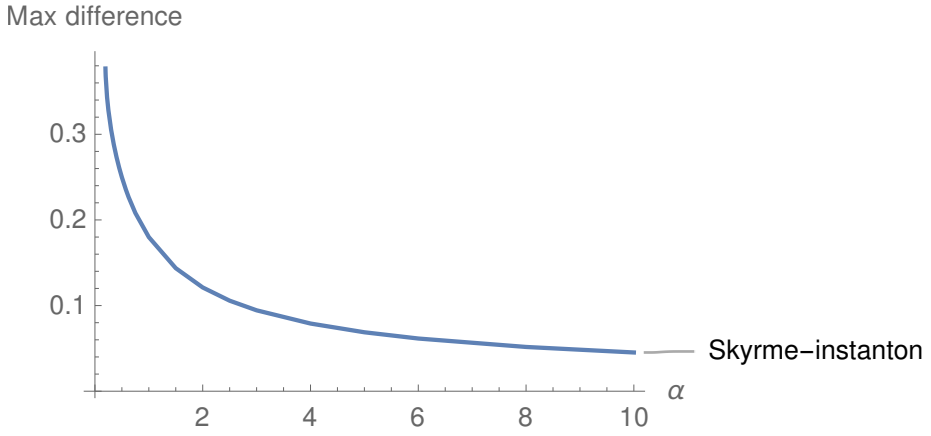

Figure 4.16: The maximum difference between the Skyrme-instanton Skyrme field, and ordinary Skyrme field, as a function of α.

In the case of the Skyrme-monopoles, the difference is seen to be the greatest of all configuration types studied, but still below 0.48 for all examples, which is $\approx 15\%$ of the maximum absolute value of the skyrmion's profile function ($|f(0)| = \pi$). As α varies, this measure of deviation is relatively constant, remaining between 0.45 and 0.48. Contrary

to this, the difference between the Skyrme-instantons, and the ordinary skyrmions starts similarly to the Skyrme-monopoles, and then becomes almost negligible as α increases. This is in fact very much expected – as a result of the discussion in section 4.2.2, we know that as $\alpha \longrightarrow \infty$, the family of spherically-symmetric Skyrme-instantons that we have described will converge in some way to the ordinary spherically-symmetric skyrmion.

4.5.1 Approximating skyrmions with calorons and monopoles

To finish our discussions on calorons, gauged skyrmions, and skyrmions, we shall make one last set of comparisons. Part of the motivation for studying this topic was to see how well calorons, and in particular monopoles, approximate ordinary skyrmions. This has, as already mentioned, been investigated in part in [36, 96], but without the knowledge of the family of gauged Skyrme models (4.40), and the intermediate relationship between calorons and gauged skyrmions.

In the same way as with the gauged skyrmions, we compare the optimal Harrington-Shepard calorons, and BPS monopoles with $\nu = \pi$, by measuring the maximum difference between the profile functions. The results for varying $0 \leq \alpha \leq 10$ are plotted in figure 4.17. In light of the observations in section 4.4.3, it is unsurprising that the strength of the BPS monopole approximation diminishes as α increases, with the difference between the profile functions growing fairly rapidly. On the other hand, the Harrington-Shepard caloron approximation improves as α increases, but of course, this is expected as the caloron appeared to better approximate the Skyrme-instantons in this way, as seen in figure 4.11. These two plots meet at $\alpha = 0$, and importantly, the difference between them and the ordinary Skyrme field is small, at approximately 0.25, which is only 8% of the maximum absolute value of the skyrmion's profile function.[18] The conclusion of this brief analysis is that calorons appear to be good approximations

[18] This is actually not the minimum value found. A smaller value of the max difference may be obtained at $\alpha \sim -0.2$, namely a difference of 0.21.

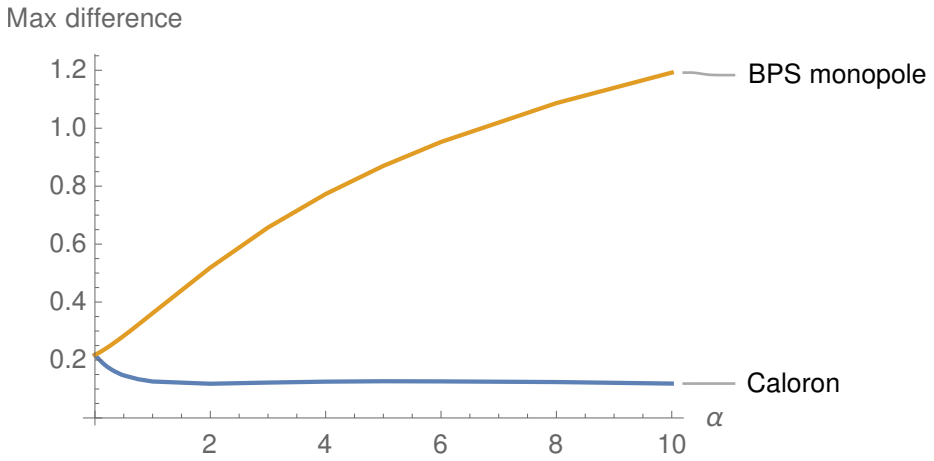

Figure 4.17: The maximum difference between the Skyrme field profile function for the charge 1 BPS monopole, and optimum Harrington-Shepard caloron, as a comparison with the ordinary spherically-symmetric skyrmion.

of skyrmions at all length and energy scales (for optimal choices of the parameter λ), and crucially, monopoles are a good approximation when the length and energy scales are those which align with $\alpha \approx 0$.

4.6 Summary and open problems

By utilising the Atiyah-Manton-Sutcliffe methods for constructing approximate Skyrme fields from instantons [8, 113], we have shown how to similarly construct approximate *gauged Skyrme fields* from periodic instantons, also known as calorons. One nice property of this construction is that it considers an expansion of the caloron in terms of the ultra-spherical functions, which leads to a one-parameter family of gauged Skyrme models (4.40), parameterised by the ultra-spherical parameter $\alpha > -\frac{1}{2}$. In particular, this family, with any number of vector mesons included, reduces to the corresponding Sutcliffe model [113] in a limit where $\alpha \longrightarrow \infty$.

We have studied the relationships between calorons and gauged skyrmions in the case

of spherically symmetric examples. The main conclusion is that the model appears to interpolate between different favoured boundary conditions as α varies, with 'monopole-like' boundary conditions preferred as $\alpha \longrightarrow 0$, and 'instanton-like' conditions preferred as $\alpha \longrightarrow \infty$. This is rather interesting given the similar interpolation between monopoles and instantons that calorons exhibit. We have also studied how monopoles and calorons can be in some cases seen to be reasonable approximations to ordinary skyrmions. This is a small step of progress in the objective of understanding the soliton trinity, as outlined in the introduction of this thesis.

There is of course a lot of work still to be done here. Crucially, we have only considered the most basic examples, and a lot more is likely to be revealed by looking at less symmetric field configurations. The next most simple example would be to consider axially symmetric examples. The famous $(1,1)$-calorons of Kraan-van Baal and Lee-Lu [73, 75], with non-trivial holonomy, contain a family of calorons with precisely this symmetry. Like with the Harrington-Shepard calorons, the holonomies of these calorons generate (less trivial) examples of Skyrme-instantons of charge 1. Since the Skyrme-instanton boundary condition (4.75) for non-zero μ breaks the gauge symmetry to $U(1)$, there may be a relationship with the $U(1)$-gauged skyrmions found in [102], which also exhibit an axial symmetry, in addition to a non-zero dipole moment, which is similar to the interpretation of $(1,1)$-calorons as two oppositely charged magnetic monopoles [72].

It would be particularly interesting to compare other examples of symmetric calorons to the skyrmions of this model. For example, Ward presents in [122] examples of (k,k)-calorons, with trivial holonomy, in the cases $k = 2, 3,$ and 4, which exhibit symmetries corresponding to platonic symmetries of instantons and monopoles, and in addition, these instantons and monopoles occur as limiting cases. It would be very interesting to see whether there exist corresponding symmetric gauged skyrmions, how well these calorons approximate them, and of course, how they relate to the ordinary skyrmions. In particular, it would be good to see if this comparison evinces the apparent correlation between the

symmetries of certain monopoles and skyrmions. It would also be interesting to study the more obscure symmetric examples of calorons in the context of skyrmions, for example the crossed solutions and oscillating solutions described in section 3.6.3.

Bibliography

[1] M Abramowitz and I A Stegun, *Handbook of mathematical functions: with formulas, graphs, and mathematical tables*, vol. 55, Courier Corporation, 1964.

[2] R Alkofer and J Greensite, *Quark confinement: the hard problem of hadron physics*, J. Phys. G: Nuclear and Particle Physics **34** (2007), no. 7, S3.

[3] J P Allen and P M Sutcliffe, *ADHM polytopes*, J. H. E. P. **2013** (2013), no. 5, 1–36.

[4] K Arthur and D H Tchrakian, $SO(3)$ *gauged soliton of an* $O(4)$ *sigma model on* $\mathbb{R}^3$, Phys. Lett. B **378** (1996), no. 1-4, 187–193.

[5] M Atiyah and P Sutcliffe, *Skyrmions, instantons, mass and curvature*, Phys. Lett. B **605** (2005), no. 1-2, 106–114.

[6] M F Atiyah, V G Drinfeld, N J Hitchin, and Y I Manin, *Construction of instantons*, Phys. Lett. A **65** (1978), no. 3, 185–187.

[7] M F Atiyah and N J Hitchin, *The geometry and dynamics of magnetic monopoles*, Princeton University Press, 1988.

[8] M F Atiyah and N S Manton, *Skyrmions from instantons*, Phys. Lett. B **222** (1989), no. 3, 438–442.

[9] M F Atiyah and R S Ward, *Instantons and algebraic geometry*, Commun. Math. Phys. **55** (1977), no. 2, 117–124.

[10] R A Battye and P M Sutcliffe, *Symmetric skyrmions*, Phys. Rev. Lett. **79** (1997), no. 3, 363.

[11] A Ao Belavin, A M Polyakov, A S Schwartz, and Yu S Tyupkin, *Pseudoparticle solutions of the Yang-Mills equations*, Phys. Lett. B **59** (1975), no. 1, 85–87.

[12] R Bielawski, *Monopoles and the Gibbons–Manton metric*, Commun. Math. Phys. **194** (1998), no. 2, 297–321.

[13] E Braaten, L Carson, and S Townsend, *Novel structure of static multisoliton solutions in the Skyrme model*, Phys. Lett. B **235** (1990), no. 1-2, 147–152.

[14] H W Braden, *Cyclic monopoles, affine Toda and spectral curves*, Commun. Math. Phys. **308** (2011), no. 2, 303–323.

[15] HW Braden and VZ Enolski, *The construction of monopoles*, Commun. Math. Phys. **362** (2018), no. 2, 547–570.

[16] Y Brihaye, B Hartmann, and D H Tchrakian, *Monopoles and dyons in $SO(3)$ gauged Skyrme models*, J. Math. Phys. **42** (2001), no. 8, 3270–3281.

[17] Y Brihaye, C T Hill, and C K Zachos, *Bounding gauged skyrmion masses*, Phys. Rev. D **70** (2004), no. 11, 111502.

[18] F Bruckmann, D Nógrádi, and P van Baal, *Constituent monopoles through the eyes of fermion zero-modes*, Nucl. Phys. B **666** (2003), no. 1, 197–229.

[19] F Bruckmann and P van Baal, *Multi-caloron solutions*, Nucl. Phys. B **645** (2002), no. 1, 105–133.

[20] A Chakrabarti, *Periodic generalizations of static, self-dual $SU(2)$ gauge fields*, Phys. Rev. D **35** (1987), no. 2, 696.

[21] B Charbonneau and J Hurtubise, *The Nahm transform for calorons*, The many facets of geometry: a tribute to Nigel Hitchin (2010) (2007).

[22] B Charbonneau and J Hurtubise, *Calorons, Nahms equations on S^1 and bundles over $\mathbb{P}^1 \times \mathbb{P}^1$*, Commun. Math. Phys. **280** (2008), no. 2, 315–349.

[23] T-P Cheng and L-F Li, *Gauge theory of elementary particle physics*, Clarendon press Oxford, 1984.

[24] S A Cherkis, *Moduli spaces of instantons on the Taub-NUT space*, Commun. Math. Phys. **290** (2009), no. 2, 719–736.

[25] S A Cherkis, *Instantons on gravitons*, Commun. Math. Phys. **306** (2011), no. 2, 449–483.

[26] S A Cherkis and J Hurtubise, *Monads for instantons and bows*, arXiv preprint arXiv:1709.00145 (2017).

[27] S A Cherkis, A Larrain-Hubach, and M Stern, *Instantons on multi-Taub-NUT spaces I: Asymptotic form and index theorem*, arXiv preprint arXiv:1608.00018 (2016).

[28] S Coleman, *Aspects of symmetry: selected Erice lectures*, Cambridge University Press, 1988.

[29] J Cork, *Skyrmions from calorons*, arXiv preprint arXiv:1810.04143 (2018).

[30] J Cork, *Symmetric calorons and the rotation map*, J. Math. Phys. **59** (2018), no. 6, 062902.

[31] E Corrigan and D B Fairlie, *Scalar field theory and exact solutions to a classical $SU(2)$ gauge theory*, Phys. Lett. B **67** (1977), no. 1, 69–71.

[32] S K Donaldson, *Instantons and geometric invariant theory*, Commun. Math. Phys. **93** (1984), no. 4, 453–460.

[33] S K Donaldson, *Nahm's equations and the classification of monopoles*, Commun. Math. Phys. **96** (1984), no. 3, 387–407.

[34] S K Donaldson and P B Kronheimer, *The geometry of four-manifolds*, Oxford University Press, 1997.

[35] M Dunajski, *Skyrmions from gravitational instantons*, Proc. R. Soc. A **469** (2013), no. 2151, 20120576.

[36] K J Eskola and K Kajantie, *Thermal skyrmion-like configuration*, Zeitschrift für Physik C Particles and Fields **44** (1989), no. 2, 347–348.

[37] M J Esteban, *A direct variational approach to Skyrme's model for meson fields*, Commun. Math. Phys. **105** (1986), no. 4, 571–591.

[38] M J Esteban, *Existence of 3-D skyrmions*, Commun. Math. Phys. **251** (2004), no. 1, 209–210.

[39] L D Faddeev, *Some comments on the many-dimensional solitons*, Lett. Math. Phys. **1** (1976), no. 4, 289–293.

[40] D T J Feist, P H C Lau, and N S Manton, *Skyrmions up to baryon number 108*, Phys. Rev. D **87** (2013), no. 8, 085034.

[41] S Flood and J M Speight, *Chern-Simons deformation of vortices on compact domains*, J. Geom. Phys. **133** (2018), 153–167.

[42] G Frobenius, *Ueber die integration der linearen differentialgleichungen durch reihen.*, Journal für die reine und angewandte Mathematik **76** (1873), 214–235.

[43] M Furuta and Y Hashimoto, *Invariant instantons on S^4*, J. Fac. Sci. Univ. Tokyo **37** (1990), 585–600.

[44] H Garland and M K Murray, *Kac-Moody monopoles and periodic instantons*, Commun. Math. Phys. **120** (1988), no. 2, 335–351.

[45] H Garland and M K Murray, *Why instantons are monopoles*, Commun. Math. Phys. **121** (1989), no. 1, 85–90.

[46] C Gattringer, *Calorons, instantons, and constituent monopoles in $SU(3)$ lattice gauge theory*, Phys. Rev. D **67** (2003), no. 3, 034507.

[47] M Göckeler and T Schücker, *Differential geometry, gauge theories, and gravity*, Cambridge University Press, 1989.

[48] D Y Grigoriev, P M Sutcliffe, and D H Tchrakian, *Skyrmed monopoles*, Phys. Lett. B **540** (2002), no. 1-2, 146–152.

[49] D G Harland, *Large scale and large period limits of symmetric calorons*, J. Math. Phys. **48** (2007), no. 8, 082905.

[50] D G Harland, *Kinks, chains, and loop groups in the $\mathbb{C}P^n$ sigma models*, J. Math. Phys. **50** (2009), no. 12, 122902.

[51] D G Harland and R S Ward, *Chains of skyrmions*, J. H. E. P. **2008** (2008), no. 12, 093.

[52] B J Harrington and H K Shepard, *Periodic euclidean solutions and the finite-temperature Yang-Mills gas*, Phys. Rev. D **17** (1978), no. 8, 2122.

[53] P Hekmati, M K Murray, and R F Vozzo, *The general caloron correspondence*, J. Geom. Phys. **62** (2012), no. 2, 224–241.

[54] N J Hitchin, A Karlhede, U Lindström, and M Roček, *Hyperkähler metrics and supersymmetry*, Commun. Math. Phys. **108** (1987), no. 4, 535–589.

[55] N J Hitchin, N S Manton, and M K Murray, *Symmetric monopoles*, Nonlinearity **8** (1995), no. 5, 661.

[56] N J Hitchin, G B Segal, and R S Ward, *Integrable systems: Twistors, loop groups, and Riemann surfaces*, Oxford University Press, 2013.

[57] G 't Hooft, unpublished.

[58] G 't Hooft, *How instantons solve the $U(1)$ problem.*, Phys. Rep. **142** (1986), no. 6, 357–387.

[59] C J Houghton, N S Manton, and P M Sutcliffe, *Rational maps, monopoles and skyrmions*, Nucl. Phys. B **510** (1998), no. 3, 507–537.

[60] C J Houghton and P M Sutcliffe, *Octahedral and dodecahedral monopoles*, Nonlinearity **9** (1996), no. 2, 385.

[61] C J Houghton and P M Sutcliffe, *Tetrahedral and cubic monopoles*, Commun. Math. Phys. **180** (1996), no. 2, 343–361.

[62] C J Houghton and P M Sutcliffe, *$SU(N)$ monopoles and platonic symmetry*, J. Math. Phys. **38** (1997), no. 11, 5576–5589.

[63] J Hurtubise, *The classification of monopoles for the classical groups*, Commun. Math. Phys. **120** (1989), no. 4, 613–641.

[64] J Hurtubise and M K Murray, *On the construction of monopoles for the classical groups*, Commun. Math. Phys. **122** (1989), no. 1, 35–89.

[65] E-M Ilgenfritz, M Müller-Preussker, and D Peschka, *Calorons in $SU(3)$ lattice gauge theory*, Phys. Rev. D **71** (2005), no. 11, 116003.

[66] M Jardim, *A survey on Nahm transform*, J. Geom. Phys. **52** (2004), no. 3, 313–327.

[67] S Jarvis, *Euclidian monopoles and rational maps*, Proc. Lond. Math. Soc. **77** (1998), no. 1, 170–192.

[68] S Jarvis, *A rational map of euclidean monopoles via radial scattering*, Journal fur die Reine und Angewandte Mathematik **524** (2000), 17–42.

[69] T Kato, A Nakamula, and K Takesue, *Magnetically charged calorons with non-trivial holonomy*, J. H. E. P. **2018** (2018), no. 6, 24.

[70] T C Kraan, *Instantons, monopoles and toric hyperkähler manifolds*, Commun. Math. Phys. **212** (2000), no. 3, 503–533.

[71] T C Kraan and P van Baal, *Exact T-duality between calorons and Taub-NUT spaces*, Phys. Lett. B **428** (1998), no. 3, 268–276.

[72] T C Kraan and P van Baal, *Monopole constituents inside $SU(n)$ calorons*, Phys. Lett. B **435** (1998), no. 3-4, 389–395.

[73] T C Kraan and P van Baal, *Periodic instantons with non-trivial holonomy*, Nucl. Phys. B **533** (1998), no. 1, 627–659.

[74] K Langfeld and H Reinhardt, *$SU(N)$ instantons and exotic skyrmions*, Phys. Lett. B **317** (1993), no. 4, 590–595.

[75] K Lee and C Lu, *$SU(2)$ calorons and magnetic monopoles*, Phys. Rev. D **58** (1998), no. 2, 025011.

[76] R A Leese and N S Manton, *Stable instanton-generated Skyrme fields with baryon numbers three and four*, Nucl. Phys. A **572** (1994), no. 3-4, 575–599.

[77] N S Manton, *A remark on the scattering of BPS monopoles*, Phys. Lett. B **110** (1982), no. 1, 54–56.

[78] N S Manton, *Geometry of skyrmions*, Commun. Math. Phys. **111** (1987), no. 3, 469–478.

[79] N S Manton and B M A G Piette, *Understanding skyrmions using rational maps*, European Congress of Mathematics, Springer, 2001, pp. 469–479.

[80] N S Manton and T M Samols, *Skyrmions on S^3 and H^3 from instantons*, J. Phys. A: Mathematical and General **23** (1990), no. 16, 3749.

[81] N S Manton and P M Sutcliffe, *Skyrme crystal from a twisted instanton on a four-torus*, Phys. Lett. B **342** (1995), no. 1-4, 196–200.

[82] N S Manton and P M Sutcliffe, *Topological solitons*, Cambridge University Press, 2004.

[83] N S Manton and P M Sutcliffe, *Platonic hyperbolic monopoles*, Commun. Math. Phys. **325** (2014), no. 3, 821–845.

[84] L J Mason and N M J Woodhouse, *Integrability, self-duality, and twistor theory*, no. 15, Oxford University Press, 1996.

[85] D Muranaka, A Nakamula, N Sawado, and K Toda, *Numerical Nahm transform for 2-caloron solutions*, Phys. Lett. B **703** (2011), no. 4, 498–503.

[86] W Nahm, *All self-dual multimonopoles for arbitrary gauge groups*, Structural elements in particle physics and statistical mechanics, Springer, 1983, pp. 301–310.

[87] H Nakajima, *Monopoles and Nahm's equations*, Lecture Notes in Pure and Applied Mathematics (1993), 193–193.

[88] H Nakajima, *Instantons on ALE spaces, quiver varieties, and Kac-Moody algebras*, Duke Mathematical Journal **76** (1994), no. 2, 365–416.

[89] A Nakamula and J Sakaguchi, *Multicalorons revisited*, J. Math. Phys. **51** (2010), no. 4, 043503.

[90] A Nakamula and N Sawado, *Cyclic calorons*, Nucl. Phys. B **868** (2013), no. 2, 476–491.

[91] A Nakamula, N Sawado, and K Takesue, *Aspects of $C3$-symmetric calorons from numerical Nahm transform*, J. Phys.: Conference Series, vol. 563, IOP Publishing, 2014, p. 012032.

[92] C Naya and P Sutcliffe, *Skyrmions in models with pions and rho mesons*, J. H. E. P. **2018** (2018), no. 5, 174.

[93] D Nógrádi, *Multi-calorons and their moduli*, Ph.D. thesis, Institute Lorentz for Theoretical Physics, University of Leiden, 2005.

[94] P Norbury, *Periodic instantons and the loop group*, Commun. Math. Phys. **212** (2000), no. 3, 557–569.

[95] P Norbury and N M Romão, *Spectral curves and the mass of hyperbolic monopoles*, Commun. Math. Phys. **270** (2007), no. 2, 295–333.

[96] M A Nowak and I Zahed, *Skyrmions from instantons at finite temperature*, Phys. Lett. B **230** (1989), no. 1-2, 108–112.

[97] T M W Nye, *The geometry of calorons*, Ph.D. thesis, The University of Edinburgh, 2001.

[98] T M W Nye and M A Singer, *An L^2-index theorem for Dirac operators on $S^1 \times \mathbb{R}^3$*, J. Funct. Anal. **177** (2000), 203.

[99] R S Palais, *The principle of symmetric criticality*, Commun. Math. Phys. **69** (1979), no. 1, 19–30.

[100] S Palmer and C Sämann, *M-brane models from non-abelian gerbes*, J. H. E. P. **2012** (2012), no. 7, 10.

[101] V Paturyan and D H Tchrakian, *Monopole–antimonopole solutions of the skyrmed $SU(2)$ Yang–Mills–Higgs model*, J. Math. Phys. **45** (2004), no. 1, 302–309.

[102] B M A G Piette and D H Tchrakian, *Static solutions in the $U(1)$ gauged Skyrme model*, Phys. Rev. D **62** (2000), no. 2, 025020.

[103] P Plansangkate, *Skyrmions, multi-instantons and $SU(\infty)$-Toda equation*, arXiv preprint arXiv:1611.01444 (2016).

[104] M K Prasad and P Rossi, *Construction of exact Yang-Mills-Higgs multimonopoles of arbitrary charge*, Phys. Rev. Lett. **46** (1981), no. 13, 806.

[105] M K Prasad and C M Sommerfield, *Exact classical solution for the 't Hooft monopole and the Julia-Zee dyon*, Phys. Rev. Lett. **35** (1975), no. 12, 760.

[106] A Pressley and G Segal, *Loop groups*, The Clarendon Press, D. Reidel Publishing Co., 1984.

[107] P Rossi, *Propagation functions in the field of a monopole*, Nucl. Phys. B **149** (1979), no. 1, 170–188.

[108] T Sakai and S Sugimoto, *Low energy hadron physics in holographic QCD*, Prog. Th. Phys. **113** (2005), no. 4, 843–882.

[109] R P d Santos, *Monopoles on $\mathbb{R}^5$ and generalized Nahm's equations*, arXiv preprint arXiv:1610.00563 (2016).

[110] T Schäfer and E V Shuryak, *Instantons in QCD*, Rev. Mod. Phys. **70** (1998), no. 2, 323.

[111] M A Singer and P M Sutcliffe, *Symmetric instantons and Skyrme fields*, Nonlinearity **12** (1999), no. 4, 987.

[112] D Stuart, *The geodesic approximation for the Yang-Mills-Higgs equations*, Commun. Math. Phys. **166** (1994), no. 1, 149–190.

[113] P Sutcliffe, *Skyrmions, instantons and holography*, J. H. E. P. **2010** (2010), no. 8, 19.

[114] P Sutcliffe, *Skyrmions in a truncated BPS theory*, J. H. E. P. **2011** (2011), no. 4, 45.

[115] P M Sutcliffe, *BPS monopoles*, Int. J. Mod. Phys. A **12** (1997), no. 26, 4663–4705.

[116] P M Sutcliffe, *Cyclic monopoles*, Nucl. Phys. B **505** (1997), no. 1-2, 517–539.

[117] P M Sutcliffe, *Instantons and the buckyball*, Proc. R. Soc. Lon. A: Mathematical, Physical and Engineering Sciences, vol. 460, The Royal Society, 2004, pp. 2903–2912.

[118] Y Takayama, *Nahm's equations, quiver varieties and parabolic sheaves*, (2016).

[119] C H Taubes, *Differential geometry: Bundles, connections, metrics and curvature*, vol. 23, Oxford University Press, 2011.

[120] K K Uhlenbeck, *Removable singularities in Yang-Mills fields*, Commun. Math. Phys. **83** (1982), no. 1, 11–29.

[121] P van Baal, *A review of instanton quarks and confinement*, AIP Conference Proceedings, vol. 892, AIP, 2007, pp. 241–244.

[122] R S Ward, *Symmetric calorons*, Phys. Lett. B **582** (2004), no. 3, 203–210.

[123] R S Ward, *Symmetric instantons and discrete Hitchin equations*, J. Int. Sys. **1** (2016), no. 1.

[124] R S Ward and R O Wells, *Twistor geometry and field theory*, Cambridge University Press, 1991.

[125] G Wilson, *Notes on the vector adelic grassmannian*, arXiv preprint arXiv:1507.00693 (2015).

[126] E Witten, *Some exact multipseudoparticle solutions of classical Yang-Mills theory*, Phys. Rev. Lett. **38** (1977), no. 3, 121.

[127] E Witten, *Baryons in the 1N expansion*, Nucl. Phys. B **160** (1979), no. 1, 57–115.